1996

# The self-assembly of metallosupramolecular architectures

Jeffrey Ronald Hall
*University of Windsor*

# INFORMATION TO USERS

This manuscript has been reproduced from the microfilm master. UMI films the text directly from the original or copy submitted. Thus, some thesis and dissertation copies are in typewriter face, while others may be from any type of computer printer.

**The quality of this reproduction is dependent upon the quality of the copy submitted.** Broken or indistinct print, colored or poor quality illustrations and photographs, print bleedthrough, substandard margins, and improper alignment can adversely affect reproduction.

In the unlikely event that the author did not send UMI a complete manuscript and there are missing pages, these will be noted. Also, if unauthorized copyright material had to be removed, a note will indicate the deletion.

Oversize materials (e.g., maps, drawings, charts) are reproduced by sectioning the original, beginning at the upper left-hand corner and continuing from left to right in equal sections with small overlaps. Each original is also photographed in one exposure and is included in reduced form at the back of the book.

Photographs included in the original manuscript have been reproduced xerographically in this copy. Higher quality 6" x 9" black and white photographic prints are available for any photographs or illustrations appearing in this copy for an additional charge. Contact UMI directly to order.

# The Self-Assembly of Metallosupramolecular Architectures

by

Jeffrey Ronald Hall

A Thesis
Submitted to the
Faculty of Graduate Studies and Research
through the Department of Chemistry
and Biochemistry in Partial Fulfillment
of the Requirements for the Degree
of Master of Science at
The University of Windsor

Windsor, Ontario, Canada

September, 1996

Canada

# University of Windsor

# Faculty of Graduate Studies and Research

## Certificate of Examination
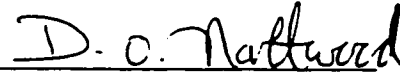
Chief Advisor                                  Examining Board

_____
Dr. Stephen J. Loeb

                                        _____
                                        Dr. Douglas W. Stephan
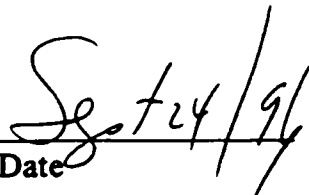
                                        _____
                                        Dr. Derek O. Northwood
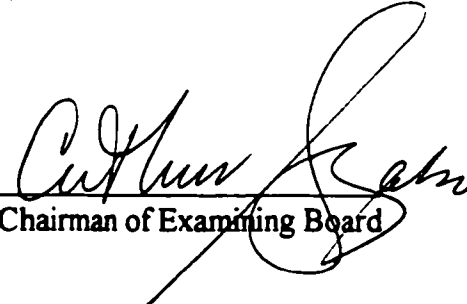
The Dissertation by
Jeffrey Ronald Hall
entitled

Self-Assembly of Metallosupramolecular Architectures

is Accepted in Partial Fulfillment of the
Requirements for the Degree of
Master of Science

_____
Date

                                        _____
                                        Chairman of Examining Board

# Abstract

This thesis describes the design, synthesis and characterization of

metallosupramolecular cleft and box-shaped molecules. These compounds are generated

via the self-assembly of building block compounds; metallated thioether complexes and

aromatic N-donor ligands.

Chapter Two describes the synthesis and characterization of the building block

compounds. Cyclometallation of the thioether ligand 1,3-bis(phenylthio-methyl)benzene

(PhS$_2$) with [Pd(CH$_3$CN)$_4$][BF$_4$]$_2$ produced the species [Pd(PhS$_2$)(CH$_3$CN)][BF$_4$]. By

varying the S-R group, a family of compounds were synthesized each possessing different

physical properties. The metallated ligands exhibited inversion of sulfur and this was

studied via variable temperature $^1$H NMR spectroscopy. As well, several ligands of the

form 1,2,4,5-tetrakis-(phenylthiomethyl)benzene (PhS$_4$) were synthesized. These ligands

underwent the cyclometallation reaction twice, forming the doubly palladated compound

[Pd$_2$(PhS$_4$)(CH$_3$CN)$_2$][BF$_4$]$_2$. In an attempt to produce a trigonal bipyramidal Pd(II)

complex with 1,10-phenanthroline, an uncommon square pyramidal geometry was

produced. These building block compounds were characterized through the use of

$^{13}$C{$^1$H} and $^1$H NMR spectroscopy as well as X-ray crystallography.

Chapter Three describes the synthesis of molecular clefts and boxes from the

building block compounds developed in Chapter Two. When mixed in a ratio of 2:1,

[Pd(PhS$_2$)(CH$_3$CN)][BF$_4$]:4,7-phenanthroline, the molecular cleft

[(Pd(PhS$_2$))$_2$(4,7-phen)][BF$_4$]$_2$ (Ph-Cleft) can be isolated in quantitative yields. This was

found to be the case with the n-butyl version of the ligand as well. The self-assembly of a

molecular box was achieved by the addition of $[Pd_2(PhS_4)(CH_3CN)_2][BF_4]_2$ to

4,7-phenanthroline in a 1:1 ratio. The sole product of this reaction is the molecular box, a

cyclic complex containing three wall units, $[Pd_2(PhS_4)][BF_4]_2$ and three corner pieces;

4,7-phenanthroline. Similar results were obtained utilizing the

$[Pd_2(BuS_4)(CH_3CN)_2][BF_4]_2$ compound with 4,7-phenanthroline. These supramolecular

species were characterized by $^1H$ NMR and mass spectrometry as well as X-ray

crystallography.

.

v

This work is dedicated to my parents.

I seem to have been only like a boy playing on the seashore, and diverting myself in now and then finding a smoother pebble or a prettier shell than ordinary, whilst the great ocean of truth lay all undiscovered before me.

**Sir Isaac Newton**

# Acknowledgments

I would like to thank my supervisor, Professor Steve Loeb for his friendship, patience and guidance. These past few years will always be appreciated and remembered.

There are several people in particular who have made the past few years an enjoyable period. Past and present members of the Loeb group, Sonia Corrent, Beth Cameron, Shannon Murphy, James Wisner and Chris Deslippe are sincerely thanked for their camaraderie and support. Thanks to the faculty and staff of the chemistry department for their help and assistance, particularly Mike Fuerth and Dr. Doug Stephan.

The Chemistry softball team provided great release from the lab. The roaring Mike Siwek hitting mammoth home runs, Dr. Jim Green's burning competitiveness, perennial MVP Dave Platt and the tremendous talent and devotion from the members of the Loeb group, Chris, Sonia, Beth, Shannon and Steve Loeb. All are thanked for their friendship and the great memories.

A special thank-you to my family, Mom, Dad, Jeremy and Ernie the wiener dog for their love and support.

Finally I would like to thank Shannon Murphy, who never ceases to amaze and amuse me with her understanding and wit.

viii

# Table of Contents

ix

x

xi

# List of Figures

xii

xiii

# List of Tables

xiv

# List of Abbreviations

| | |
|---|---|
| δ | chemical shift |
| λ | wavelength |
| μ | absorption coefficient |
| ρ | density |
| ν | frequency |
| Å | Angstrom |
| °C | degrees centigrade |
| anh. | anhydrous |
| br | broad |
| Bu | n-butyl |
| cm | centimetre |
| d | doublet |
| dd | doublet of doublets |
| dpp | 3,6-bis(2'pyridyl)pyridazine |
| DMF | N,N'-dimethylformamide |
| ESI-MS | electrospray ionization mass spectrometry |
| FAB-MS | fast atom bombardment mass spectrometry |

| | |
|---|---|
| fw | formula weight |
| g | grams |
| h | hours |
| Hz | hertz |
| IR | Infrared |
| J | Joule |
| k | rate constant |
| K | degrees Kelvin |
| kJ | kilojoules |
| LSI-MS | liquid secondary ionization mass spectrometry |
| *m* | meta |
| m | multiplet |
| m/z | mass to charge ratio |
| Me | methyl |
| MHz | megahertz |
| min | minutes |
| mL | millilitres |
| mmol | millimoles |

| | |
|---|---|
| mol | moles |
| NaOAc | sodium acetate |
| NMR | nuclear magnetic resonance |
| Ph | phenyl |
| ppm | parts per million |
| q | quartet |
| quin. | quintet |
| R | agreement factor |
| $R_w$ | weighted agreement factor |
| s | singlet |
| t | triplet |
| T | temperature |
| TFA | trifluoroacetic acid |
| UV-vis | ultraviolet-visible |
| V | unit cell volume |
| X-ray | X-ray diffraction |
| Z | number of molecules in the unit cell |

# Chapter One

## 1.1 Supramolecular Chemistry

"Just as there is a field of *molecular chemistry* based on the covalent bond, there is a field of *supramolecular chemistry*, the chemistry of molecular assemblies and of the intermolecular bond."[1] Supramolecular chemistry involves the assembly of two or more species forming a *supermolecule* held together by noncovalent interactions. The intermolecular forces involved are forces such as hydrogen bonding, hydrophobic/ hydrophilic interactions, $\pi$-$\pi$ and ion-dipole interactions and metal-ligand interactions. Although molecular associations have been recognized for years, the concept and term supramolecular chemistry was only introduced in 1978.[2] It has been a slow process of recognizing the significance of scattered results and seemingly unrelated observations to establish what is now considered supramolecular chemistry.

Supramolecular chemistry grew primarily from alkali complexation of crown ethers and cryptands. The interactions between a crown ether and an alkali earth metal led to the concept of molecular receptors; a molecule complexed by another molecule. Covalent organic hosts are synthesized to selectively bind specific molecules. Driven largely by the desire to selectively complex molecules, host molecules have become increasingly complex. From Pedersen's first crown ethers[3] have emerged organic molecules with such figurative names as cryptands[4], spherands[5], cavitands[6], carcerands[7] and cyclophanes.

1

These molecules are not limited to organic chemistry as an example from Sanders

illustrates.[8]
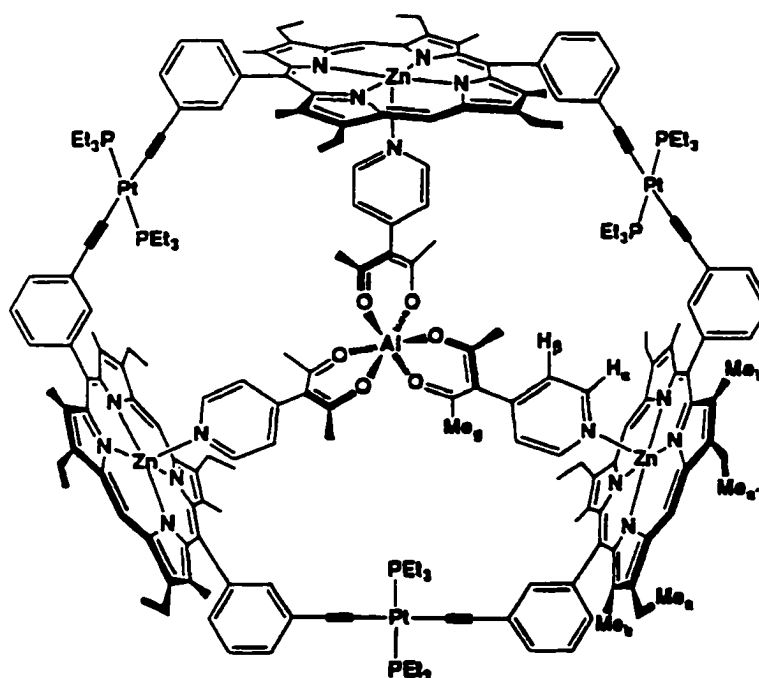


*Figure 1.1    Platinum linked cyclic porphyrin.*

This cyclic trimer porphyrin is synthesized from monomeric porphyrin units through

Glaser coupling of the terminal alkynes with trans-Pt(PR$_3$)$_2$Cl$_2$. Subsequent binding of the

octahedral aluminium tris[3-(4-pyridyl)acetylacetonate] guest induces an asymmetry which

is detected by NMR spectroscopy. The coupling produces the cyclic trimer in yield of

16-20%, the remainder being polymeric material.

As these molecules become more complex, the number of steps required in their

syntheses typically results in final product yields of less than 5%. The number of steps

required to synthesize a large complex molecule would take an excessive amount of time

and enormous amounts of starting materials. The use of template syntheses has brought

dramatic increases in synthetic efficiency.

## 1.2  Template Syntheses

### 1.2.1  Introduction

The term *template effects* has been around since the 1960's.[9] The template effect is generally described as occurring when a neutral molecule or ion as guest "coordinates" a ligand or host molecule, and by doing so organizes the ligand into a conformation suitable for the formation of a specific product.

### 1.2.2  Template Syntheses with Metal Cations

The most frequently used and longest known templates have been based on metal ions. The most recognized being the formation of crown ethers in good yield.[3] The ligand building blocks wrap themselves around the metal ion, favoring ring closure to the macrocycle.
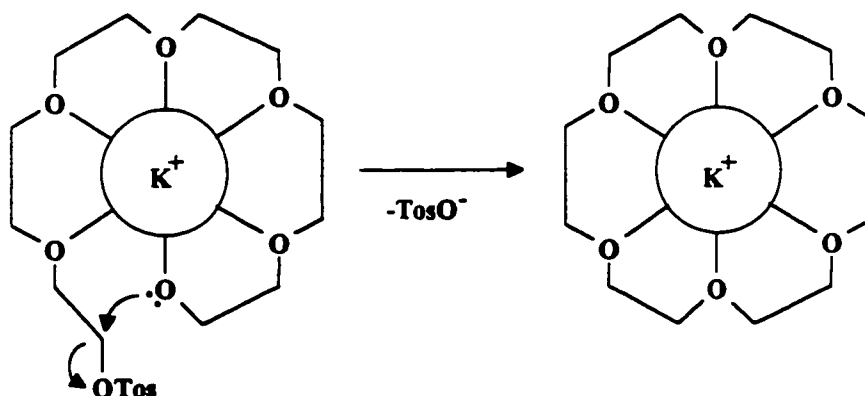


**Figure 1.2**    *Template synthesis of [18]crown-6.  The potassium ion acts as a convex template.*

A particularly interesting use of metal template synthesis has been the construction of interlocked macrocycles known as catenanes. Metal ions may be used to complex two ligands so that connecting their ends favours the formation of the catenane.

Sauvage's catenanes[10] are some of the most impressive examples of all

supramolecular compounds. The catenanes are based on tetrahedral coordination of Cu[1]

by functionalized phenanthroline ligands.
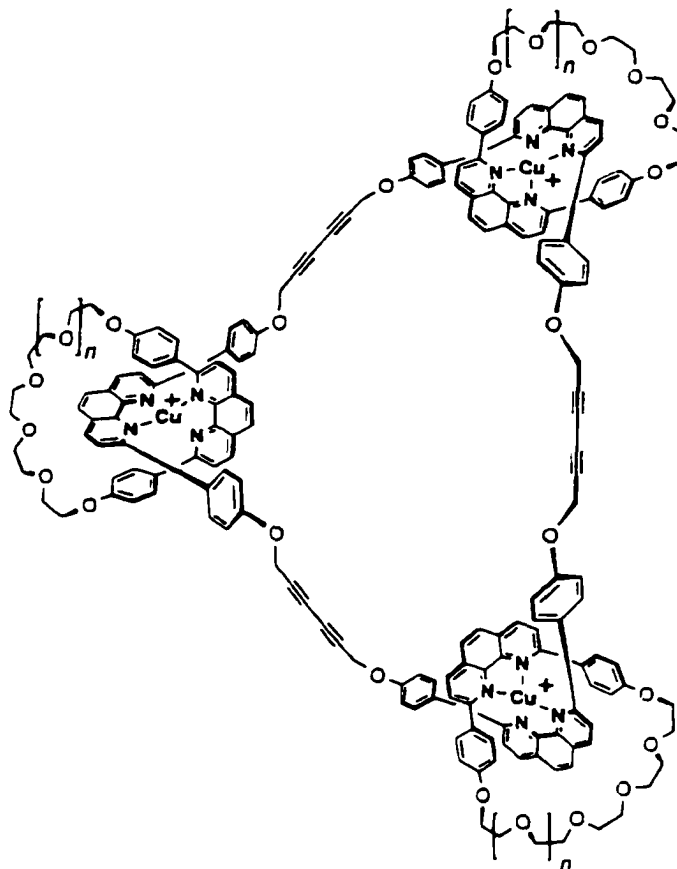


*Figure 1.3  A [3]catenate using Cu(I) as a convex template.*

## 1.2.3 Molecules as Templates

Stoddart has developed an efficient template-directed one pot synthesis of a

[2]catenane.[11] The template is based on the π-donor and π-acceptor stacking of the

electron rich hydroquinone ether unit and the electron poor bipyridinium groups. The

arrangement of the groups leads to an orthogonal arrangement of the building blocks.

The result was a highly efficient formation of [2]catenanes in remarkable yield.

Stoddart has also recently made a two-dimensional array based on π-donor/π-acceptor square cyclophanes with the inclusion of ferrocene.[12] The array is based on hydroquinone and bipyridinium units, arranged to provide a self-complementary framework. This self-complementarity allows for the assembly of the two-dimensional array.
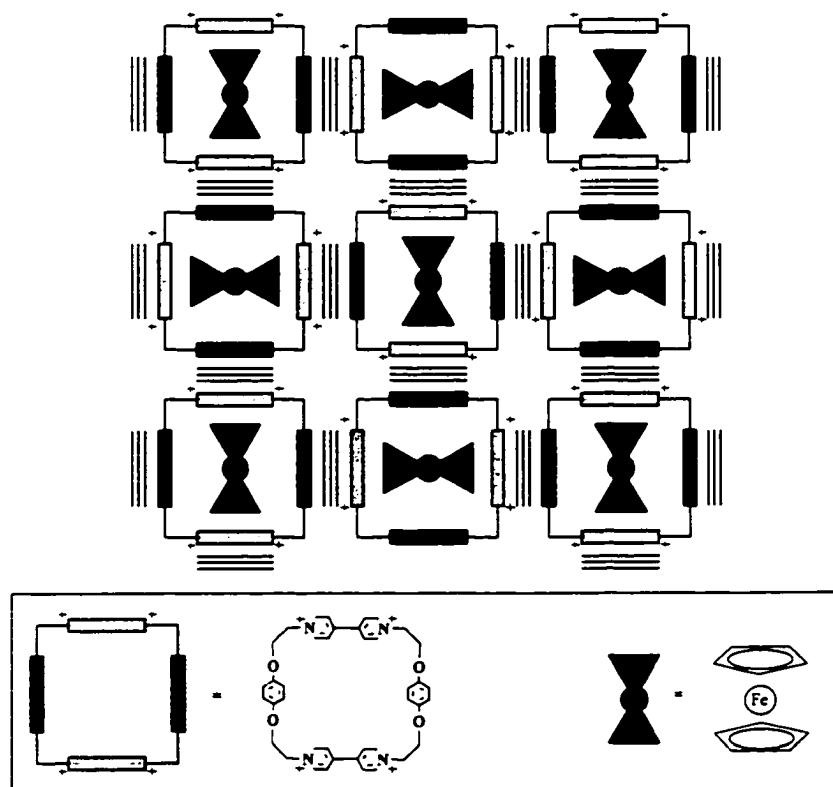


*Figure 1.4    Schematic representation of the 1:1 adduct*

The formation of a 1:1 adduct produces a bright green solution upon addition of an equimolar quantity of ferrocene. An X-ray crystallographic analysis showed the solid state structure to be a 1:1 adduct with the cyclopentadienyl rings sandwiched between the faces of the bipyridinium units. The use of template synthesis allows the construction of this *molecular mosaic* possible.

## 1.3 Self-Assembly

### 1.3.1 Introduction

Somehow nature created the molecules of life from the primordial soup without a chemist or genetic material to direct the synthesis. Wald first proposed that building block molecules could spontaneously assemble into an intact cell.[13] These building block molecules contained all the necessary information to recognize and interact with other appropriate molecules. From template effect to self-assembly is only a small jump, if even that. In recent literature, the term self-assembly has been used where the term template effect had been used in previous communications. The prevailing terminology seems to be that a template is used to direct the self assembly process to form the desired product. The term template effect is reserved for situations in which a template is used to bring something into a suitable conformation at which point further covalent synthesis is required to obtain the desired product. Self-assembly is a highly convergent process which may be defined as the spontaneous assembly of individual components into higher ordered structures due to their reversible binding at thermodynamic equilibrium. This process offers some advantages over stepwise covalent syntheses. Yields may be dramatically higher since there is a form of error checking involved. Defective assemblies are rejected during self-assembly because they are not thermodynamically stable with respect to the target compound. Furthermore, since the process is convergent, fewer steps are required to obtain the final product compared to that of a stepwise synthesis. The utilization of self-assembly has been a boon to the field of Supramolecular chemistry where increasing complexity of the target molecule has strained the classical stepwise methods of synthesis.

## 1.3.2 Multiple Equilibria and Self-Assembly

The noncovalent interactions that drive self-assembly are weak compared to their covalent counterparts. As a consequence, supramolecular complexes may exist in equilibria with component parts as well as other unwanted complexes. The equilibria are often significantly affected by subtle environmental factors such as concentration, solvent temperature and light. Typically stable multimeric complexes are required. In nature, the self assembly process is used only in high molecular weight aggregates where a legion of noncovalent interactions preserve the structural integrity of the molecule. At the current level of progress in supramolecular chemistry, the relatively small molecules in use do not possess the multitude of noncovalent interactions required to effectively drive the self-assembly process. This difficulty may be addressed by controlling factors which promote the formation of small self-assembling complexes.

The most important factor for controlling supramolecular assemblage is ensuring that subunit design allows good interaction. Without complementarity in subunit design, nature will find an alternate structure that best utilizes complementary forces. CPK models may be used for indications of size and shape complementarity. Computer modelling of noncovalent interactions using molecular mechanics are available although coordination compounds involving metal ions with organic ligands have yet to be well parametrized.[14,15]

The use of an appropriate solvent can enhance the strength of the noncovalent interactions that are responsible for maintaining the structural integrity of the complex. If the species are designed to interact via hydrophobic interactions, then self-assembly is best

conducted under aqueous conditions. In contrast, hydrogen bonds and electrostatic interactions are strongest in apolar aprotic solvents.

In accordance with LeChatelier's principle, a large excess of one of the components can be employed to drive the self-assembly process to completion. Unfortunately, in this case, the large excess of free subunits may disrupt the ability of the complex to perform the task for which it was designed. Although the complex may be the predominant complex in solution under these conditions, it will still be in equilibrium with its component parts and isolation may not be possible. Under these conditions, characterization may be difficult.

The supramolecular complex can be selectively removed from solution to prevent dissociation of the complex back to its component parts. Characterization should be more tractable than with an equilibrium mixture of complexes since the complex is isolated. This approach is fine if characterization is the only goal; if the isolated end product is almost completely dissociated in solution, then it may have limited usefulness as a functionally active complex.

This apparent liability for self-assembly may also prove to be it's most powerful attribute. The assembly and disassembly of microtubules is an extraordinary example of self-assembly. The chameleon changes colour in response to external stimuli by assembling microtubules to convey pigment to specialized cells on the skin surface. A supramolecular complex which can rapidly assemble and disassemble based on a change in the environment may be used for parts in nanoscale machines. These molecular sized

machines could make decisions and perform functions based on a set of environmental conditions.

## 1.4 Self-Assembling Metallosupramolecular Complexes

### 1.4.1 Introduction

Just as classical chemistry is divided into organic and inorganic chemistry, supramolecular chemistry may be divided into analogous areas. Becoming prevalent in the literature is the term *metallosupramolecular*. Metallosupramolecular chemistry encompasses the supramolecular complexes which utilize metal-ligand interactions to drive the self-assembly process. Using metal-ligand interactions to design molecular building blocks has led to the idea of a meccano set for chemists. Chemists have been expanding their meccano sets and have created complexes which have geometry mimicked from macroscopic structures. The following is a survey of metallosupramolecular structures.

### 1.4.2 One and Two Dimensional Arrays , Three Dimensional Networks

One dimensional molecules with very long $\pi$-systems have been investigated for uses in conductive polymers, semiconductors and third-order nonlinear optical materials. Anderson has used non-covalent interactions to hold adjacent porphyrin units planar in order to maximize $\pi$-overlap.[16] The square pyramidal geometry of zinc(II) allows for a linking of two one dimensional polymers. The coordination of pyrazine to zinc produces an infinite ladder like structure with pyrazine rungs.
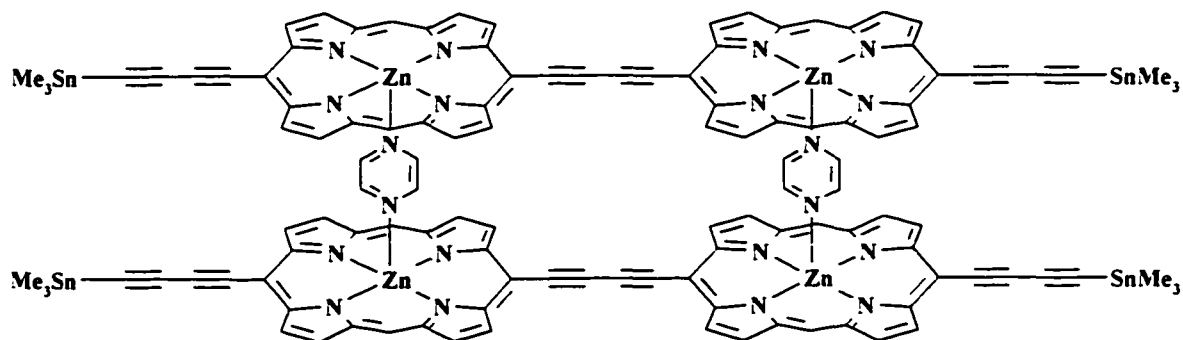
*Figure 1.5  Anderson's conjugated porphyrin ladder*

Ogura has used the term molecular ladders and bricks to describe the two-dimensional arrays formed based on cadmium(II) and pyridine based ligands.[17] When an aqueous solution of $Cd(NO_3)_2$ and an ethanol solution of ligand were combined an allowed to stand for three days, colourless crystals were formed in 63% yield. Subsequent X-ray crystallographic analysis showed the solid state structure to be analogous to a ladder. When the hydrogen atoms of the central aromatic unit on the ligand were replaced with fluorine a significantly different solid state structure was observed. In this case the resulting formation was described as a triply interpenetrated infinite brick structure.
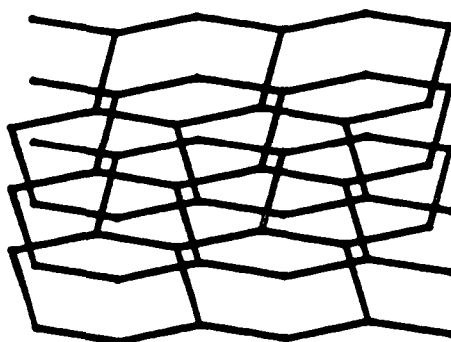


*Figure 1.6  Ogura's triply interpentrated brick structure.  Only the Cd(II) centres are shown: framework is shown as heavy connections*

## 1.4.3 Racks, Ladders and Grids

The construction of infinite arrays is a relatively simple task. A current trend is to produce discrete structures ultimately leading to the development of parts for molecular size machines. Racks ladders and grids represent some of the attempts to reproduce real world objects on the nanometre scale. These are discrete structures as depicted below. The circles represent a metal and the bars the supporting ligands.



Racks          Ladders                    Grids
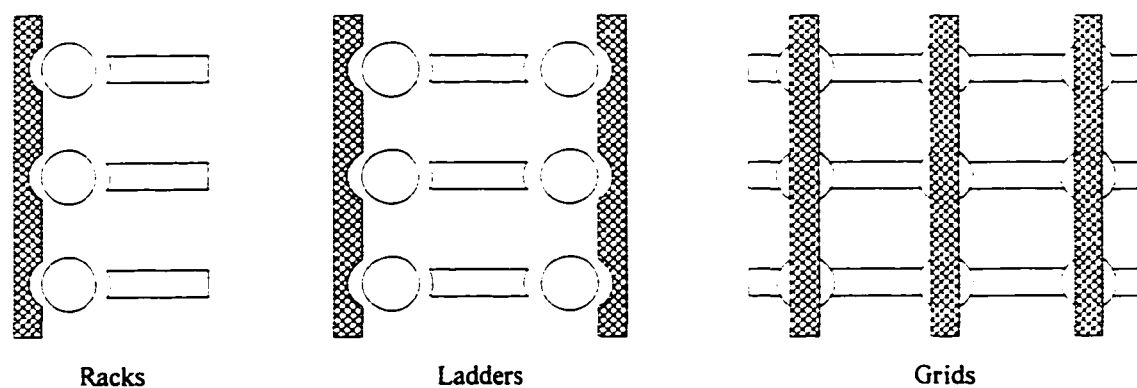
*Figure 1.7     Basic structure of racks, ladders and grids*

Lehn's group has designed di- and trimetallic racks using a ruthenium (II) complex on a poly-terpyridyl backbone to hang terpyridyl moieties. Interesting to note is that regardless of the stoichiometry of the reagents, the fully complexed rack was the primary product. Incomplete racks were recovered in only minute quantities.
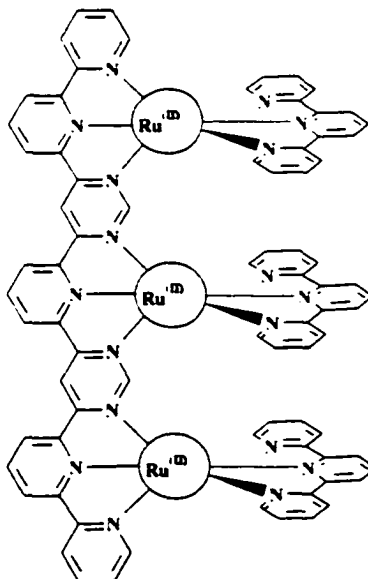
*Figure 1.8    Rigid rack of tris-terpyridine with Ru(II) and terpyridine*

Another interesting example also from Lehn's group, is a macrocyclic

1,10-phenanthroline derivative hung on a poly-bipyridyl backbone using tetrahedral

copper (I).[18] The macrocyclic structure was used to prevent two ligands from coordinating

to the same copper centre and thereby competing with the desired assemblage.
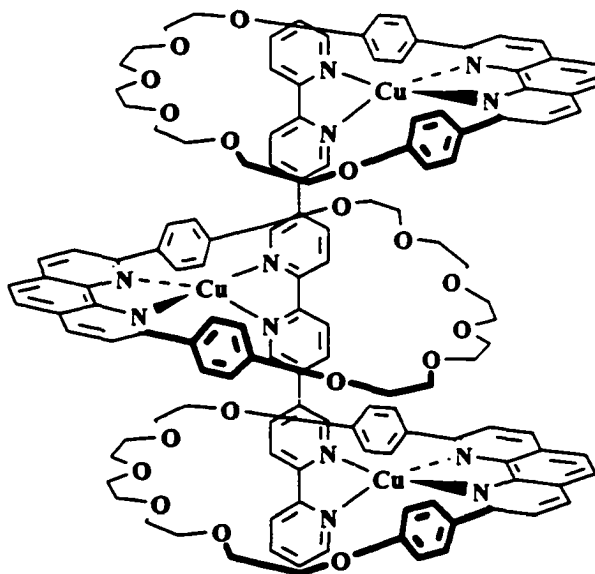


*Figure 1.9    Trimetallic copper (I) rigid rack*

A 2x2 grid has been constructed from four Cu(I) centres coordinated to the ligand 3,6-bis(2'pyridyl)pyridazine (dppn).[19] An X-ray structure as well as a FAB mass spectrum characterized the product. While the compound self-assembles and can be isolated in 85% yield, polymeric products can be obtained when greater than three fold excess of dppn per copper atom is used.
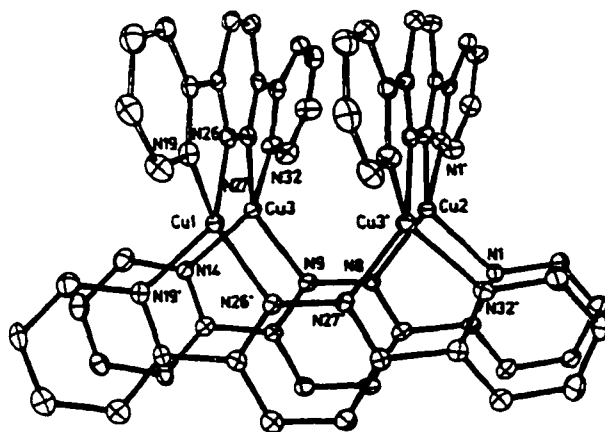


Figure 1.10  ORTEP representation of the crystal structure of a 2x2 Cu(I) grid[19]

The self-assembly and characterization of a 3x3 grid has been accomplished by Lehn's group. Using tetrahedral Ag(I) with the ligand, 6,6'-bis[2-(6-methylpyridyl)]-3,3'bipyridazine, resulted in the quantitative formation of the 3x3 grid.[20] The [109]Ag NMR spectrum show three resonances in the ratio 4:4:1 as expected for the corners, midpoints of the sides and the central silver ions respectively. This is an impressive example of the self-assembly process; a total of fifteen components, six ligands and nine metal ions spontaneously assemble to the desired superstructure.
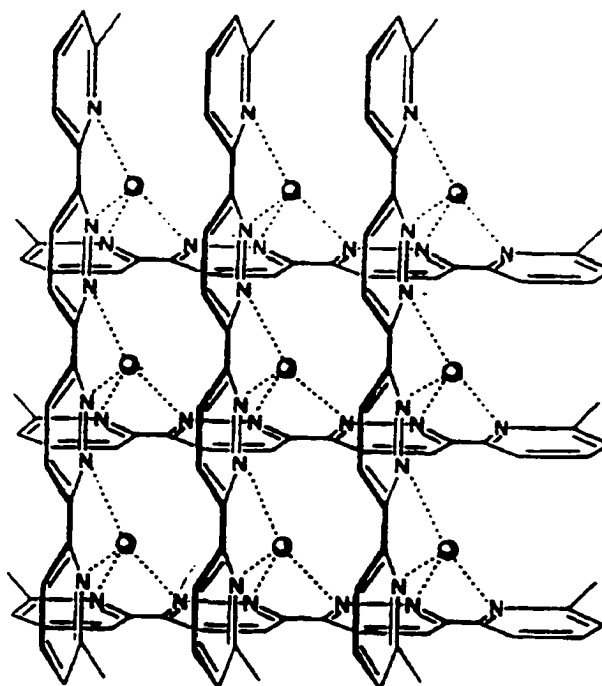
*Figure 1.11 Representation of the self-assembled 3x3 grid*

## 1.4.4 Helical Arrays

Inspired by the DNA double helix, the helical array has attracted a great deal of attention. Using segmental ligands as strands which intertwine about transition metals, several double and triple helical assemblies have been constructed.[21,22,23] All that is required is the incorporation of suitable donor atoms into the molecular threads. The stereochemical requirements of the transition metal ion directs the spatial orientation of the threads.

The general strategy for formation of a double helix is the use of a four coordinate metal typically tetrahedral, coordinated to bis-bidentate ligands.
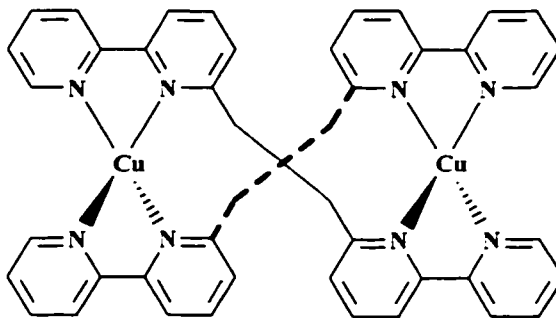
*Figure 1.12    Formation of a double-helical complex by interaction of a bis-bipyridyl ligand with tetrahedral Cu(I).*[24]

Claude Piguet has recently published a heterodinuclear triple helix complex.[25] The ligand incorporates two different sites for metal binding. Quantitative formation of the mixed metal Zn (II) and Eu(III) complex with three segmental ligands results at concentrations larger than $10^{-2}$ mol dm$^{-3}$ in acetonitrile.
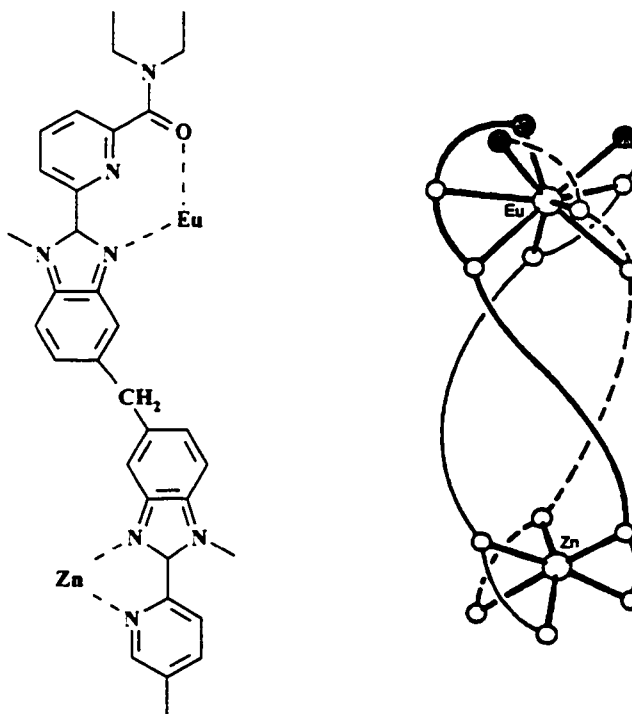


*Figure 1.13    Piguet's triple helix, heterodinuclear d-f complex*

## Dendrimers

Dendrimers or arborols are classified as branching or cascade molecules. The branching is controlled, resulting in discrete molecules as opposed to uncontrolled branching resulting in a polymer. Dendrimers are commonly prepared in a stepwise manner through the use of covalent bonds. At present there are few examples of *self-assembling* dendrimeric structures.[26,27] The dendrimeric structure described here uses $[Ru(2-3-dpp)_3]^{2+}$ as the starting point.



[Ru(2-3-dpp)₃]²⁺          [Ru(2,3-Medpp)₃Cl₂
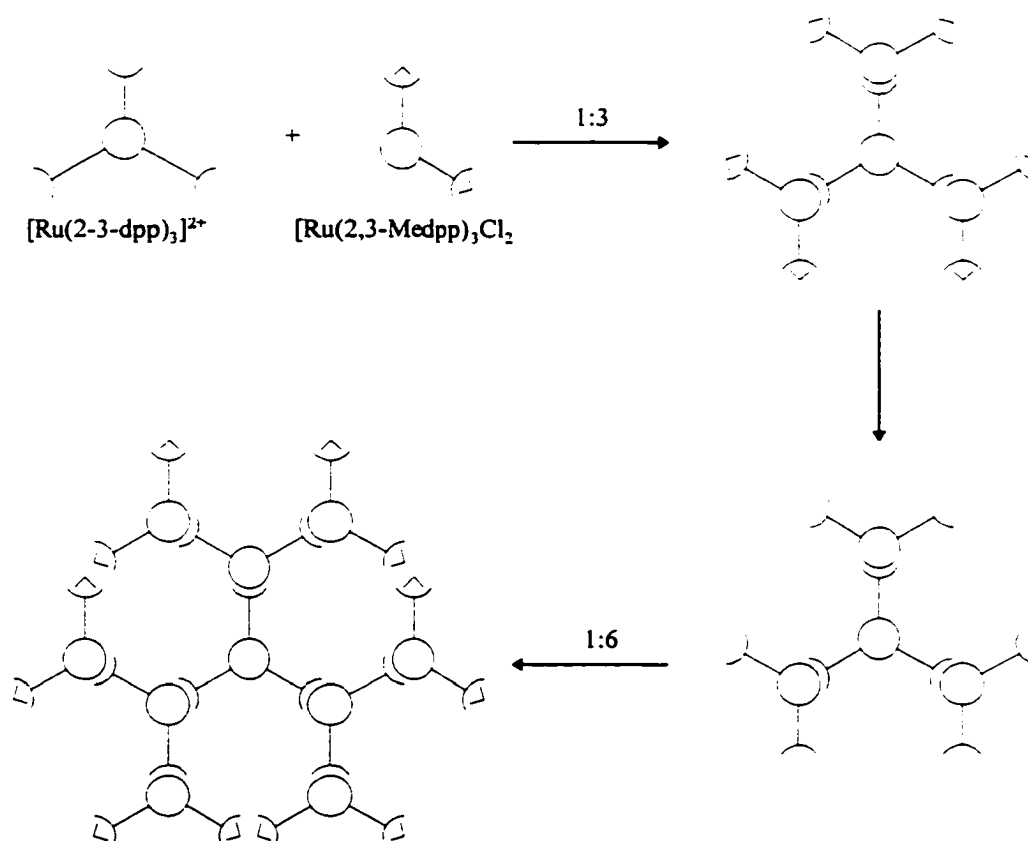
*Figure 1.14    Synthesis of a ruthenium (II) dendrimer*

This contains three separate sites for complexation of the building block $[Ru(2,3-Medpp)_3Cl_2]^{2+}$. Upon addition of the building block compound to the starting material, the first generation tetranuclear complex is formed. This species is blocked from

further ruthenium coordination due to the presence of the methylated ring nitrogen. Upon removal of the methyl groups. and addition of further building block complex. a second generation dendrimer if formed. Ultimately a third generation complex was produced with 22 metal ions having a molecular weight of 10890. The first and second generation dendrimers were characterized by NMR. IR. elemental analysis. UV-vis and luminescence spectroscopy. Electrochemical oxidation of the third generation complex yields a peak corresponding to 12 electrons (there are 12 equivalent subunits that lie on the periphery of the complex).

## Catenanes and Rotaxanes

Catenanes and rotaxanes are interlocked molecules. The catenanes are classified as two or more molecules linked together as links in a chain. Rotaxanes are analogous to a washer on a nut and bolt.

[2]Catenane        [2]Rotaxane
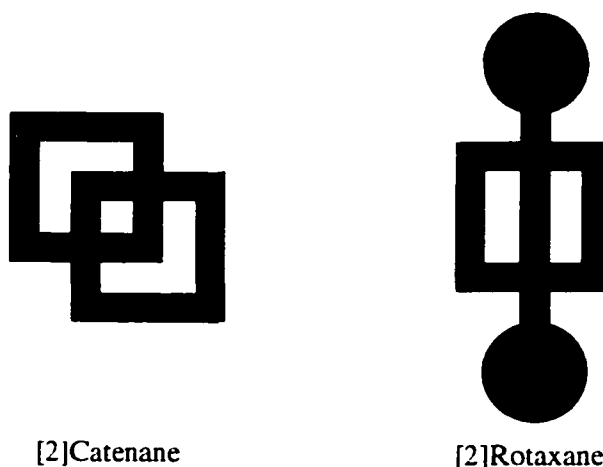
*Figure 1.15 Schematic representation of a [2]catenane and [2]rotaxane*

Most catenanes and rotaxanes have been synthesized utilizing templates along with self-assembly. In Sauvage's trefoil knot, two 1,10-phenanthroline based ligands are

brought into a favourable arrangement by coordination to tetrahedral Cu(I). When arranged, classical organic synthesis was used to connect the ends of the phenanthroline forming the trefoil knot.
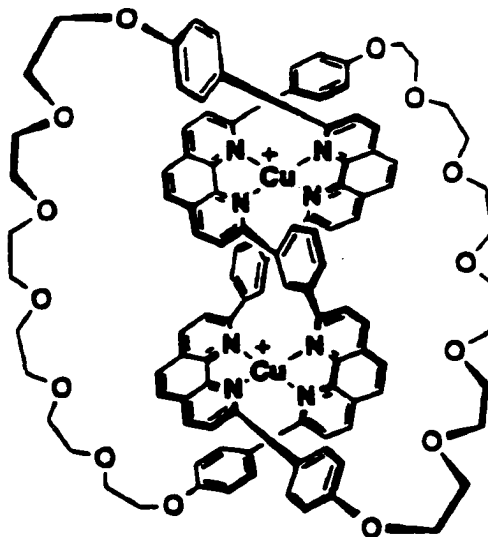


*Figure 1.16 Sauvage's trefoil knot synthesized in 30% yield via templating and self-assembly.*[28]

Fujita and Ogura have demonstrated a molecular lock in the context of unlocking a single molecular ring and locking two molecular rings together.[29] Exploiting the kinetic nature of the platinum(II)-pyridine coordination bond under ordinary conditions, there is no thermodynamic equilibrium with other structures. However in polar media at elevated temperature, the bond becomes reversible and a thermodynamic equilibrium between the molecular ring and its catenated dimer is established. In polar media, the equilibrium is strongly pushed towards the catenane by edge to face aromatic contact. Upon cooling, the catenane was isolated in 50% yield. The palladium analog exhibits catenation in equilibrium with other species under standard conditions.
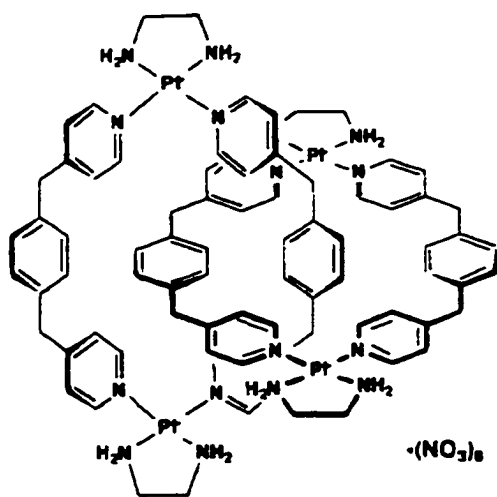
*Figure 1.17 A self-assembled [2]catenane, a molecular lock*

Rotaxanes have also been exploited utilizing metal-ions as templates. Sauvage has

an interesting rotaxane structure. Using a similar scheme to the synthesis of the trefoil

knot, a rotaxane stoppered with $C_{60}$ fullerene was constructed.
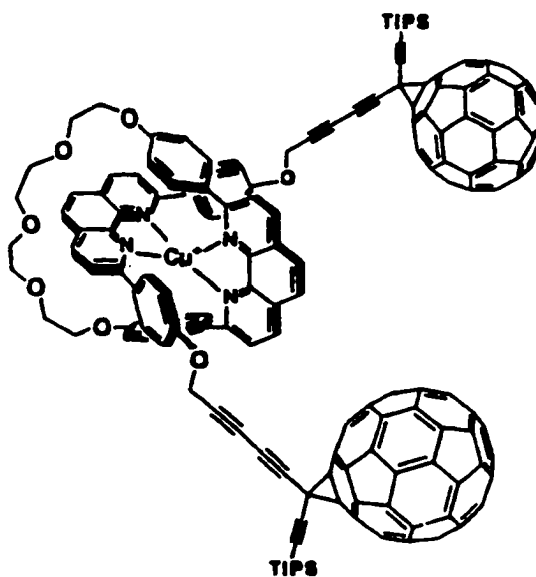


*Figure 1.18 Sauvage's $C_{60}$ stoppered pseudo-rotaxane*

The compound depicted below still retains the Cu(I) used in templating.[30] A true rotaxane was produced by the removal of the Cu(I). Treating with aqueous KCN removes the Cu(I) resulting in the formation of the rotaxane in 15% yield.

### 1.4.7 Cyclic Arrays

To make cyclic arrays, the individual subunits have the opportunity to assemble into either a cyclic or linear array. Since cyclic structures generally exhibit more order than their linear counterparts, their formation should be favored from an entropic point of view. Also, the formation of the cyclic structure should be favoured from an enthalphic point of view since there will be a greater number of noncovalent interactions per subunit, compared to that of a linear complex. Consider a hypothetical species that self-associates to form a cyclic trimercomplex through hydrogen bonds. There will be three subunits and three hydrogen bonds for an average 1.0 hydrogen bonds per monomer. However in the linear trimer, there are 2 bonds with 3 subunits, for an average 0.67 per monomer. As the number of bonds between subunits increase, for example 2 bonds between subunits, the enthalpic advantage increases, with an average 2 bonds in the cyclic version versus 1.33 for the linear trimer. Under these conditions, (neglecting entropic factors) one might predict that the cyclic species would be favoured. Nevertheless, the enthalpic advantage is diminished as the size of the aggregate increases. In a 20-mer composed of one hydrogen bond between monomers, the cyclic version averages 1.0 bonds per monomer, and the linear version 0.95 bonds per monomeric unit.

## 1.5 Scope of this Thesis

The goal of this work has been to synthesize and characterize a specific cyclic supramolecular complex, known as a molecular box. To form this structure, a toolbox of wall units and corner pieces was developed. These components are described in Chapter two. Background literature on known molecular boxes is presented in Chapter three, along with the synthesis and characterization of the supramolecular species prepared en route to the molecular box.

# Chapter Two

## Introduction

This chapter develops the components necessary for construction of molecular

clefts and molecular boxes. The goal was to develop suitable corner pieces and wall

units to synthesize a cleft and a box utilizing self-assembly. These corner pieces and wall

units must have the appropriate geometry and complementary binding sites for the

desired thermodynamic product to result.

Construction of a Cleft

Construction of a Molecular Box
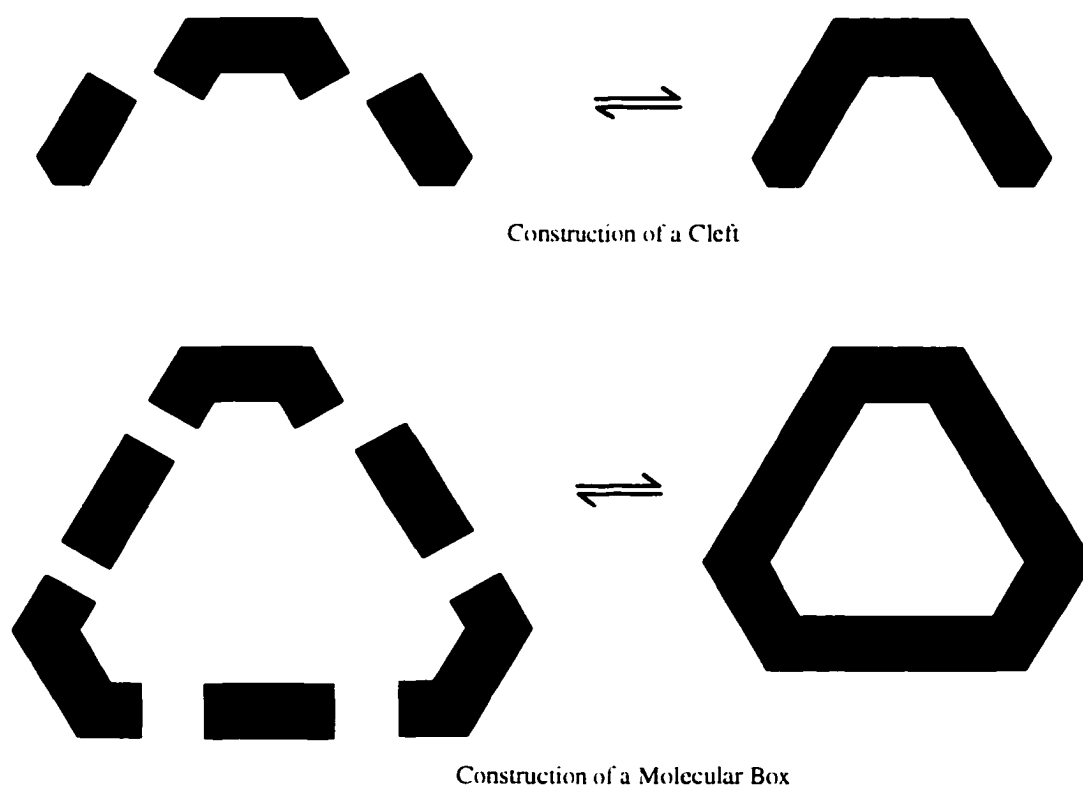
Figure 2.1 Schematic representations of the construction of a supramolecular cleft and box from appropriate corner and wall components.

22

Previous work in our laboratory demonstrated that the thioether ligand 1,2,4,5-

tetrakis(phenylthiomethyl)benzene could be metallated at both unsubstituted positions on

the central aromatic ring.[32]
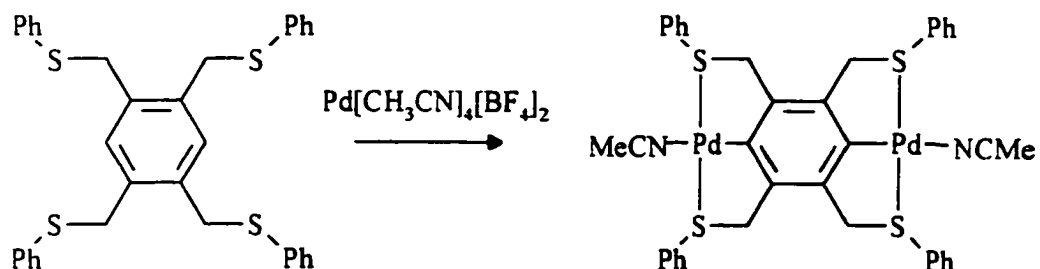


*Figure 2.2 Original synthesis of the dipalladated building block complex from
1,2,4,5-tetrakis(phenylthiomethyl)benzene*

The doubly palladated fragment was subsequently reacted with aromatic N-donors to form

linear organometallic coordination polymers.
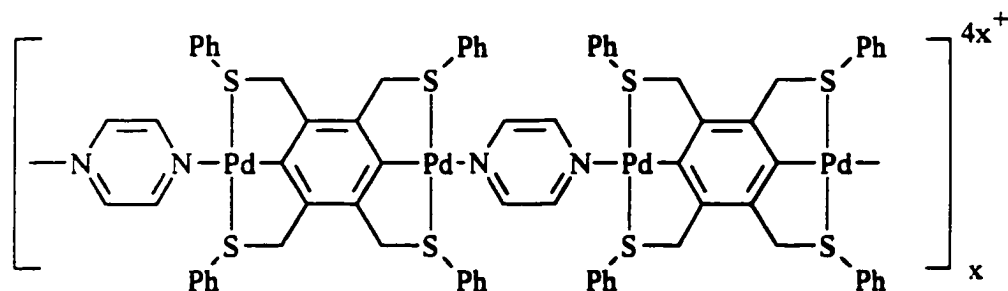


*Figure 2.3 Organometallic coordination polymers from building block complexes*

This chapter deals with this doubly palladated fragment and variations of it, as

components in the design and synthesis of discrete molecular assemblies. These molecules

have properties which make them excellent components in supramolecular assemblies.

Metallation of the basic ligand with a square planar metal creates a fragment with a linear

coordination geometry through two metal sites. Coordinated to corner pieces with suitable

geometry, these molecules make excellent wall sections for a supramolecular container.

To this end, several ligands were synthesized and subsequently metallated to determine their usefulness as walls in such a supramolecular assemblage. Although emphasis was placed on the design of the wall, suitable corner pieces were also examined.

### 2.1.1 The Metallation Reaction

In general, the reaction that results in a covalent σ-bond to a transition metal is termed a metallation reaction. A reaction where an intramolecular cyclization occurs between a transition metal and a ligand is referred to as *cyclometallation*. The result is the formation of a chelate ring and a metal-carbon σ-bond. More specifically, when the carbon atom is part of an aromatic ring, the reaction is an *orthometallation*. A typical cyclometallation occurs via C-H bond activation with the metal possessing a ligand which functions as a good leaving group. There are many examples of orthometallation involving palladium.[33,34,35] The single and double palladations presented in this thesis are all orthometallation reactions and proceed at room temperature within 24 hours. At reflux in acetonitrile the reaction generally complete within 4 hours.

## 2.2 Experimental

General Comments: Thiophenol, 4-butanethiol, 1-bromooctane, ammonium chloride, ammonium iodide, sodium acetate (anh.) and all deuterated solvents were purchased from Aldrich and used as received. $K_2PdCl_4$ was purchased from Strem Chemicals. α,α'-Dibromo-*m*-xylene ,tetrabromodurene, *m*-Xylene-α,α'-dithiol and 1,2,4,5 tetrakis(thiomethyl)benzene were prepared from literature preparations.[36,37,38] All reactions were conducted under an atmosphere of $N_2$ using standard Schlenk techniques and all

solvents were distilled and degassed prior to use. $^1$H, $^{13}$C$\{^1$H$\}$, spectra were recorded at

300.1 and 75.4 Mhz respectively, on a Brüker AC300 spectrometer locked to the

deuterated solvent. $^{19}$F$\{^1$H$\}$ NMR spectra were recorded unlocked at 188.3 Mhz on a

Brüker AC200 spectrometer with the TFA as a standard.

## 2.2.1 Preparation of 1,3-Bis(phenylthiomethyl)benzene (1) (PhS₂)

Thiophenol (4.170g, 37.9 mmol) was added to anhydrous ethanol (100 mL), in

which Na metal (0.870 g, 37.9 mmol) had been dissolved. This mixture was allowed to

stir for 4 h and the solution was observed to take on a pale yellow colour. To this solution

was added α,α'-dibromo-m-xylene (5.000g, 19.0 mmol) and allowed to stir for an

additional 4 h. The ethanol was removed on the rotary evaporator leaving a white solid.

This residue was extracted with CH₂Cl₂ (50 mL) and the white NaBr filtered off. The

CH₂Cl₂ was then removed on the rotary evaporator and the product recrystallized from

ethanol. Yield: 5.803 g (95%). $^1$H NMR (CDCl₃): δ (ppm) 7.1-7.3 (m , 14H, aromatic),

4.06 (s, 4H, benzylic). $^{13}$C $\{^1$H$\}$ NMR (CDCl₃): δ (ppm) 137.87, 130.10, 129.43, 128.94,

128.72, 127.78, 126.52 (aromatic), 39.10 (benzylic).

## 2.2.2 Preparation of [Pd(PhS₂)(CH₃CN)][BF₄] (2)

[Pd(CH₃CN)₄][BF₄]₂ (0.425g, 0.957 mmol) and PhS₂ were combined in CH₃CN

(50 mL) and stirred for 8 h. The solution changed from an orange colour to a bright

yellow colour indicative of the complexed material. Diethyl ether was added (40 mL) and

the precipitate collected by filtration. Yield: 0.287g (54%) $^1$H NMR (d3-acteonitrile) : δ

(ppm) 7.96-7.92 (m , 4H, aromatic), 7.57 (m, 6H, aromatic), 7.13 (m, 3H, aromatic),

4.91(br s, 4H, benzylic).

### 2.2.3 Preparation of [Pd(PhS₂)Cl] (3)

To a solution of [Pd(PhS₂)(CH₃CN)][BF₄] (0.322 g, 0.569 mmol) in acetonitrile (15 mL) was added NH₄Cl (30.4 mg, 0.569 mmol). The solution was allowed to stir for 24 h after which the product had precipitated and was collect by vacuum filtration. Yield: 0.266 g, (99%). ¹H NMR (CD₂Cl₂): δ (ppm) 7.86-7.83 (m , 4H, aromatic), 7.43-7.41 (m, 6H, aromatic), 7.01 (m, 3H, aromatic), 4.64(br s, 4H, benzylic).

Alternatively this compound could be made in a single step from a solution of PhS₂ (0.493 g, 1.53 mmol) in ethanol (50 mL) by adding K₂PdCl₄ (0.498 g, (1.53 mmol), and NaOAc (0.125g, 1.53 mmol) and refluxing. After 48 h, the dark green solution was stripped down in vacuo and chloroform (50 mL) added. This was stirred under medium heat with decolourizing charcoal for 1 h then filtered through celite resulting in a bright yellow filtrate. Hexane (40 mL) was added and the product collected by vacuum filtration. Yield: 0.553 g, (78%.)

### 2.2.4 Preparation of 1,3-Bis(n-butylthiomethyl)benzene (4) (BuS₂)

n-Butanethiol (3.417g, 37.9 mmol) was added to anhydrous ethanol (100 mL), in which Na metal (0.870 g, 37.9 mmol) had been dissolved. This mixture was allowed to stir for 4 h and the solution was observed to take on a pale yellow colour. To this solution was added α,α'-dibromo-m-xylene (5.000g, 19.0 mmol) and allowed to stir for an additional 4 h. The ethanol was removed on the rotary evaporator leaving a white solid and light orange liquid. This residue was extracted with CH₂Cl₂ (50 mL) and H₂O (50 mL) and the CH₂Cl₂ separated and dried over MgSO₄. The MgSO₄ was then filtered off and the CH₂Cl₂ removed on the rotary evaporator. Yield: 5.084 g (95%). ¹H NMR

(CDCl$_3$): δ (ppm) 7.24-7.14 (m . 4H, aromatic), 3.66 (s, 4H, benzylic), 2.38(t, 4H, S-CH$_2$), 1.52(quin, 4H, S-CH$_2$-CH$_2$), 1.33(sextet, 4H, S- CH$_2$- CH$_2$- CH$_2$), 0.86(t, 6H, CH$_2$-CH$_3$). $^{13}$C {$^1$H} NMR (CDCl$_3$): δ (ppm) 138.97, 129.39, 128.62, 127.50 (aromatic), 36.28 (benzylic), 31.44(S-CH$_2$), 31.16(S-CH$_2$-CH$_2$), 22.09(S- CH$_2$- CH$_2$- CH$_2$), 13.81(CH$_2$-CH$_3$).

## 2.2.5 Preparation of [Pd(BuS$_2$)(CH$_3$CN)][BF$_4$] (5)

[Pd(CH$_3$CN)$_4$][BF$_4$]$_2$ (0.513g, 1.15 mmol) and (BuS$_2$) (0.326 g, 1.15 mmol) were combined in CH$_3$CN (50 mL) and stirred for 8 h. The solution changed from an orange colour to a bright yellow colour indicative of the complexed material. Diethyl ether was added (40 mL) and the precipitate collected by filtration. Yield: 0.344 g (58%) $^1$H NMR (CDCl$_3$) : δ (ppm) 7.09 (m, 3H, aromatic), 4.13 (br s, 4H, benzylic), 3.25 (t, 4H, S-CH$_2$), 2.26 (s, 3H, CH$_3$CN), 1.77 (quin, 4H, S-CH$_2$-CH$_2$), 1.46 (sextet, 4H, S- CH$_2$- CH$_2$- CH$_2$), 0.90 (t, 6H, CH$_2$-CH$_3$). $^{13}$C {$^1$H} NMR (CDCl$_3$): δ (ppm) 150.36, 126.00, 123.38 (aromatic), 44.33 (S-CH$_2$) 38.81 (benzylic), 31.44 (S-CH$_2$-CH$_2$), 21.80(S- CH$_2$- CH$_2$-CH$_3$), 13.62 (CH$_2$-CH$_3$), 2.41 (CH$_3$CN).

## 2.2.6 Preparation of [Pd(BuS$_2$)Cl] (6)

To a solution of [Pd(BuS$_2$)(CH$_3$CN)][BF$_4$] (0.322 g, 0.569 mmol) in acetonitrile (15 mL) was added NH$_4$Cl (30.4 mg, 0.569 mmol). The solution was allowed to stir for 24 h after which the product had precipitated and was collect by vacuum filtration. Yield: 0.266 g, (99%). $^1$H NMR (CDCl$_3$): δ (ppm) 6.94 (m , 3H, aromatic), 4.17 (br s, 4H, benzylic), 3.15 (t, 4H, S-CH$_2$), 1.85 (quin, 4H, S-CH$_2$-CH$_2$), 1.47 (sextet, 4H, S- CH$_2$-CH$_2$- CH$_2$), 0.91 (t, 6H, CH$_2$-CH$_3$).

Alternatively this compound could be made in a single step from a solution of

$BuS_2$ (0.500 g, 1.77 mmol) in ethanol (50 mL) by adding $K_2PdCl_4$ (0.578 g, (1.77 mmol),

and NaOAc (0.145g, 1.77 mmol) and refluxing. After 48 h, the dark green solution was

stripped down in vacuo and chloroform (50 mL) added. This was stirred under medium

heat with decolourizing charcoal for 1 h then filtered through celite resulting in a bright

yellow filtrate. Hexane (40 mL) was added and the product collected by vacuum

filtration. Yield: 0.554 g, (74%.)

### 2.2.7 Preparation of 1,2,4,5 Tetrakis(phenylthiomethyl)benzene (7) (PhS₄)

This compound has been previously prepared by George Shimizu. A slight

modification of the preparation from his Ph.D. thesis follows for completeness. After

dissolving Na metal (0.941 g, 40.9 mmol) in a solution of anhydrous ethanol (150 mL),

thiophenol (4.292 g, 40.0 mmol) was added and stirred. During 2 hours of stirring the

solution took on a pale yellow colour. Tetrabromodurene (4.501 g, 10.0 mmol) was

added to the solution and the mixture brought to reflux for 4 hours. The ethanol was

removed on the rotary evaporator and the white precipitate extracted with $CH_2Cl_2$

(40 mL). The white NaBr was then filtered off and the $CH_2Cl_2$ removed on the rotary

evaporator. The white product was recrystallized from ethanol to give air-stable

colourless crystalline plates. Yield: 5.385 g (95 %). $^1H$ NMR ($CDCl_3$): δ (ppm) 7.25-

7.18 (m, 20H, aromatic), 6.99 (s, 2H, durene), 4.08 (s, 8H, benzylic). $^{13}C$ {$^1H$} NMR

($CDCl_3$): δ (ppm) 134.90, 132.77, 130.54, 128.91, 126.72 (aromatic), 36.34 (benzylic).

## 2.2.8 Preparation of [Pd₂(PhS₄)(CH₃CN)₂][BF₄]₂ (8)

An acetonitrile solution (25 mL) containing [Pd(CH₃CN)₄][BF₄]₂ (0.548 g, 1.234

mmol) was added to an acetonitrile solution of 1,2,4,5-tetrakis(phenylthiomethyl)benzene

(0.300 g, 0.617 mmol). The solution was allowed to stir at room temperature for 4 h.

Over this time, the solution was observed to change from an orange colour to a bright

yellow. Diethyl ether was added (25 mL) and the solution refrigerated. The complex

crystallized from solution as yellow blocks. Yield: 0.618 g (97%). ¹H NMR (CDCl₃):

δ (ppm) 7.80 (m, 8H, aromatic), 7.51 (m, 12H, aromatic), 4.60 (br s, 8H, benzylic), 1.94

(s, 6H, CH₃CN).

## 2.2.9 Preparation of [Pd₂(PhS₄)Cl₂] (9)

To a solution of [Pd₂(PhS₄)(CH₃CN)₂][BF₄]₂ (0.532 g, 0.515 mmol) in

acetonitrile (25 mL) was added ammonium chloride (0.055 g, 1.03 mmol). This solution

was allowed to stir at room temperature for 24 h. The resulting precipitate was filtered

off and used as is. Yield (0.433 g) (99%) ¹H NMR (CDCl₃) δ (ppm) 7.79 (dd, 8H,

aromatic), 7.37 (m, 12H, aromatic), 4.43 (br s, 8H, benzylic).

## 2.2.10 Preparation of 1,2,4,5-Tetrakis(n-butylthiomethyl)benzene (10) (BuS₄)

n-Butanethiol (2.400g, 26.6 mmol) was added to a solution of ethanol (100 mL) in

which was previously dissolved Na metal (0.614g, 26.6 mmol) and allowed to stir for 4 h.

To this colourless solution was then added tetrabromodurene (3.000g, 6.7 mmol) and the

solution allowed to stir for an additional 4 h. The ethanol was removed on the rotary

evaporator leaving a white solid. This residue was extracted with CH₂Cl₂ (50 mL) and the

white NaBr filtered off. The CH₂Cl₂ was then removed on the rotary evaporator and the

product recrystallized from ethanol. Yield: 2.95 g, (91%). $^1$H NMR (CDCl$_3$) δ (ppm) 7.10 (s, 2H, durene), 3.81 (s, 8H, benzylic), 2.44 (t, 8H, S-CH$_2$), 1.54 (quintet, 8H, S-CH$_2$-CH$_2$), 1.37 (sextet, 8H, CH$_2$-CH$_3$), 0.87 (t, 12H, CH$_2$-CH$_3$). $^{13}$C {$^1$H} NMR (CDCl$_3$): δ (ppm) 135.44, 132.76 (aromatic), 33.33 (S-CH$_2$), 31.89, 31.63, 22.13, 13.81 (n-butyl).

### 2.2.11 Preparation of [Pd$_2$(BuS$_4$)(CH$_3$CN)$_2$][BF$_4$]$_2$ (11)

To a solution of BuS$_4$ (0.139 g, 0.286 mmol) in acetonitrile (50 mL) was added [Pd(CH$_3$CN)$_4$][BF$_4$]$_2$ (0.254 g, 0.571 mmol). The solution immediately turned dark orange. After refluxing the solution for 12 h, the solution became a pale yellow. The acetonitrile was then concentrated down to 25 mL in vacuo and diethyl ether added until precipitation occurs (10 mL). After placing in the freezer (0°C) for 2 h, the off white precipitate is collected by vacuum filtration. Yield: 0.245 g, (90%). $^1$H NMR (CD$_3$CN) δ (ppm) 4.27 (br s, 8H, benzylic), 3.19 (t, 8H, S-CH$_2$), 1.93 (quintet, 8H, S-CH$_2$-CH$_2$), 1.37 (sextet, 8H, CH$_2$-CH$_3$), 1.06 (t, 12H, CH$_2$-CH$_3$).

### 2.2.12 Preparation of [Pd$_2$(BuS$_4$)I$_2$] (12)

To a solution of [Pd$_2$(BuS$_4$)(CH$_3$CN)$_2$][BF$_4$]$_2$ (0.542 g, 0.568 mmol), was added ammonium iodide (0.165 g, 1.14 mmol). This solution was allowed to stir at room temperature for 24 h. The resulting precipitate was filtered off and used as is. Yield (0.432 g) (99%) $^1$H NMR (CDCl$_3$) δ (ppm) 4.37 (br s, 8H, benzylic), 3.15 (t, 8H, S-CH$_2$), 1.87 (quintet, 8H, S-CH$_2$-CH$_2$), 1.39 (sextet, 8H, CH$_2$-CH$_3$), 1.12 (t, 12H, CH$_2$-CH$_3$).

### 2.2.13 Preparation of 1,3-Bis(n-octylthiomethyl)benzene (13) (OctS₂)

m-xylene-α,α'-dithiol (2.042 g, 9.5 mmol) was added to anhydrous ethanol (100 mL), in which Na metal (0.437 g, 19 mmol) had been dissolved. This mixture was allowed to stir for 4 h and the solution was observed to take on a pale yellow colour. To this solution was added 1-bromooctane (3.670 g, 19.0 mmol) and allowed to stir for an additional 4 h. The ethanol was removed on the rotary evaporator leaving a pale yellow oil and white solid. To this residue was added $CH_2Cl_2$ (25 mL) and the white NaBr filtered off. The $CH_2Cl_2$ was then allowed to evaporate resulting in a pale yellow oil. Yield: 3.412 g (91%). $^1H$ NMR ($CDCl_3$): δ (ppm) 7.20 (m, 4H, aromatic), 3.76 (s, 4H, benzylic), 2.39 (t, 4H, S-CH₂), 1.53 (quin, 4H, S-CH₂-CH₂), 1.20 (m, 20H), 0.84 (t, 6H, CH₃).

### 2.2.14 Preparation of [Pd(OctS₂)(CH₃CN)][BF₄] (14)

To a solution of OctS₂ (0.283 g, 0.717 mmol) in acetonitrile (50 mL) was added [Pd(CH₃CN)₄][BF₄]₂ (0.318 g, 0.717 mmol). The solution immediately turned dark orange. After refluxing the solution for 12 h, the solution became a pale yellow. The acetonitrile was then concentrated down to 25 mL in vacuo and diethyl ether added until precipitation occurs (10 mL). After placing in the freezer (0°C) for 2 h, the off white precipitate is collected by vacuum filtration. Yield: 0.212 g, (47%). $^1H$ NMR ($CD_3CN$): δ (ppm) 7.14 (m, 3H, aromatic), 4.24 (s, 4H, benzylic), 3.26 (t, 4H, S-CH₂), 2.05 (quin, 4H, S-CH₂-CH₂), 1.57 (m, 20H), 0.96 (t, 6H, CH₃).

### 2.2.15 Preparation of [Pd(OctS₂)Cl] (15)

To a solution of [Pd(OctS₂)(CH₃CN)][BF₄] (0.245 g, 0.390 mmol) in acetonitrile

(25 mL) was added ammonium chloride (0.021 g, 0.390 mmol). This solution was

allowed to stir at room temperature for 24 h. The resulting precipitate was filtered off and

used as is. Yield (0.206 g) (99%) $^1$H NMR (CDCl₃): δ (ppm) 7.02 (m , 3H, aromatic),

4.07 (s, 4H, benzylic), 3.14 (t, 4H, S-CH2), 2.03 (quin, 4H, S-CH2-CH2), 1.55 (m, 20H),

0.94 (t, 6H, CH3).

### 2.2.16 Preparation of 1,2,4,5-Tetrakis(n-octylthiomethyl)benzene (16) (OctS₄)

1,2,4,5 Tetrakis(thiomethyl)benzene (0.542 g, 2.07 mmol) was added to anhydrous

ethanol (100 mL), in which Na metal (0.190 g, 8.26 mmol) had been dissolved. This

mixture was allowed to stir for 4 h and the solution was observed to take on a pale yellow

colour. To this solution was added 1-Bromooctane (1.595 g, 8.26 mmol) and allowed to

stir for an additional 4 h. The ethanol was removed on the rotary evaporator leaving a

pale yellow oil and white solid. To this residue was added CH₂Cl₂ (25 mL) and the white

NaBr filtered off. The CH₂Cl₂ was then allowed to evaporate resulting in a pale yellow

oil. Yield: 1.369 g (93%). $^1$H NMR (CDCl₃): δ (ppm) 7.09 (s , 2H, aromatic), 3.81 (s,

8H, benzylic), 2.44 (t, 8H, S-CH₂), 1.55 (quin, 8H, S-CH₂-CH₂), 1.24 (m, 40H), 0.86 (t,

CH₃). $^{13}$C {$^1$H} NMR (CDCl₃): δ (ppm) 135.45 (t aromatic), 132.75 (q, aromatic), 33.35,

32.25, 31.92, 29.56, 29.34, 29.08, 24.71, 22.77 (benzylic and CH₂), 14.20 (CH₃) .

### 2.2.17 Preparation of [Pd₂(OctS₄)(CH₃CN)₂][BF₄]₂ (17)

To a solution of OctS₄ (0.242 g, 0.340 mmol) in acetonitrile (50 mL) was added

[Pd(CH₃CN)₄][BF₄]₂ (0.302 g, 0.680 mmol). The solution immediately turned dark

orange. After refluxing the solution for 12 h, the solution became a pale yellow. The acetonitrile was then concentrated down to 25 mL in vacuo and diethyl ether added until precipitation occurs (10 mL). After placing in the freezer (0°C) for 2 h, the off white precipitate is collected by vacuum filtration. Yield: 0.368 g, (92%). $^1$H NMR (CD$_3$CN) δ (ppm) 4.34 (br s, 8H, benzylic), 3.23 (t, 8H, S-CH$_2$), 1.90 (quintet, 8H, S-CH$_2$-CH$_2$), 1.34 (sextet, 8H, CH$_2$-CH$_3$), 1.02 (t, 12H, CH$_2$-CH$_3$).

### 2.2.18 Preparation of 1,2,4,5-Tetrakis(pentafluorophenylthiomethyl)benzene (18) (F$_5$PhS$_4$)

Pentafluorothiophenol (.210 g, 9.53 mmol) was added to a solution of ethanol in which Na metal (.219 g, 9.53 mmol) had been previously dissolved. After stirring for 4 hours the solution was a pale yellow. To this solution was added tetrabromodurene (1.072 g, 2.38 mmol) and allowed to stir for an additional 4 h. The ethanol was removed on the rotary evaporator leaving an off white solid. To this residue was added CH$_2$Cl$_2$ (25 mL) and the white NaBr filtered off. The CH$_2$Cl$_2$ was then evaporated and the product recrystallized from ethanol resulting in a white solid. Yield: 1.610 g (73%). $^1$H NMR (CDCl$_3$): δ (ppm) 6.81 (s, 2H, aromatic), 4.15 (s, 8H, benzylic). $^{19}$F NMR (ref. TFA) -55 (m, 8F), -73 (t, 4F), -83 (m, 8F).

### 2.2.19 Preparation of [Pd$_2$(F$_5$PhS$_4$)(CH$_3$CN)$_2$][BF$_4$]$_2$ (19)

To a solution of F$_5$PhS$_4$ (0.050 g, 0.054 mmol) in acetonitrile (50 mL) was added [Pd(CH$_3$CN)$_4$][BF$_4$]$_2$ (0.048 g, 0.108 mmol). The solution immediately turned light yellow. After refluxing the solution for 24 h, the solution remained light yellow. The acetonitrile was then concentrated down to 25 mL in vacuo and diethyl ether added until

precipitation occurs (10 mL). After placing in the freezer (0°C) for 2 h, the light yellow

precipitate is collected by vacuum filtration. Yield: 0.012 g (18%). $^1$H NMR (CD$_3$CN). δ

(ppm) 4.48 (br s, benzylic).

### 2.2.20 Preparation of 1,2,4,5-Tetrakis(4-methoxyphenylthiomethyl)benzene (20) (MeOPhS$_4$)

4-methoxythiophenol (1.012 g, 7.22 mmol) was added to a solution of ethanol in

which Na metal (0.166 g, 7.22 mmol) had been previously dissolved. After stirring for 4

hours the solution was a pale yellow. To this solution was added tetrabromodurene (0.812

g, 1.80 mmol) and allowed to stir for an additional 4 h. The ethanol was removed on the

rotary evaporator leaving an off white solid. To this residue was added CH$_2$Cl$_2$ (25 mL)

and the white NaBr filtered off. The CH$_2$Cl$_2$ was then evaporated and the product

recrystallized from ethanol resulting in a white solid. Yield: 1.050 g (93%). $^1$H NMR

(CDCl$_3$): δ (ppm) 7.17 (d, 8H, aromatic), 6.76 (d, 8H, aromatic), 6.70 (s, 2H, aromatic),

3.89 (s, 8H, benzylic), 3.77 (s, 12H, CH$_3$O). $^{13}$C {$^1$H} NMR (CDCl$_3$): δ (ppm) 159.52

(COCH$_3$), 135.15 , 134.54, 132.93, 126.02, 114.56, 55.42 (OCH$_3$), 38.25 (benzylic).

### 2.2.21 Preparation of [Pd$_2$(MeOPhS$_4$)(CH$_3$CN)$_2$][BF$_4$]$_2$ (21)

To a solution of MeOPhS$_4$ (0.202 g, 0.322 mmol) in acetonitrile (50 mL) was

added [Pd(CH$_3$CN)$_4$][BF$_4$]$_2$ (0.286 g, 0.644 mmol). The solution immediately turned

blood red. After refluxing the solution for 24 h, the solution maintained the blood red

colour. The acetonitrile was then removed in vacuo then dissolved in acetone (20 mL).

The solution was filtered with vacuum to remove the NaBr. The acetone solution was

then allowed to evaporate and then recrystallized repeatedly from acetone until a light

orange solid was obtained. Yield: 0.183 g, (52%). $^1$H NMR (d6-acetone) δ (ppm) 7.86

(d, 8H aromatic), 7.09 (d, 8H, aromatic), 4.82 (br s, 8H, benzylic), 3.87 (s, 12H, OCH$_3$)

### 2.2.22 Preparation of [Pd$_2$(MeOPhS$_4$)(CH$_3$CN)$_2$][SO$_3$CF$_3$]$_2$ (22)

[Pd(CH$_3$CN)$_4$][SO$_3$CF$_3$]$_2$ was prepared from PdCl$_2$ and AgSO$_3$CF$_3$.

[Pd(CH$_3$CN)$_4$][SO$_3$CF$_3$]$_2$(0.247 g, 0.434 mmol) was added to a solution of MeOPhS$_4$

(0.136 g, 0.217 mmol) in acetonitrile (50 mL). The solution turned orange and after

refluxing for 24 h, the solution was a pale yellow colour. The acetonitrile was then

concentrated to 25 mL in vacuo and diethyl ether added until precipitation started to

occur. After placing in the freezer (0°C) for 4 h, the yellowish orange precipitate is

collected by vacuum filtration. Yield: 0.233 g, (88%).$^1$H NMR (see compound (21)

above)

### 2.2.23 Preparation of Quino[5,6-b]1,7-phenanthroline (23)

This preparation is based on a preparation of quinoline from aniline.[39] In a 100 mL

round bottom flask was added FeSO$_4$ (0.750 g, 4.94 mmol), glycerol (12.701 g, 137.9

mmol), acriflavin (4.81 g, 23.0 mmol), nitrobenzene (1.415 g, 11.5 mmol) to 20 mL of

sulphuric acid. The solution was brought to reflux for 12 hours then cooled to room

temperature. Concentrated NaOH solution was added until the solution was slightly basic.

The black tarry substance was extracted with hot ethanol several times. During cooling to

room temperature a white precipitate formed in the ethanol solution. This product was

clean and used as is. Yield: 1.552 g, (24%). $^1$H NMR (d5-pyridine) δ (ppm) 9.92 (d, 2H

aromatic), 9.22 (dd, 2H, aromatic), 8.72 (s, 1H, aromatic), 8.25 (d, 2H, aromatic) 8.10 (d,

2H aromatic), 7.74 (dd, 2H, aromatic). $^{13}C$ {$^{1}H$} NMR (d5-pyridine): δ (ppm) 152.94, 151.77, 146.57, 134.08, 130.74, 130.57, 128.25, 126.48, 124,92, 123.46.

### 2.2.24 Preparation of [Pd$_2$(PhS$_4$)(1,10 Phen)$_2$][BF$_4$]$_2$ (24)

Complex [Pd$_2$(PhS$_4$)(CH$_3$CN)$_2$][BF$_4$]$_2$ (0.052 g, 0.050 mmol) was dissolved in CH$_3$CN (15 mL). 1,10-Phenanthroline (0.0182 g, 0.100 mmol) was dissolved in CH$_3$CN (10 mL) and syringed into the stirred solution of [Pd$_2$(PhS$_4$)(CH$_3$CN)$_2$][BF$_4$]$_2$. A much more intense yellow colour was observed upon addition of the phenanthroline. Slow evaporation of this solution resulted in t yellow crystals of this complex. Yield 0.064 g, (98%). $^{1}H$ NMR (d6-acetone) δ (ppm) 9.18 (d, 4H aromatic 1,10-phen), 8.64 (d, 4H, aromatic 1,10-phen), 8.04 (s, 4H, aromatic 1,10-phen), 7.92 (dd, 4H, aromatic 1,10-phen) 7.31 (d, 8H aromatic), 7.16 (t, 4H, aromatic), 7.05 (t, 8H, aromatic), 5.09 (s, 8H, benzylic).

### 2.2.25 Preparation of [Pd$_2$(PhS$_4$)(Quinoline)$_2$][BF$_4$]$_2$ (25)

Complex [Pd$_2$(PhS$_4$)(CH$_3$CN)$_2$][BF$_4$]$_2$ (0.058 g, 0.056 mmol) was dissolved in CH$_3$CN (15 mL). Quinoline (0.014 g, 0.112 mmol) was dissolved in CH$_2$Cl$_2$ (10 mL) and syringed into the stirred solution of [Pd$_2$(PhS$_4$)(CH$_3$CN)$_2$][BF$_4$]$_2$. A intense yellow colour was observed upon addition of the quinoline. Slow evaporation of this solution resulted in yellow crystals of this complex. Yield 0.066 g, (97%). $^{1}H$ NMR (CD$_2$Cl$_2$) δ (ppm) 8.24 (d, 2H quinoline), 7.83 (m, 4H, quinoline), 7.68 (m, 8H, aromatic), 7.50 (m, 8H, aromatic) 7.32 (m, 12H aromatic), 4.85 (br s, 8H, benzylic).

## 2.3  General Comments about X-ray Structure Determinations

All diffraction experiments were carried out on a Rigaku AFC6s four circle diffractometer with graphite-monochromatizied MoKα radiation. The orientation matrices and unit cell parameters were obtained from 25 centred reflections ($15°<2\theta<35°$). Standard reflections were measure every 150 reflections and a linear correction applied for significant changes over the course of a data collection. Data was collected in four shells ($2\theta<30,40,45,50°$) using the ω-2θ technique. Weak reflections ($I<10.0\sigma(I)$) were rescanned a maximum four times and the counts averaged. The data was processed using the TeXsan software package on an SGI Challenge XL on a remote X-terminal. Refinements were carried out by using full-matrix least-square techniques on F by minimizing the function $\Sigma w(|F_o|-|F_c|)^2$ where $w=1/\sigma^2(F_o)$ and $F_o$ and $F_c$ are the observed and calculated structure factors. Absorption corrections were applied from azimuthal scans. All data were corrected for Lorentz and polarization effects.

## 2.4  X-ray Structure Determinations

### 2.4.1  Structure Determination of [Pd(PhS₂)(CH₃CN)][BF₄] (2)

Pale yellow crystals were grown from slow evaporation of methylene chloride solution. Cell parameters were determined from a least squares refinement of 24 reflections and the space group was uniquely determined from the systematic absences to be $P2_1/n$. A total of 3265 reflections were collected with 1512 being unique with $F_o^2>3\sigma(F_o^2)$ and subsequently used in the refinement. A trial structure was obtained from the SHELX-86 direct methods from the TeXsan package. The structure was expanded using successive difference Fourier maps until all non-hydrogen atoms were located. Disorder

in the $BF_4^-$ was modeled as two $BF_4^-$'s each with half occupancy, sharing a common boron. In the final cycles all non-hydrogen atoms in the cation were refined anisotropically. All hydrogen atom positions were calculated for ideal positions with C-H bonds lengths fixed at $0.95\text{Å}$. Hydrogen atom thermal parameters were fixed at a factor of 1.20 of the carbon atoms to which they were bonded. This resulted in R=0.049 and $R_w$=0.040 at final convergence. The goodness of fit was 2.02 and a $\Delta/\sigma$ value for any parameter in the final cycle was less than 0.021. A final difference Fourier map calculation showed no peaks of chemical significance; the largest being $0.8 \ e^-/\text{Å}^3$, which was associated with $BF_4^-$ disorder. Listings of atomic positional parameters and selected bond distances and angles are deposited in Appendix B.

## 2.4.2 Structure Determination of [Pd(PhS$_2$)Cl] (3)

Yellow crystals were grown by slow evaporation of a chloroform/hexane solution of this compound. A statistical analysis of intensity distributions was consistent with the space group $P\overline{1}$ and this was confirmed by a successful solution refinement. A total of 12979 reflections were collected and 4886 unique reflections with $F_o^2 > 3\sigma(F_o^2)$ were used in the refinement. The position of the palladium atoms were determined by Patterson methods and the remaining atoms were located from difference Fourier map calculations. In the final cycles of refinement all palladium, sulphur and chlorine atoms were assigned anisotropic thermal parameters. This resulted in R=0.052 and $R_w$=0.051 at final convergence. The goodness of fit was 1.65 and a $\Delta/\sigma$ value for any parameter in the final cycle was less than 0.005. A final difference Fourier map calculation showed no peaks of chemical significance; the largest being $0.7 \ e^-/\text{Å}^3$, which was associated with Pd. Listings

of atomic positional parameters and selected bond distances and angles are deposited in Appendix B.

### 2.4.3 Structure Determination of [Pd$_2$(PhS$_4$)(CH$_3$CN)$_2$][BF$_4$]$_2$ (8)

Yellow crystals were grown by slow evaporation of an acetonitrile solution. Cell parameters were determined from a least square refinement of 24 reflections and the space group was uniquely determined from the systematic absences to be $P2_1/n$. A total of 3811 reflections were collected with 1059 being unique with $F_o^2 > 3\sigma(F_o^2)$ and subsequently used in the refinement. A trial structure was obtained from the SHELX-86 direct methods from the TeXsan package. The structure was expanded using successive difference Fourier maps until all non-hydrogen atoms were located. In the final cycles S, and Pd atoms were refined anisotropically. All hydrogen atom positions were calculated for ideal positions with C-H bonds lengths fixed at 0.95Å. Hydrogen atom thermal parameters were fixed at a factor of 1.20 of the carbon atoms to which they were bonded. This resulted in R=0.074 and R$_w$=0.065 at final convergence. The goodness of fit was 2.41 and a $\Delta/\sigma$ value for any parameter in the final cycle was less than 0.019. A final difference Fourier map calculation showed no peaks of chemical significance; the largest being 0.7 e$^-$/Å$^3$, which was associated with BF$_4^-$ disorder. Listings of atomic positional parameters and selected bond distances and angles are deposited in Appendix B.

### 2.4.4 Structure Determination of [Pd$_2$(PhS$_4$)Cl$_2$] (9)

Yellow crystals were grown by slow evaporation from a dimethylformamide solution. Cell parameters were determined from a least square refinement of 24 reflections and the space group was uniquely determined from the systematic absences to be $P2_1/c$. A

total of 3100 reflections were collected with 1789 being unique with $F_o^2 > 3\sigma(F_o^2)$ and subsequently used in the refinement. A trial structure was obtained from the SHELX-86 direct methods from the TeXsan package. The structure was expanded using successive difference Fourier maps until all non-hydrogen atoms were located. In the final cycles all N, S, and Pd atoms were refined anisotropically. All hydrogen atom positions were calculated for ideal positions with C-H bonds lengths fixed at 0.95Å. Hydrogen atom thermal parameters were fixed at a factor of 1.20 of the carbon atoms to which they were bonded. This resulted in R=0.033 and $R_w$=0.026 at final convergence. The goodness of fit was 1.33 and a $\Delta/\sigma$ value for any parameter in the final cycle was less than 0.005. A final difference Fourier map calculation showed no peaks of chemical significance; the largest being 0.5 e/Å$^3$, which was associated with palladium. Listings of atomic positional parameters and selected bond distances and angles are deposited in Appendix B.

## 2.4.5 Structure Determination of [Pd$_2$(PhS$_4$)(1,10-phen)$_2$][BF$_4$]$_2$ (24)

Pale yellow crystals were grown by slow diffusion of diethyl ether into a methylene chloride solution. Cell parameters were determined from a least square refinement of 24 reflections and the space group was uniquely determined from the systematic absences to be $P2_1a$. A total of 5520 reflections were collected with 1714 being unique with $F_o^2 > 3\sigma(F_o^2)$ and subsequently used in the refinement. A trial structure was obtained from the SHELX-86 direct methods from the TeXsan package. The structure was expanded using successive difference Fourier maps until all non-hydrogen atoms were located. In the final cycles all N, S, and Pd atoms were refined anisotropically. All hydrogen atom positions were calculated for ideal positions with C-H bonds lengths fixed at 0.95Å. Hydrogen

atom thermal parameters were fixed at a factor of 1.20 of the carbon atoms to which they were bonded. This resulted in R=0.069 and $R_w$=0.065 at final convergence. The goodness of fit was 2.03 and a $\Delta/\sigma$ value for any parameter in the final cycle was less than 0.005. A final difference Fourier map calculation showed no peaks of chemical significance; the largest being 0.6 e/$\text{Å}^3$, which was associated with palladium. Listings of atomic positional parameters and selected bond distances and angles are deposited in Appendix B.

## 2.5 Results and Discussion

### 2.5.1 General Synthesis of Building Blocks

Ligands were synthesized in nearly quantitative yields using a thioether equivalent of a Williamson ether synthesis. From the benzyl bromide or benzyl thiol, a one step synthesis can afford a wide variety of ligands in high yield. All resulting ligands were air and moisture stable and possessed excellent solubility in common organic solvents such as chloroform, methylene chloride or diethyl ether.
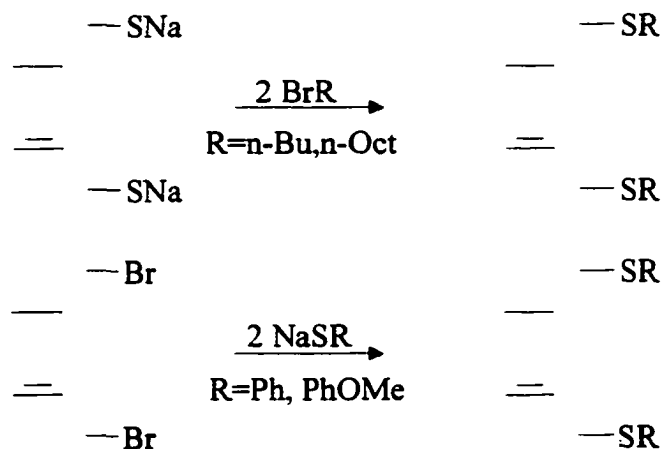


*Figure 2.4*    *Generic $S_2$ ligand syntheses also applicable to the $S_4$ ligands.*

There are a few general observations for the metallation of these compounds. The initial colour of the complexed palladium varied from orange to bright yellow depending

on the R group at sulphur. Those with aromatic R-groups tended to be orange while those with aliphatic groups yellow. As the reaction progressed, the solution would become lighter. The final colour of the products tended to be bright yellow for compounds with aromatic groups on the sulphur and nearly colourless for compounds with aliphatic R-groups.

### 2.5.2 Metallation of (PhOMeS₄) Ligand

The initial metallations of this ligand were different from the metallation of other ligands. Upon addition of the $[Pd(CH_3CN)_4][BF_4]_2$ the solution became blood red and an uncharacteristically low yield of 52% was obtained. This was eventually attributed to the $BF_4^-$ anion converting the methoxy group to the alcohol. It is common to protect a phenolic hydroxyl group as mono- or polymethyl-aryl ether and deprotection may be accomplished with boron trifluoride at room temperature at 1/3 mole equivalent. The compound was synthesized using palladium with triflate as the counter-ion and the blood red colour was not observed. A more typical yield of 88% was obtained using this method.

### 2.5.3 Metallation of (F₅PhS₄) Ligand

Early attempts at preparing molecular boxes using aromatic molecules as corner pieces indicated limited solubility and complicated aromatic regions in the ¹H NMR. The pentafluorophenyl ligand was made to investigate its solubility and to simplify the ¹H NMR spectrum. Unfortunately the metallation did not proceed effectively yielding only 18% doubly metallated product. Presumably the electron withdrawing power of the

pentafluorophenyl groups significantly reduces the ability of the sulphur to coordinate effectively to palladium.

## 2.5.4 Characterization of Building Blocks by $^1$H NMR Spectroscopy

A common feature in the $^1$H NMR spectra of these compounds is the observance of a broadened peak for the benzylic protons after metallation. Since sulphur has two lone pairs, a fluxional process exists where the lone pairs alternate coordinating to the palladium. This process was first demonstrated in 1966 by E. W. Abel using the chelate compound $PtCl_2$(2,5-dithiahexane). [40] This process is referred to as *inversion of sulphur*, since the stereochemistry of the sulphur centre inverts each time the lone pairs alternate coordination with the metal. Abel later determined that this process occurs via a non-dissociative mechanism, as coupling to $^{195}Pt$ was retained in the high temperature spectra. [41] The rate of exchange can be measured via NMR spectroscopy and allows the calculation of the barriers to exchange. The thermodynamic activation parameters ($\Delta G^{\ddagger}$ $\Delta S^{\ddagger}$ $\Delta H^{\ddagger}$ ) of a chemical system can be obtained by fitting calculated spectra to experimental spectra.

The rate at which exchange occurs depends on the temperature. At sufficiently low temperatures, a fluxional process can be slowed to a point where the molecule is considered to be rigid on the NMR time scale and peaks from all conformers are observed. As the temperature is raised, the rate of exchange is increased and the peaks broaden and coalesce. At sufficiently high temperatures, the rate of exchange exceeds the sampling time on the NMR and a single, narrow averaged peak is observed. This process was studied in detail using the component [Pd(PhS$_2$)Cl].

## 2.5.5  Fluxional Behavior of [Pd(PhS₂)Cl]

The metallation of the $S_2$ molecule should produce two diastereomers, a racemic mixture of R-R and S-S enantiomers and the mesoform R-S.



S-R *meso* form            R,R and S,S enantiomers
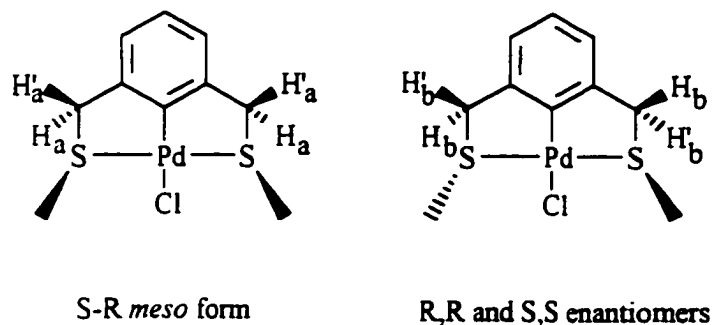
*Figure 2.5 Diagram depicting the diastereotopic protons H and H ' for the two possible diastereomers of [Pd(PhS₂)Cl].*

The benzylic protons are diastereotopic and should appear as separate signals in the $^1H$ NMR spectrum for each isomer. This is not observed since the inversion of sulphur stereochemically exchanges protons which results in the observance of a single broadened peak. The rate of inversion is temperature dependent and is directly responsible for the shape of the peak. The inversion of sulphur can be monitored through variable temperature $^1H$ NMR spectroscopy by observing its effects on the benzylic protons. The room temperature spectrum shows the benzylic protons as a broad singlet at $\delta=4.64$ ppm. At 313 K, the spectrum is a relatively sharp singlet and the sulphurs can be considered to be in an averaged planar conformation. At low temperature, the chirality of each sulphur is locked on the NMR timescale and barring chance overlap, resonances for both isomers can be seen. The low temperature $^1H$ NMR spectrum shows two sets of peaks; a pair of doublets for each isomer. The variable temperature spectra for this compound are shown below.
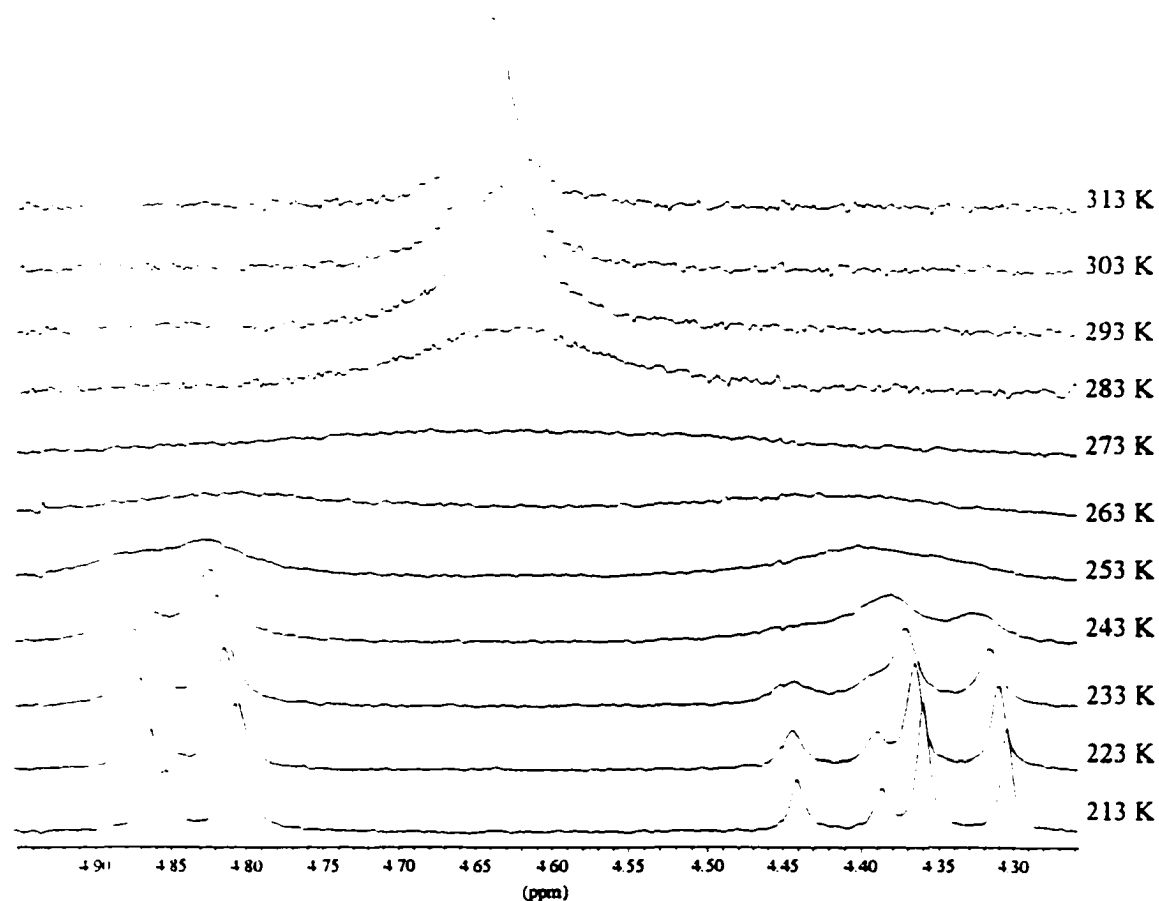
Figure 2.6 *VT $^1H$ NMR spectra showing the benzylic protons of [Pd(PhS$_2$)Cl] in CD$_2$Cl$_2$*

## 2.5.6 $^1$H NMR Line-shape Analysis

Line-shape analysis may be used in exchange broadened bandshapes to determine

the parameters affecting the system. The parameters that affect the line-shape in a $^1$H

NMR spectrum are iterated upon until a calculated line-shape matches an experimental

line-shape within a given error or a set number of iterations. The particular parameter of

interest is the rate of exchange. From transition state theory, the rate of a chemical

process can be expressed in the form $k = \dfrac{k_b T}{h} e^{\frac{\Delta S^{\ddagger}}{R}} e^{\frac{-\Delta H^{\ddagger}}{RT}}$. A plot known as an Eyring plot

takes the form $\ln(k/T)$ vs $1/T$ resulting in a linear equation with $m = -\Delta H^{\ddagger}/R$ and

$b = \Delta S^{\ddagger}/R + \ln(k_b/h)$. By performing a line-shape analysis and determining the rate of the

exchange process at several different temperatures, the thermodynamic variables for the

exchange process can be calculated.

Before embarking on this experiment, several items must be obtainable.

Immediately obvious is the necessity of obtaining a program capable of performing line-

shape analysis. The program used in these calculations was DNMR5.[42] There must also

be a way to get the data points from the experimental spectrum into a format readable by

the fitting program. Typically thousands of points are present in only a small portion of a

spectrum and a program must be written to convert the native format of the NMR

computer to the format required by the fitting program. There is no reason why points

cannot be measured directly from a printed spectrum and entered manually. It turns out

that these are the two hurdles to overcome before a line-shape analysis can be attempted.

The parameters required for the program will be covered below.

The number of coupled nuclei and the number of chemical configurations of the

molecule are required. A chemical configuration is defined as an NMR differentiable

species. Processes that occur too rapidly to detect on the NMR timescale are ignored in

this treatment. For example, at temperatures above -70 °C, the interconversion between

cyclohexane chair and boat conformations occurs too rapidly to affect the linewidths, and

for purposes of assigning chemical configurations cyclohexane is considered to be planar.

Typically achiral solvents are used and enantiomers are not distinguishable, but a chiral solvent may be used in cases where interconversion between enantiomers is of interest and the chemical shift differences are observable. Initial guesses for chemical shift and coupling as well as effective transverse relaxation times ($T_2$) and rate constants must also be given. Depending on the nature of the problem and the exchange region of interest, these variables may be iterated upon or left constant.

Initial chemical shifts ($\delta v$) typically come from low temperature spectra and exhibit mild linear temperature dependence. This may be corrected for by linear least-squares analysis of $\delta v$ versus temperature. Chemical shifts can only be allowed to vary in the slow exchange region as the rate constant and chemical shifts become covariant from coalescence up to the fast exchange limit. From coalescence up, extrapolated chemical shift values must be used and held constant.

Coupling constants are obtained from the slow exchange region. Sometimes mild temperature dependence is observed and in this case coupling constants may be iterated upon over the entire range. Typically, coupling constants are measured in the slow exchange limit and iterated on. The results are then used as constants for the remainder of the fittings.

Effective transverse relaxation times ($T_2'$) are ideally measured outside of the exchange regions and interpolated. Care must be used to ensure a constant resolution is maintained over the temperature range. The relaxation time may be calculated from the width at half height ($W_{1/2H}$) for the peak of interest. $W_{1/2H} = 1/\pi T_2$. In a system which exhibits only a singlet in the fast exchange region, the exchange rate (k) and $T_2$ are

covariant and cannot be iterated upon simultaneously. In fairly simple spin systems, k is iterated upon and $T_2$ is held constant. As the systems increase in complexity, k and $T_2$ may be iterated upon simultaneously.

In the DNMR5 input file, the experimental spectrum must follow the initial guesses for the systems parameters. The frequency of the origin and the sweep width must be specified. As well, a starting and ending frequency for the determination of noise must be specified and a starting and ending frequency for specifying the region exhibiting exchange broadening. Following these values, DNMR5 requires the number of spectral points and then all the spectral intensities. A program was written to extract this information from a collected spectrum in WINNMR format. A graphical display of the spectrum is presented and a sample region for noise and the area to fit may be quickly selected. The program outputs a file suitable for appending to the initial input for DNMR5.

Finally, the input file must include a list of parameters to be varied independently, followed by a list of parameters to be varied but kept equal to an independent parameter. Upper and lower limits on the parameters may also be given. Although this information has been given with respect to DNMR5, the procedure is general for any program used.

## 2.5.7 Details of DNMR Fittings for [Pd(PhS$_2$)Cl]

A complete line-shape analysis was performed using DNMR5 to measure the rate of inversion of sulphur by monitoring the benzylic protons. Spectra were collected at 10 K intervals from 193 K to 313 K in $CD_2Cl_2$. Using DNMR5 with the collected spectra, a theoretical spectrum was fit to each experimental spectrum. From the fittings, the

exchange coefficient (k) was used to calculate the thermodynamic parameters from an Eyring-type plot.

The low temperature spectrum in the absence of exchange provides most of the initial values. Chemical shifts were empirically adjusted for temperature dependence by linear extrapolation. The populations of one of the configurations was fixed at 1.0 and the other estimated by integration of the low temperature spectrum. The rate constant was assumed to be nearly zero. Relaxation time was estimated from the peak width at half height. With these initial estimates, DNMR5 was allowed to iterate on the chemical shifts, populations, the rate and a parameter that corrects for baseline tilt. With these improved values, in the slow exchange region, the chemical shifts, populations and rate were allowed to vary. Coupling was kept constant and $T_2$'s were interpolated. As temperatures approached coalescence, only the rate was varied. Chemical shift, population and relaxation rates were all extrapolated. The results of the fittings are shown in Table 2.1. When the high temperature spectrum is a singlet, many variables are highly correlated. As a result, the fittings are much less accurate in the region of coalescence as indicated in the error estimates for the rate of inversion. Due to the large error at theses temperatures, the calculation of thermodynamic variables was based on the data obtained over the temperature region 213 K to 263 K. At very low temperatures, other factors, particularly viscosity broadening begin to affect line-shape, and thus the lowest temperature used in the calculations was 213K. The results of the calculations are presented in Table 2.2.

*Table 2.1 Rate of Inversion of Sulphur for [Pd(PhS₂)Cl]*

| Temperature (K) | Rate (s⁻¹) |
|---|---|
| 313 | 5760±97 |
| 303 | 1840±27 |
| 293 | 522±300 |
| 283 | 426±210 |
| 273 | 300±84 |
| 263 | 198±12 |
| 253 | 77.2±3.7 |
| 243 | 27.1±0.73 |
| 233 | 7.49±0.07 |
| 223 | 1.45±0.06 |
| 213 | 0.47±0.0003 |
| 203 | 1.01±0.03 |
| 193 | 0.12±0.0015 |

*Table 2.2 Thermodynamic Parameters for the Inversion at Sulphur in [Pd(PhS₂)Cl]*

$\Delta H^{\ddagger}$=55.9 ± 0.6  kJ/mol

$\Delta S^{\ddagger}$=13.5 ± 2  J/K/mol

$\Delta G^{\ddagger}_{300}$=51.9 ± 0.9  kJ/mol

Similar numbers have been reported by Hursthouse for a slightly less flexible

system, [Pd₂(2-dimethylamino-benzylamine)₂(pyridine-2-thionate)₂]. The reported barrier

to inversion at sulphur in this example was $\Delta G^{\ddagger}_{273}$=58.9 kJ/mol.[43] The results of our

analysis for [Pd(PhS₂)Cl] is generally applicable to the other building block species. All

the PdS₂ and Pd₂S₄ compounds have a nearly invariable coalescence temperature of

273 K. This fact suggests that the barrier to the inversion of sulphur is not significantly

affected by the identity of the R-group on sulphur or the labile ligand occupying the

fourth coordination site of palladium.

## 2.5.8 X-Ray Structure of [Pd(PhS₂)Cl]

This compound crystallizes with an unusual four molecules per asymmetric unit.

The molecules are paired by intermolecular aromatic "T" and planar $\pi$-stacking

interactions. The R-groups on sulphur adopt syn-conformations to allow the peripheral

phenyl rings to maximize intermolecular aromatic edge and facial $\pi$-interactions with the

other paired molecule. Because of this pairing, a handedness exists between them and

upon crystallization forms a racemate. These two pairs alternate in straight chains through

the lattice. The palladium atoms form nearly a perfect line through the lattice.

Considering each pair to be a molecule, the intermolecular distance from palladium to

palladium is 3.79Å, too large for any chemical bonding. Each metal centre is in a slightly

distorted square planar environment bonded to two sulphur atoms, with Pd-S distances

ranging from 2.290(4) Å to 2.310(4), Pd-C distances ranging between 1.97(1) Å and

1.99(1)Å, and Pd-Cl distances ranging between 2.391(4)Å and 2.411(4) Å. There is no

chemical significance to deviations in the bond lengths.
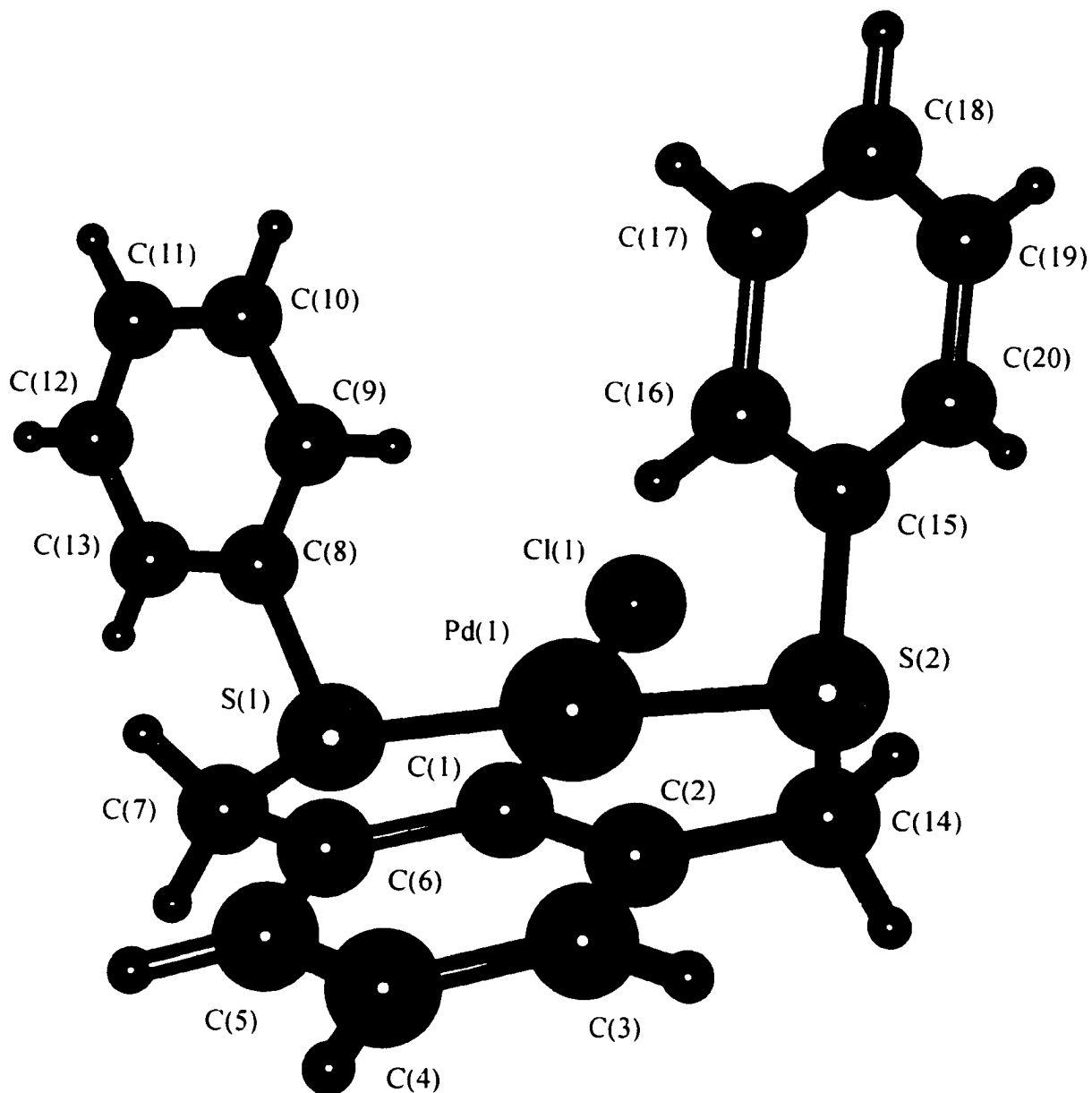
*Figure 2.7 X-ray crystal structure of [Pd(PhS₂)Cl] showing one of the four molecules in the asymmetric unit.*
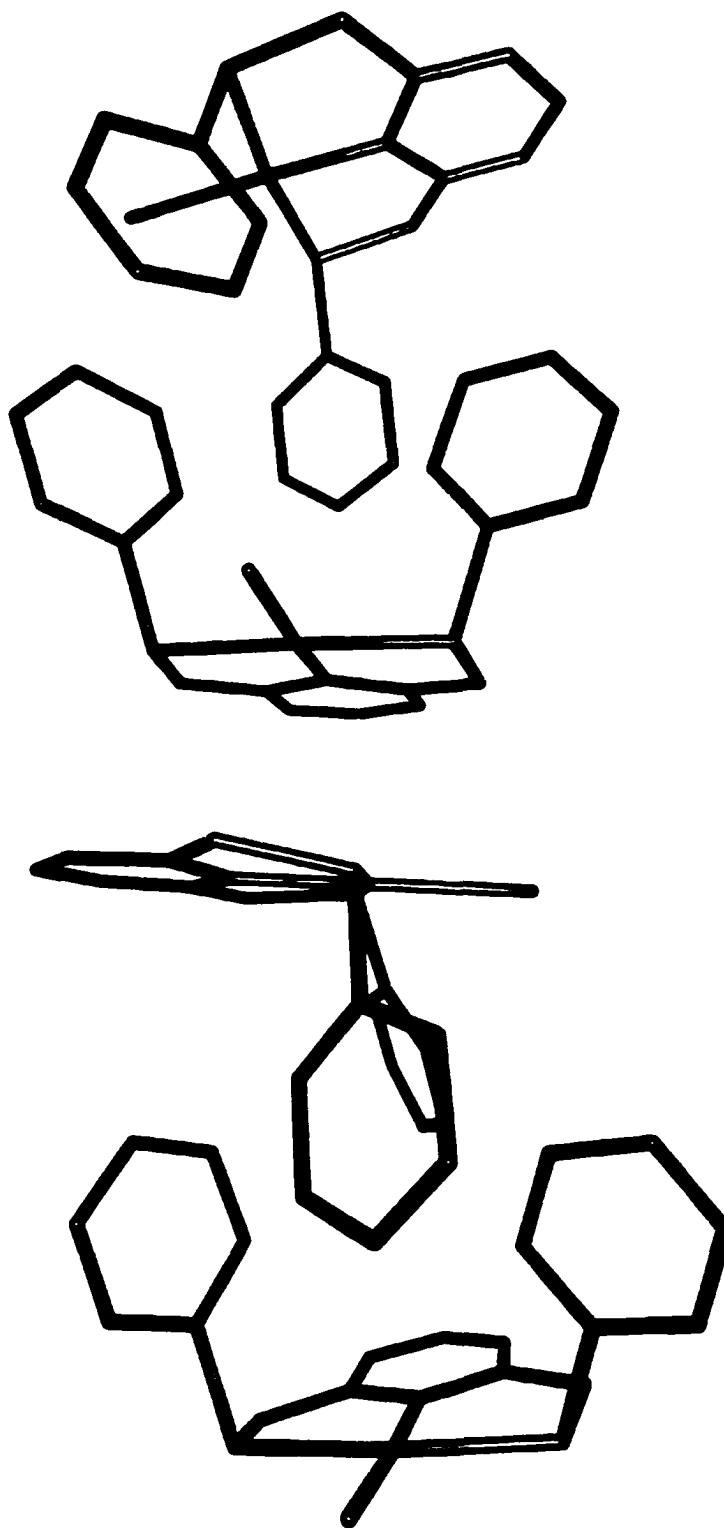
*Figure 2.8 X-ray diagram of the four [Pd(PhS₂)Cl] molecules in the unit cell displaying the alternating handed pairs.*

### 2.5.9  X-Ray Structure of [Pd(PhS$_2$)(CH$_3$CN)][BF$_4$]

This molecule crystallizes with one molecule per asymmetric unit and no crystallographically imposed symmetry. In contrast to the [Pd(PhS$_2$)Cl] structure, these molecules do not pair in the lattice. Presumably, the BF$_4^-$ counter ion is responsible for this by disrupting the packing. The phenyl groups on the sulphur atoms adopt an anti conformation as opposed to the syn conformation possessed by the [Pd(PhS$_2$)Cl] and [Pd$_2$(PhS$_4$)(1.10-phen)$_2$][BF$_4$]$_2$ structures. Palladium exists in a slightly distorted square planar geometry typical of these compounds. Palladium distances are Pd-S1 2.301(3)Å, Pd-S2 2.323(4)Å, Pd-Cl 1.99(1)Å and Pd-N1 2.10(1)Å and show no deviations of chemical significance.
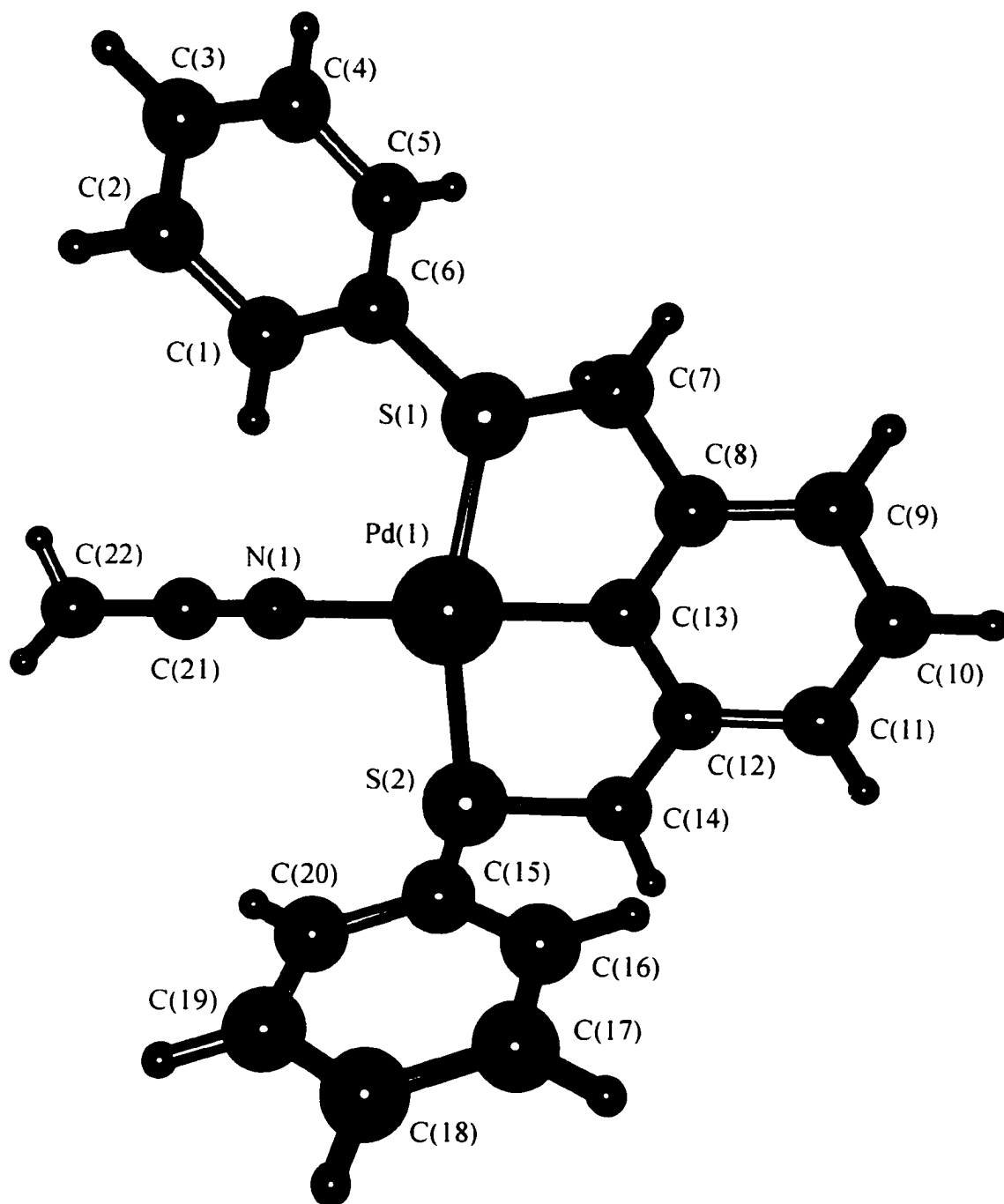
*Figure 2.9 X-ray crystal structure of [Pd(PhS₂)(CH₃CN)][BF₄]*

## 2.5.10  X-Ray Structure of [Pd$_2$(PhS$_4$)Cl$_2$]

This molecule crystallizes with two molecules per unit cell.  Each molecule possesses a crystallographically imposed centre of symmetry.  Each palladium sits in a slightly distorted square planar geometry with a CSSN coordination sphere.  The bond lengths and angles are typical and there are no deviations of chemical significance.  The phenyl groups are arranged anti from side to side and syn from end to end.  Other S$_4$ structures presented in this thesis show nearly all the possible permutations in the arrangement of these S-R groups.  There are no stabilizing interactions between aromatic groups in the lattice.

## 2.5.11  X-Ray Structure of  [Pd$_2$(PhS$_4$)(CH$_3$CN)$_2$][BF$_4$]$_2$

This molecule crystallizes with two molecules per asymmetric unit and possesses a crystallographically imposed centre of symmetry.  The phenyl groups on the sulphur atoms adopt a syn conformation.  Palladium is in a slightly distorted square planar geometry with a CSSN coordination sphere.  Palladium distances are Pd-S1 2.279(8)Å, Pd-S2 2.284(9)Å, Pd-C1 2.03(2)Å and Pd-N1 2.10(1)Å and show no deviations of chemical significance.  There was disorder of the BF$_4^-$ counter ion which was modeled as two BF$_4^-$ groups each with half occupancy.
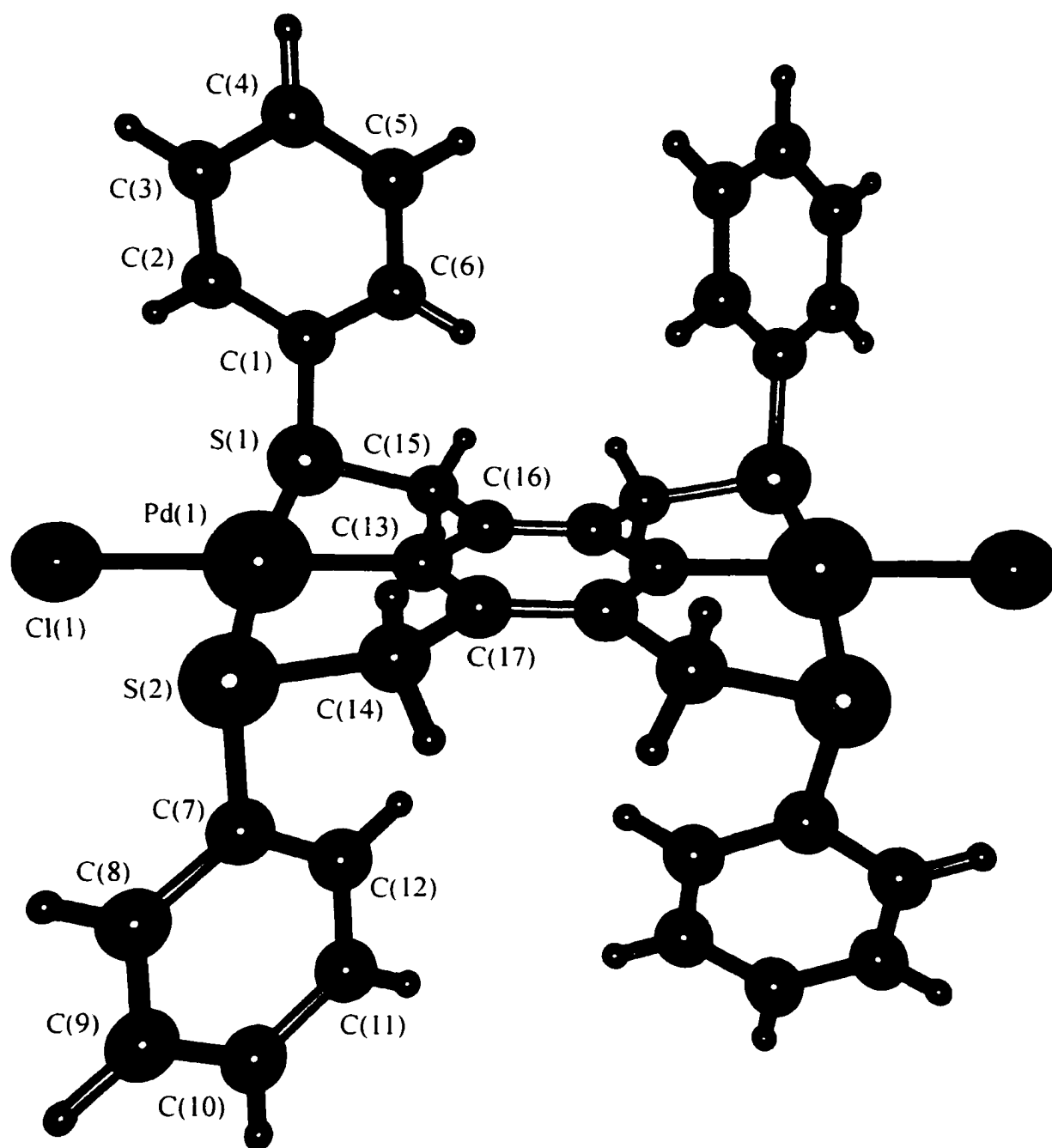
*Figure 2.10 X-ray crystal structure of [Pd₂(PhS₄)Cl₂]*
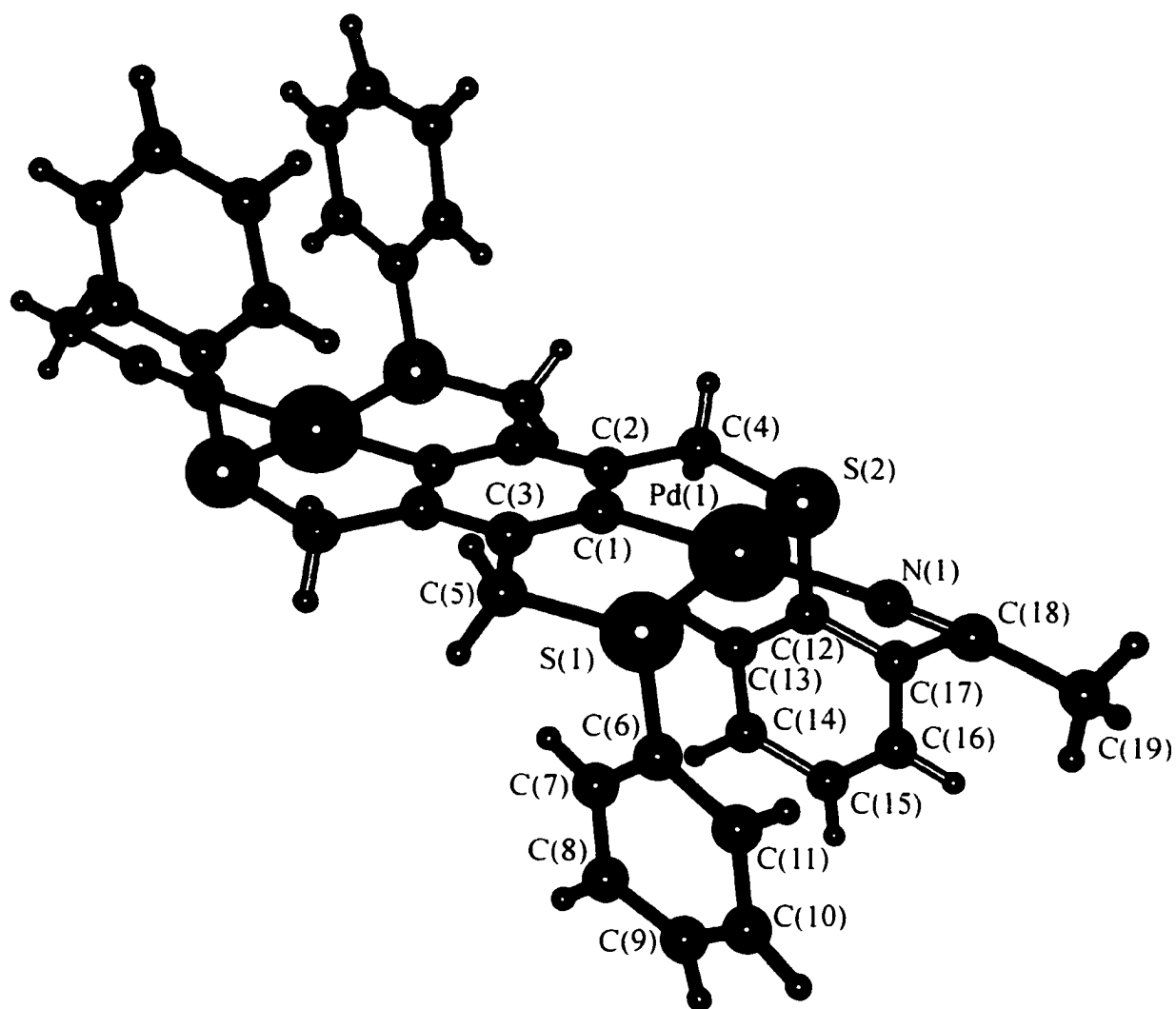
*Figure 2.11 X-ray crystal structure of [Pd₂(PhS₄)(CH₃CN)₂][BF₄]₂*

## 2.5.12 Suitability of Components for Supramolecular Assemblies

The ease with which the R-groups on the sulphur atoms may be modified resulted in a toolbox of pieces for use as wall units in cleft and box-like assemblages. The ability to vary the R-groups allows tuning for different physical properties. For example, solubility can be enhanced in different solvents with the modification of the R-groups. Furthermore, deciphering NMR spectra can be simplified by appropriate choice of R-group.

Our investigations concentrated on compounds containing the S-R groups where R=Ph and Bu since these had the most desirable physical properties. The phenyl groups were used when a crystal structure was desired. Intermolecular aromatic $\pi$-stacking forces and their rigid structure guide the packing of these molecules in the lattice. The butyl groups were used when solubility in organic solvents was an issue. Although no quantitative measurements were performed on the solubility differences between phenyl and butyl groups, it was obvious during preparations that the butyl group was significantly more soluble in organic solvents such as chloroform and methylene chloride. This effect was most noticeable when the labile acetonitrile ligand occupying the fourth coordination site on palladium was replace by a halogen. Metal halides are notoriously insoluble in non-polar solvents. When performing $^1$H NMR work, the lack of phenyl groups greatly simplified the aromatic region which would become important when aromatic corner pieces were used to replace acetonitrile on the palladium centres.

## 2.6 Attempts at Synthesizing Components for Other Supramolecular Structures

### 2.6.1 Five and Six Coordinate Pd(II)

In addition to four coordinate square planar complexes of palladium (II), a few examples of five coordinate palladium (II) complexes exist.[44,45,46] This geometry would allow the construction of ladder type assemblies using poly-2,2'-bipyridyl type units as stringers and the doubly palladated compound as rungs. It was hoped that 1,10-phenanthroline, being a rigid molecule might enforce a trigonal bipyramidal coordination geometry on palladium. Both variable temperature $^1$H NMR spectroscopy and X-ray crystallography were used to characterize the results.

Six coordinate palladium (II) compounds are very rare. These complexes all seem to possess the common feature of trans-halides occupying the fifth and six positions.[47,48] All of the known octahedral complexes exist only in the solid state, and dissociate in solution. Despite this precedent, an attempt was made at inducing an octahedral geometry around palladium employing 2,2':6',2" terpyridine (terpy) as an ancillary ligand.

Upon coordination of 1,10-phenanthroline to the doubly palladated compound [$Pd_2(PhS_4)(CH_3CN)_2$], a completely symmetric phenanthroline region was observed in the $^1$H NMR spectrum. This indicated the possibility of a trigonal bipyramidal geometry at the palladium centre. The benzylic peak was considerably sharper at room temperature than observed for previous compounds and this was attributed to a change in the geometry at palladium.

The complex crystallizes with two molecules per unit cell. Each molecule possesses a crystallographically imposed inversion centre. Solid-state evidence of the metal geometry does not support the NMR spectroscopic evidence for a trigonal bipyramidal geometry at palladium. The crystal structure shows a distorted square pyramidal environment at palladium with a CSSN+N coordination sphere. The Pd-Cl bond length is 1.98(2) Å. The Pd-S1 and Pd-S2 bond lengths are 2.281(5) Å and 2.333(5) Å respectively. The Pd-N1 bond is 2.16(1) Å and Pd-N2 distance 2.59(2) Å. This 4+1 coordination of 1,10-phenanthroline to a $d^8$ metal has been reported in a few cases.[49,50,51] There has been some debate whether to call this a square planar or square pyramidal complex since the apical nitrogen is restrained by the geometry of the 1,10-phenanthroline to occupy an elongated axial position.
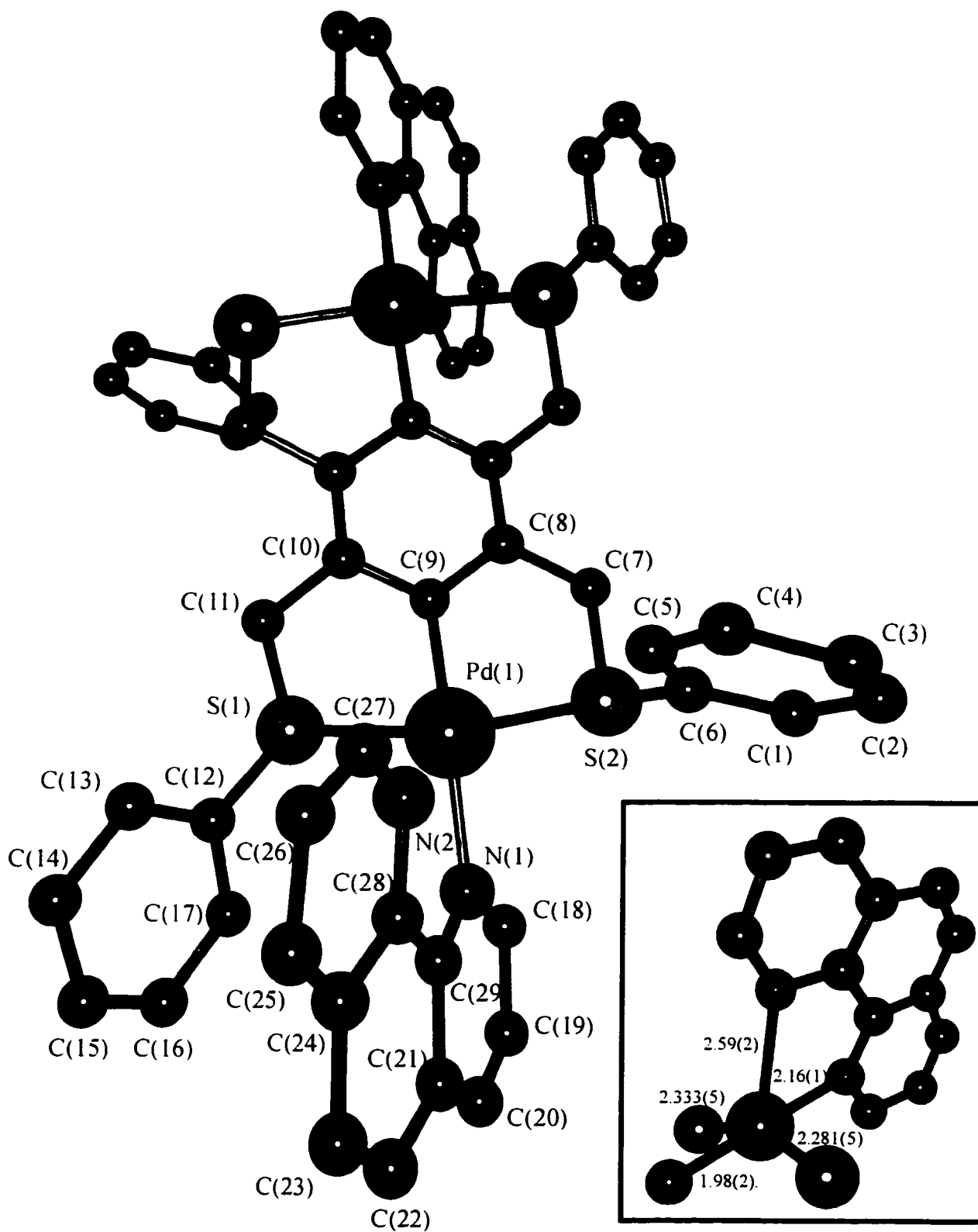
*Figure 2.12 X-ray crystal structure of [Pd₂(PhS₄)(1,10-phen)₂][BF₄]₂*

There is evidence that this should be referred to as distorted square pyramidal structure. Wieghardt has published a structure[52] with a distorted square pyramidal palladium where the fifth apical nitrogen is not restrained to occupy the site. The flexible ligand and reported palladium geometry is depicted below.
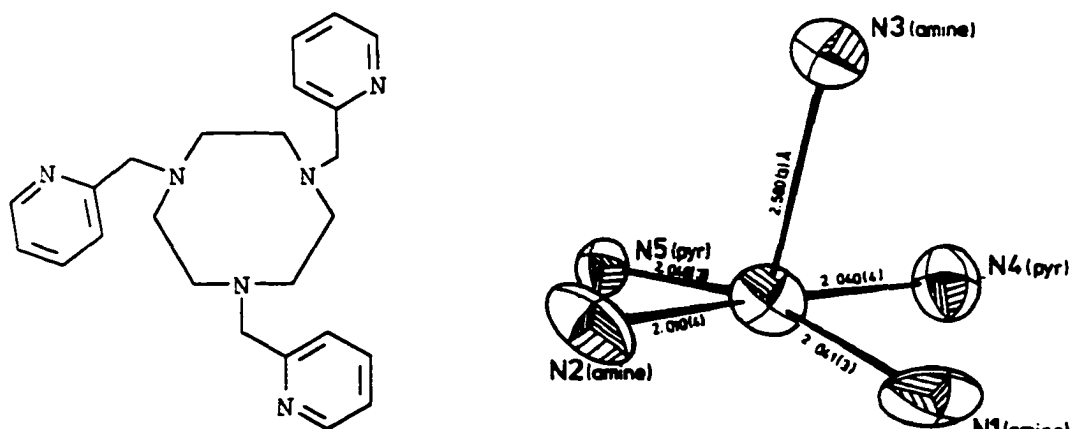


*Figure 2.13 Wieghardt's flexible ligand and the geometry of the ligand at the palladium centre.*

In a square pyramidal structure, calculations predict a $d^8$ metal to lie above the plane of the basal ligands forming an angle $\phi$ between the basal and axial ligands of approximately 103°. (See figure below) The angles in the crystal structure are consistent with this calculation. This suggests that there is an electronic interaction with the axial nitrogen producing a distorted square pyramidal structure, not a square planar geometry with the nitrogen occupying the axial position by necessity.
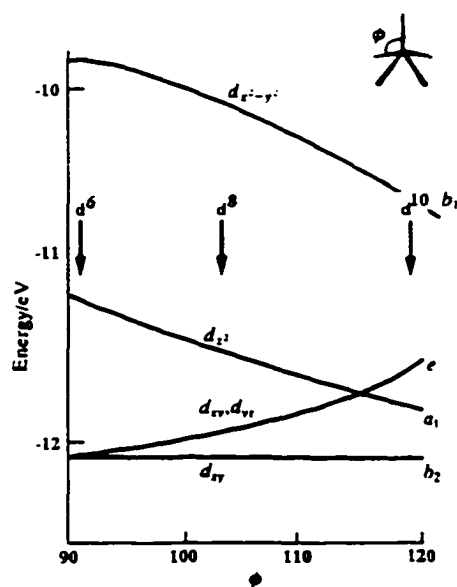
*Figure 2.14 A correlation diagram for the metal d orbitals in an ML₅ fragment*

Interestingly, 1,10-phenanthroline has been reported as being non-planar when coordinated to group 10 $d^8$ metals.[53,54,55,56] This is observed in this crystal structure as well. The two outer phenyl rings of the phenanthroline are approximately 6° out of plane. This distortion, to some degree counters the non-orthogonality of the phenanthroline to the CSSN coordination plane and positions the lone pair to sit at the apex of a square pyramid. The angle from N1 through the lone pair to palladium is 153°. This interaction of the lone pair of phenanthroline with Pd accounts for some unusual $^1H$ NMR spectroscopic results.

The pendant phenyl groups are syn at each palladium centre and anti from end to end and are involved in intermolecular π-stacking interactions. One phenyl group is involved in facial π-stacking to the 1,10-phenanthroline with distances ranging between 3.1 Å and 3.8 Å. The tetrahedral geometry of the sulphur and the square pyramidal

geometry of the palladium restrain the phenyl group and the phenanthroline so the angle between the planes of the rings is 14° from coplanarity. The other phenyl group is involved in intermolecular "T" shaped π-interactions with a pendant phenyl group of a neighboring molecule in the lattice. The deviation from 90° between the plane of phenanthroline and the plane of coordination around the palladium is not solely due to π-stacking interactions. Nearly every structure where an aromatic amine is coordinated to a square planar metal deviates from orthogonality. In this case, a typical angle of approximately 72° is observed.

After obtaining solid state evidence that the doubly palladated molecule was not in a symmetric geometry with 1,10-phenanthroline, a variable temperature NMR spectroscopic study was undertaken to determine what kind of process was responsible for the symmetric $^1$H NMR spectrum. Two potential processes were thought to be at work. Either a rapid rotation about the Pd-N bond or a rocking motion where the two N donors alternate coordinating to the Pd bond was averaging the $^1$H NMR signal. It was thought that upon cooling the compound, the dynamic process could be slowed to a point where an asymmetric phenanthroline region could be observed. Interestingly, even a 193 K, the process could not be slowed to a rate that was observable on the NMR time scale. This was found to be the case in a similar system from Yamazaki.[57] In his system, the $^1$H NMR spectra of [Pd(PPh$_3$)(1,10-phen)$_2$][PF$_6$]$_2$ and [PdCl(2,9-Me$_2$-(1,10-phen)$_2$][PF$_6$] indicated that all four nitrogen atoms of the two N-heterocyclic ligands were equivalent even at -100°C.

The same doubly palladated compound with butyl instead of phenyl groups was examined in the same manner. The coalescence temperature was found to be 220K. This temperature is still dramatically lower than the typical 273K coalescence temperature. This result implies two things. First, there is likely a cooperative mechanism involving π-stacking interactions of the 1,10-phenanthroline with the S-phenyl groups, with a rocking motion of the 1,10-phenanthroline. Secondly, the palladium is not in a square planar environment in solution. This change in geometry around the palladium accounts for the dramatically lower activation energy for the inversion of the sulphur centres.

A reaction of $[Pd_2(PhS_4)(CH_3CN)_2][BF_4]_2$ with 2,2':6',2" terpyridine was attempted in an effort to produce an octahedral geometry. Since there are no known octahedral complexes of palladium(II) in solution, there was no precedence for predicting the $^1H$ NMR spectrum. The terpyridyl region was not symmetric and many of the peaks were broad indicating a dynamic process was occurring, so analysis was not possible. It was hoped that an X-ray structure could be obtained of this material, but all attempts at obtaining crystals failed.

## 2.6.2 Preparation of Quino[5,6-b]1,7-Phenanthroline

The purpose of this experiment was to produce a corner piece to be used with the wall sections to produce a molecular square. The molecule was to become one side of a four sided box in which this ligand provided a 180° turn. However, the product of this reaction was not the desired result. The desired product was dipyrido[3,2-b:2',3'-i]acridine which is depicted in the following figure as (b). Starting from acriflavin, the

result in molecule (a) which has 11 different protons. A symmetric ring closure could produce the other two possible products (b) and (c) each having 6 different proton resonances. Only one compound was isolable and the $^1$H NMR spectrum indicated there were six different protons.



(a)                    (b)                    (c)
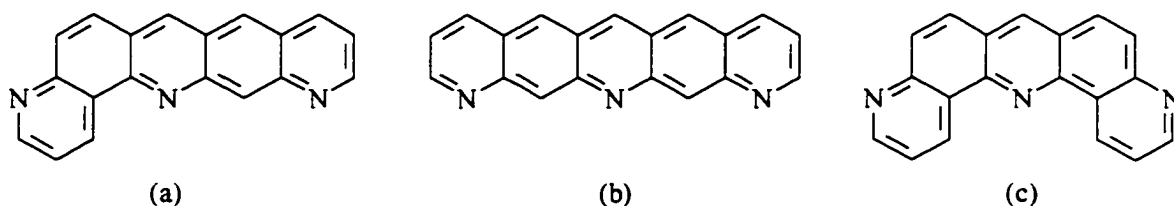
*Figure 2.15    Three possible products from cyclization reaction.*

From the $^1$H NMR spectrum, the isolated product was clearly molecule (c). The presence of only one singlet in the observed spectra is the first indication that the product is not compound (b) which should contain three singlets. A series of spin-decoupling experiments were performed to determine coupling and further verify the structure.
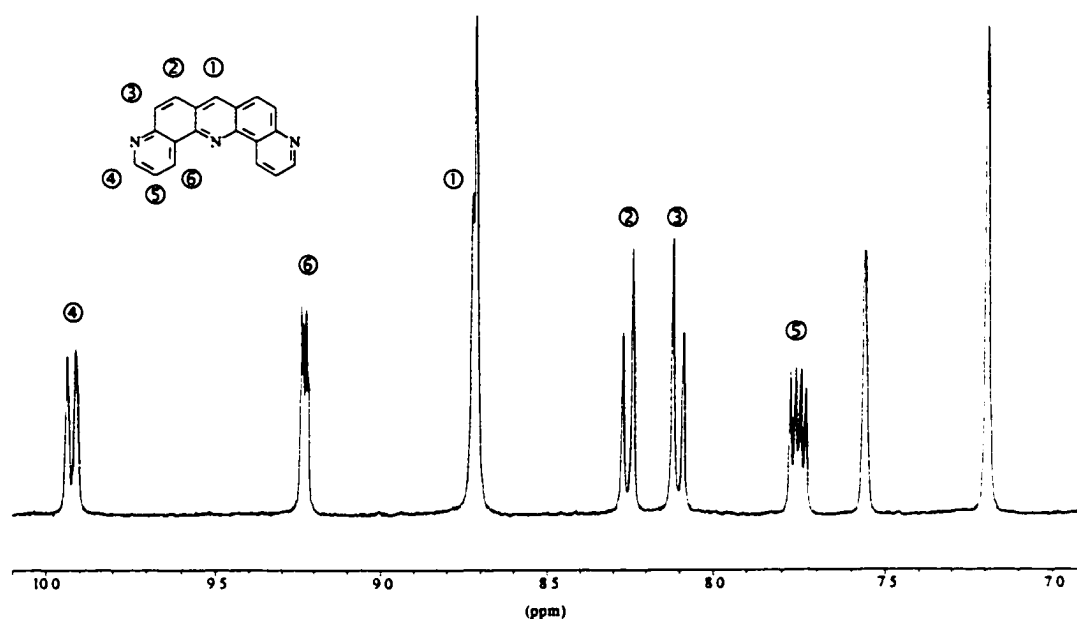


*Figure 2.16    Assignment of quino[5,6-b]1,7-phenanthroline.. Unlabeled peaks are solvent (d5-pyridine)*

Peak 1 is partly obscured under the solvent peak and is assumed to be a singlet.

The assignment of peaks 2 and 3 was based on the general observation that ortho- and

para-substituents of heterocyclic aromatic compounds tend to be significantly further

downfield than meta-substituents. Peak 5 is assigned by the magnitudes of the coupling to

the adjacent protons. Peaks 4 and 6 are assigned based on their relative shifts, with the

ortho substituent found furthest downfield.

*Table 2.3 Coupling Constants for Quino[5,6-b]1,7-phenanthroline*

| | |
|---|---|
| $J_{2-3}$ | 9.3 Hz |
| $J_{4-5}$ | 7.9 Hz |
| $J_{4-6}$ | 1.9 Hz |
| $J_{5-6}$ | 4.6 Hz |

Although the desired compound was not produced, another geometry for a corner

piece was encountered. Corner pieces did not have to turn 90° to create a molecular box.

In this case three corners could be turned at 60° and still result in a closed assemblage.

## 2.6.3 Attempted Preparation of Sulphonated 4,7-Phenanthroline

The sulphonation of 4,7-phenanthroline was attempted for two reasons. The

fragment would likely be soluble in water, and when coordinated to a metallated ligand,

could be used as the counter ion, eliminating $BF_4^-$. Sulphonation of aromatic compounds is

usually accomplished by treatment with sulphuric acid containing 5-20% sulphur trioxide

to remove the water formed in the reaction. Although aromatic hydrocarbons readily

undergo sulphonation, heterocyclic compounds are more difficult to sulphonate. Pyridine

is sulphonated with oleum at 390° in only a 13% yield.[58] The reaction was initially carried

out under conditions ranging from relatively mild in refluxing concentrated $H_2SO_4$ to the

very harsh, refluxing in $H_2SO_4$ with 80% $SO_3$. In every case, unreacted

4,7-phenanthroline was recovered quantitatively.

## 2.7 Summary and Conclusions

Several bi- and tetradentate thioether ligands were synthesized and subsequently

palladated. The resulting fragments produced a very flexible set of building blocks where

several physical properties could be controlled. These building blocks were characterized

by NMR spectroscopy, and X-ray crystallography. A full NMR line-shape analysis was

performed to determine the thermodynamic quantities, $\Delta G^{\ddagger}$, $\Delta H^{\ddagger}$ and $\Delta S^{\ddagger}$ for the

inversion of sulphur. Building blocks were investigated for use in rack and ladder rack

type assemblies. This resulted in the characterization of an uncommon square pyramidal

palladium (II) complex. The relative ease of synthesis and excellent yields makes these

compounds appealing for use as fundamental units in supramolecular assemblies. Used as

wall units, along with appropriate corner pieces they were expected to allow the

construction of cleft and box-like structures. This is discussed in Chapter Three.

# Chapter Three

## 3.1 Introduction

There has been considerable interest in nanoscale architecture as scientists attempt

to bridge the gap between device miniaturization and the chemical synthesis of small-scale

structures. The most prevalent architectures have been presented in Chapter One. This

chapter deals specifically with the synthesis of cleft and box structures.

The word box instantly conjures the image of a four sided figure and this is

reflected in the literature of the molecular box. Nearly all molecular containers have been

four sided objects. The first self-assembled molecular box is credited to Maverick.[59]

Cu(II) coordinated to the bis($\beta$-diketone) ligand produces the cofacial binuclear

compound depicted below.
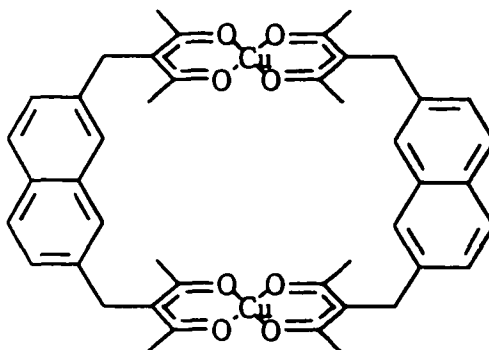


*Figure 3.1  Maverick's self-assembled molecular box*

The characteristic molecular box was first demonstrated by Fujita and Ogura.[60]

The square planar geometry of Pd(II) and Pt(II) complexes make them ideal corners. The

4,4'-bipyridine species, in the presence of ethylenediamine-palladium complex is rapidly

70

converted to the inorganic cyclophane in quantitative yield. The structure of these compounds was confirmed by NMR spectroscopy and a crystal structure. A couple of these compounds have been found to bind a variety of aromatic guests in aqueous solution [61]
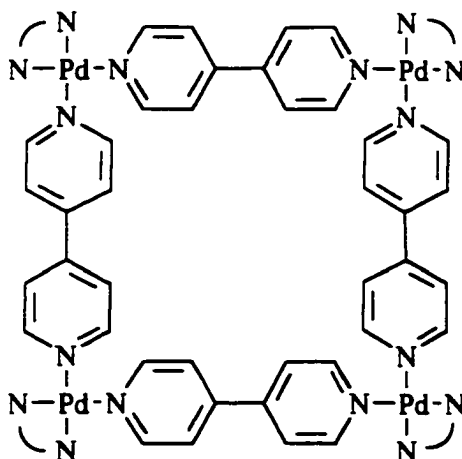


*Figure 3.2 Fujtia and Ogura's original molecular box*

Fujita has recently extended this work to a three dimensional box. The self-assembly process is not as efficient as in the previous case as the complex only assembles in high yield in the presence of specific guest molecules. This guest induced assembly produces the three dimensional cage structure shown below in >90% yield. In the absence of an appropriate guest, the cage structure is present in solution in only 60% yield.
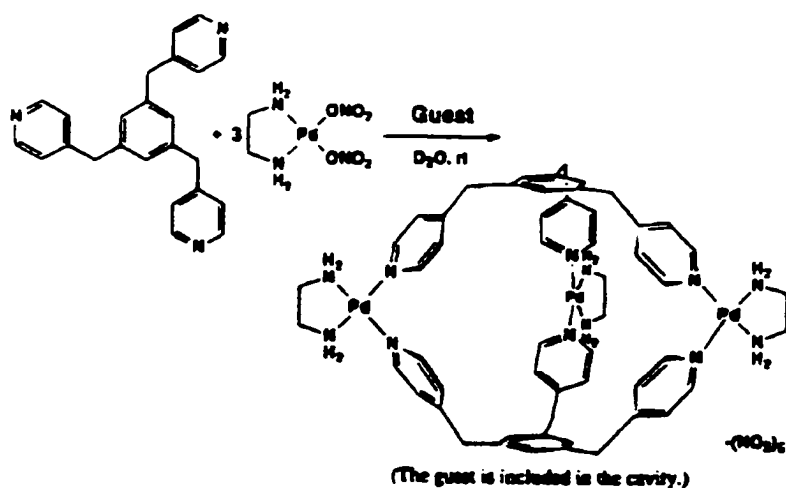
*Figure 3.3 Fujita and Ogura's three dimensional box synthesized in high yield via guest induced self-assembly.*

Stang replaced ethylenediamine in Fujita and Ogura's original molecular box with the lipophilic ligand 1,3-bis(diphenylphosphino)-propane (dppp) to generate the cyclophane in $CH_2Cl_2$.[62] The compounds were originally characterized by $^1H$, $^{13}C\{^1H\}$ and $^{31}P\{^1H\}$ NMR spectroscopy. Just recently a crystal structure of the platinum complex has been reported.[63] A further variation utilizes the ligand, 1,1'-bis(diphenylphosphino)ferrocene with Pd(II) and Pt(II) as corners of a molecular box with 2,7 diazapyrene acting as the wall units.[64]
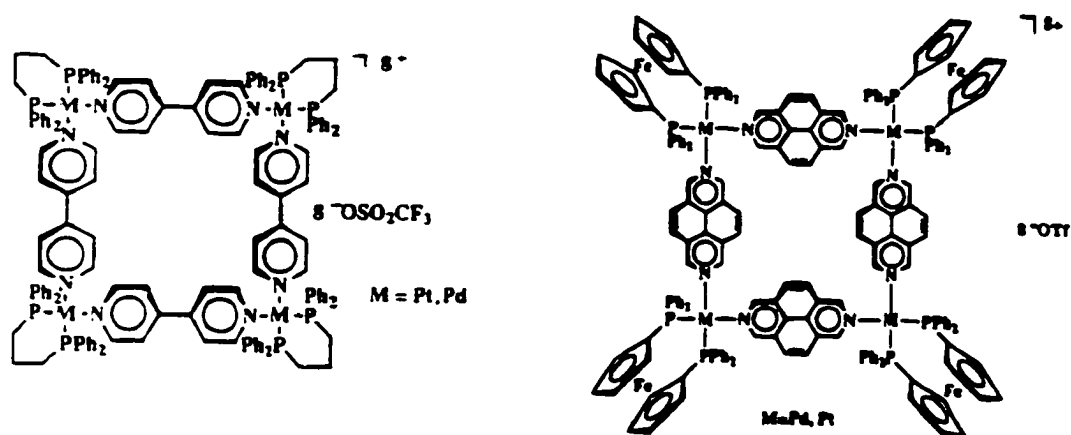
Figure 3.4 Stang's variations on Fujita and Ogura's original molecular box

Stang has also produced a mixed metal tetranuclear complex.[65] In the scheme depicted below, the all platinum and mixed platinum/palladium compounds were isolated in 90% and 96% yields respectively. These compounds were characterized through IR, $^1H$, $^{13}C\{^1H\}$ and $^{31}P\{^1H\}$ NMR spectroscopy.
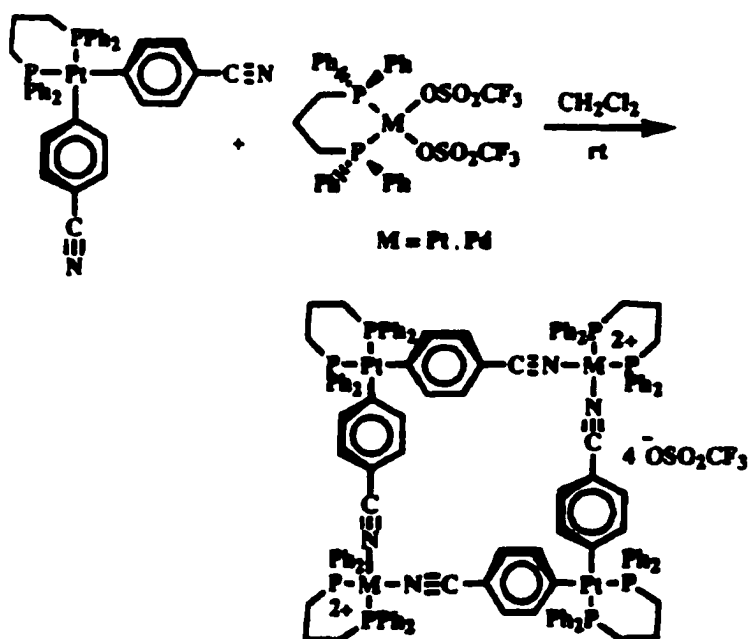


Figure 3.5 Stang's heteronuclear molecular box

Hunter's group has demonstrated cyclic dimeric[66], trimeric[67] and tetrameric[67,68]

porphyrin complexes. These compounds have been characterized by ^{1}H NMR

spectroscopy. FAB-MS has recently been attempted and the trimer and tetramer observed

as weak peaks.[68]
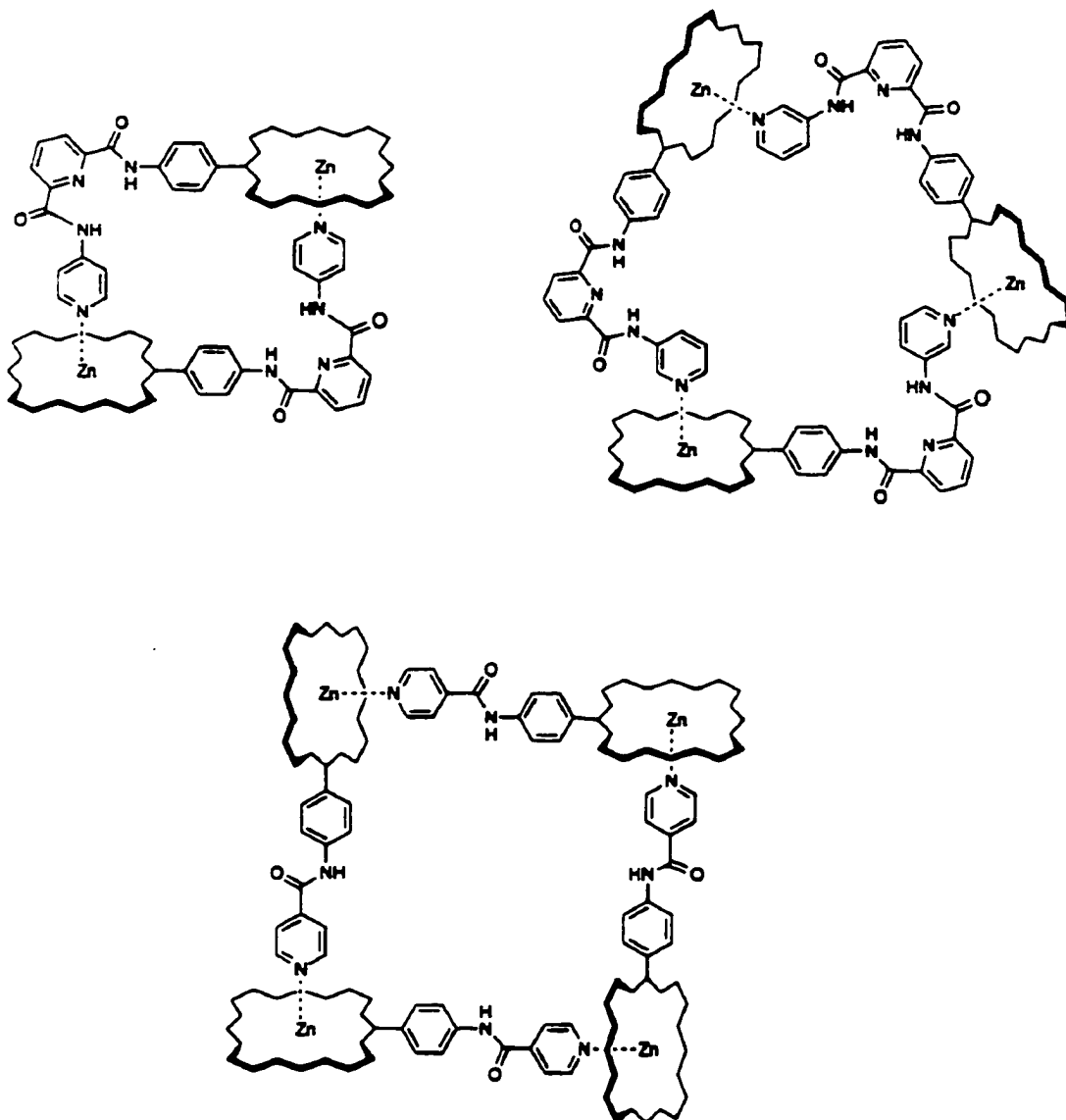


*Figure 3.6 Hunter's series of dimeric, trimeric and tetrameric porphyrin boxes*

The synthesis of all these compounds was relatively straightforward once the appropriate building blocks had been designed. Unfortunately, the synthesis cannot be considered successful unless the compound can been characterized.

## 3.2 The Characterization Problem

Self-assembly remains an emerging discipline even though it may have been the process that produced the first living cells . Structural characterization has been the largest single factor in retarding the progress of this field. The study of complexes stabilized by reversible interactions presents some difficult characterization problems.

On a biological scale, these low molecular weight complexes are often in equilibrium with their component parts. Structural information can only be readily obtained if the desired complex is isolable *and* yields X-ray quality crystals. Difficulties lie in the determination of the relative and absolute stoichiometries. The relative stoichiometry is typically determined by various titration methods, assuming that the components exhibit some measurable physical characteristics that are distinct from those features associated with the uncomplexed subunits. The assessment of absolute stoichiometry must be made after the determination of the relative ratio of the individual components. Obviously, this would be clear from the molecular weight of the complex. Mass spectrometry is most often used when the molecular weight of a compound is wanted. Unfortunately, it is not a routine experiment to determine the molecular weight of loosely coordinated species and it has not become a generally applicable technique in supramolecular chemistry. These loosely coordinated species are often not stable enough to provide a molecular ion.

As well as mass spectrometry, colligative properties may be used to estimate the molecular weight of a complex.

### 3.2.1 Mass Spectrometry

Fast Atom Bombardment mass spectrometry (FAB-MS) has been until recently, the only mild method available for the determination of molecular weight by mass spectrometry. Several supramolecular species have been investigated with this technique.[69,70] In this technique, a stream of energetic atoms (Xe or Ar) is used to ionize a sample in a condensed state. This technique, when applied to organic molecules, usually produces significant amounts of the parent ion with some fragmentation. Applied to supramolecular complexes, this technique produces mixed results. FAB-MS has a tendency to be less efficient for compounds in the range of 3000 Da and higher.[71] Liquid Secondary Ionization mass spectrometry is a technique very similar to FAB. In LSI-MS, the ionizing particle is a stream of Cs⁻ ions.

Electrospray Ionization mass spectrometry (ESI-MS) has emerged as a mild method for the characterization of a large range of molecules such as proteins, oligonucleotides, and coordination compounds[72,73,74]. No energy is required to ionize the sample, since a solution of pre-formed ions is used and only minimal energy is necessary for transferring the ions from solution to the gas phase.[75] The electrospray technique tends to produce multiply-charged species. This means that it can be use to characterize much higher molecular weight compounds.[76]. It has been possible to follow by ESI-MS, the formation of metal coordination assemblies under equilibrium conditions and obtain information about the different species present in solution.[77]

### 3.2.2 Colligative Properties

Vapour phase osmometry, freezing point depression and boiling point elevation all utilize colligative properties and have been used to assess the molecular weight of supramolecular compounds.[66,68] These methods have the advantage that they can be applied to complexes in organic solvents. These are all low resolution solution phase methods and errors can be as great as a single assembly unit. High molecular weight complexes may produce effects that are too small to be accurately measured since there is a relatively small number of molecules present under these circumstances. In boiling point elevation and freezing point depression respectively, the ebullioscopic and cryoscopic constants are solvent dependent. Since these constants must be large enough for the effects to be noticed, solvent limitations are placed on these techniques. Further, these methods based on colligative properties will only give an average molecular weight. If a mixture of oligomers has been produced, the resultant molecular weight will be an average of the oligomers.

### 3.2.3 Other Techniques

Some other techniques include, sedimentation velocity, and light scattering measurements utilizing light of comparable wavelength to the size of the particles. Equilibrium techniques include gel filtration and gel electrophoresis. The underlying assumption in these techniques is that the molecule under question is spherically shaped and evenly distributed. The use of these techniques would produce dubious results on a box like structure with a large central cavity.

Nuclear Overhauser NMR spectroscopy experiments can be used to decipher the relative position of the individual subunits. This information may provide data to determine the overall molecular architecture. Unfortunately, this method is not applicable when multiple copies of components are contained within the supramolecular complex.

## 3.3 Experimental

General Comments: 4,7-Phenanthroline and all deuterated solvents were purchased from Aldrich and used as received. All reactions were conducted under an atmosphere of $N_2$ using standard Schlenk techniques and all solvents were distilled and degassed prior to use. $^1H$, $^{13}C\{^1H\}$, spectra were recorded at 300.1and 75.4 Mhz respectively, on a Brüker AC300 spectrometer locked to the deuterated solvent. Mass spectrometry FAB was performed by the Mass Spectrometry Department, University of Alberta and University of Birmingham. LSIMS was performed an a Kratos Analytical Profile mass spectrometer at the University of Windsor. Electrospray mass spectrometry was performed by the Mass Spectrometry Department at the University of Victoria.

### 3.3.1 Preparation of [(Pd(PhS$_2$))$_2$(4,7-phen)][BF$_4$]$_2$ (26) (Ph-Cleft)

To a solution of [Pd(PhS$_2$)(CH$_3$CN)][BF$_4$] (0.184g, 0.331 mmol), in $CH_2Cl_2$ (25 mL) was added 4,7-phenanthroline (0.030g, 0.331 mmol). Diethyl ether (25 mL) was added and the precipitate collected by vacuum filtration. Crystals were grown from a diffusion of diethyl ether into a methylene chloride solution of the Ph-Cleft in $CH_2Cl_2$. Yield: 0.396g (99%). $^1H$ NMR (d6-acetone) δ (ppm) 9.36 (s, 2H, 4,7-phen), 8.93 (br s, 4H, 4,7-phen), 7.84 (s, 2H, 4,7-phen), 7.70 (s, 8H, aromatic), 7.35 (s, 8 H, aromatic), 7.24 (s, 4 H, aromatic) 5.09 (br s, 8 H, benzylic). FAB-MS [M-BF$_4$]$^+$ =1122.75 m/z.

### 3.3.2 Preparation of [(Pd(BuS₂))₂(4,7-phen)][BF₄]₂ (27) (Bu-Cleft)

To a solution of [Pd(BuS₂)(CH₃CN)][BF₄] (0.172g, 0.333 mmol), in $CH_2Cl_2$ (25 mL) was added 4,7-phenanthroline (0.030g, 0.333 mmol). Diethyl ether (25 mL) was added and the precipitate collected by vacuum filtration. Crystals were grown from a diffusion of diethyl ether into a solution of Bu-Cleft in $CH_2Cl_2$. Yield: 0.396g (99%). $^1$H NMR (d6-acetone) δ (ppm) 9.81 (br m , 2H, 4,7-phen), 9.64 (br m, 4H, 4,7-phen), 8.25 (q, 2H, 4,7-phen), 7.08 (s, 6H, aromatic), 4.56 (br s, 8 H, benzylic), 3.05 (br, 8H, S-CH₂), 1 56 (br, 8H, S-CH₂-CH₂), 1.13 (br, 8H, CH₂-CH₃), 0.65 (br, 12H, CH₂-CH₃). LSI-MS [M-BF₄]⁻ = 1042.81 m/z.

### 3.3.3 Preparation of [(Pd₂(PhS₄))₃(4,7-phen)₃][BF₄]₆ (28) (Ph-Box)

Equimolar solutions of 4,7-phenanthroline and [Pd₂(PhS₄)(CH₃CN)₂][BF₄]₂ were mixed in methylene chloride, acetone or methanol. Neither the rate of addition nor the order of the addition seems to affect the product. A broad range of concentrations were used, with the total concentration of reagents ranging from 3.17 μM to 1.47 M. The solutions were allowed to slowly evaporate. Crystals were usually obtained from methylene chloride, and pale yellow powder from either acetone or methanol. The precipitated material was clean and did not require further recrystallization. In all cases the yield was in excess of 90%. $^1$H NMR (333K) (d6-acetone) δ (ppm) 9.42 (d, 6H, 4,7-phen), 9.00 (br s, 6H, 4,7-phen), 8.84 (br s, 6H, 4,7-phen), 7.82 (q, 6H, 4,7-phen), 7.71 (m, 24 H, aromatic), 7.44 (m, 36H, aromatic) 5.27 (dd, 24H, benzylic). FAB-MS [M-BF₄]⁻ = 1122.75 m/z, [M-2BF₄]²⁺ = 1610.0 m/z. LSI-MS [M-3BF₄]³⁺ = 1044 m/z.

### 3.3.4 Preparation of [(Pd₂(BuS₄))₃(4,7-phen)₃][BF₄]₆ (29) (Bu-Box)

Equimolar solutions of 4,7-phenanthroline and $[Pd_2(BuS_4)(CH_3CN)_2][BF_4]_2$ were added to methylene chloride or acetone. The range of concentrations studied ranged from 3.29 $\mu M$ to 1.54 M in total component concentration. The solutions were allowed to slowly evaporate. Nearly colourless crystals were sometimes obtained from acetone, and very light yellow powder from methylene chloride. The precipitated material was clean and did not require further recrystallization. In all cases the yield was in excess of 90%.

$^1H$ NMR (d6-acetone) $\delta$ (ppm) 9.81 (m, 12H, 4,7-phen), 9.68 (m, 6H, 4,7-phen), 8.28 (quartet, 6H, 4,7-phen), 4.69 (br s, 24 H, benzylic), 3.10 (br, 24H, S-C$\underline{H}_2$), 1.63 (br, 24H, S-C$\underline{H}_2$-CH₂), 1.18 (br, 8H, C$\underline{H}_2$-CH₃), 0.69 (br, 36H, CH₂-C$\underline{H}_3$). FAB-MS $[M-3BF_4]^{3+}$ = 964 m/z.

## 3.4 X-ray Structure Determinations

### 3.4.1 Structure Determination of Bu-Cleft

The diffraction experiment was carried out on a Rigaku AFC5s four circle diffractometer with graphite-monochromatizied MoKα radiation. The orientation matrices and unit cell parameters were obtained from 25 centred reflections (15°<2θ<35°). Standard reflections were measure every 150 reflections and a linear correction applied for significant changes over the course of a data collection. Data was collected in four shells (2θ<30,40,45,50°) using the Weak reflections (I<10.0σ(I)) were rescanned a maximum four times and the counts averaged. The data was processed using the TeXsan software package on an SGI Challenge XL on a remote X-terminal. Refinements were carried out by using full-matrix least-square techniques on F by

minimizing the function $\Sigma w(|F_o| - |F_c|)^2$ where $w = 1/\sigma^2(F_o)$ and $F_o$ and $F_c$ are the observed

and calculated structure factors. Absorption corrections were applied from azimuthal

scans. All data were corrected for Lorentz and polarization effects.

Pale yellow crystals were grown by slow evaporation of an acetone solution of this

compound. A statistical analysis of intensity distributions was consistent with the space

group $P\bar{1}_n$ and this was confirmed by a successful solution refinement. A total of 9686

reflections were collected and 2303 unique reflections with with $F_o^2 > 3\sigma(F_o^2)$ were used in

the refinement. A trial structure was obtained from the SHELX-86 direct methods from

the TeXsan package. The structure was expanded using successive difference Fourier

maps until all non-hydrogen atoms were located. In the final cycles palladium, sulphur and

nitrogen atoms were refined anisotropically. All hydrogen atom positions were calculated

for ideal positions with C-H bonds lengths fixed at 0.95Å. Hydrogen atom thermal

parameters were fixed at a factor of 1.20 of the carbon atoms to which they were bonded.

The resulting fit was R=0.084 and $R_w$=0.072 at final convergence. The goodness of fit

was 2.65 and a $\Delta/\sigma$ value for any parameter in the final cycle was less than 0.026. A final

difference Fourier map showed no peaks of chemical significance, the largest being 1.1 e⁻

/Å³ associated with $BF_4^-$ disorder. Listings of atomic positional parameters and selected

bond distances and angles are deposited in Appendix B.

### 3.4.2 Structure Determination of Ph-Box

The diffraction experiment was carried out on Siemen's SMART system with the

CCD detector under graphite-monochromatizied MoKα radiation. The data was collected

in 1321 frames covering 1.3 hemispheres at -120°C over 13 hours. The data was

processed using the Shelx software package on an SGI Challenge XL. Refinements were carried out by using conjugate gradient least square techniques on $F^2$ by minimizing the function $\Sigma(F_o^2-F_c^2)^2/\Sigma[(F_o^2)^2]^{1/2}$ where $F_o^2$ and $F_c^2$ are the observed and calculated structure factors. All data were corrected for Lorentz and polarization effects.

Pale yellow crystals were grown by slow evaporation of a methylene chloride solution of this compound. The space group initially chosen was $P\bar{1}$ with $Z=4$. During structure refinement, large discrepancies between observed and calculated structure factors prompted the change in space group to $P1$. Initial refinements displayed no correlation of the heavy atom positions. A total of 49179 reflections were collected and 22772 unique reflections with with $F_o^2>4\sigma(F_o^2)$ were used in the refinement. A trial structure was obtained from SHELXS-93 direct methods. The structure was expanded using successive difference Fourier maps. Palladium and sulphur atoms were refined anisotropically. The structure is currently in a preliminary stage of refinement.

## 3.5 Results and Discussion of Clefts

### 3.5.1 Synthesis of Clefts

The cleft structure represents the transition from simple building blocks to the supramolecular box in as much as it represents a single corner or vertex. Before attempting to characterize a box, it was necessary to determine if the box was feasible by examining the cleft. The $Pd(BuS_2)$ and $Pd(PhS_2)$ compounds were chosen from the toolbox of pieces. The corner piece chosen was 4,7-phenanthroline. With these two pieces, the cleft is the only possible structure expected to form. In a non-competitive solvent such as acetone or methylene chloride, the better donor, 4,7-phenanthroline

displaces the labile acetonitrile which normally occupies the fourth coordination position

of palladium. When mixed in a ratio 2:1, $PdS_2$:4,7-phen, the expected result is the cleft.

### 3.5.2 $^1H$ NMR Spectroscopy

The $^1H$ NMR spectra are consistent with the proposed cleft-like structures. The

ratio of wall unit to phenanthroline is 2:1 and the phenanthroline region is symmetrical.

As a result of coordination to the electron deficient metal, the protons on 4,7-

phenanthroline exhibit a significant downfield shift. The $^1H$ NMR spectrum of Bu-Cleft

is labeled below with the protons of interest and their shift relative to free 4,7-
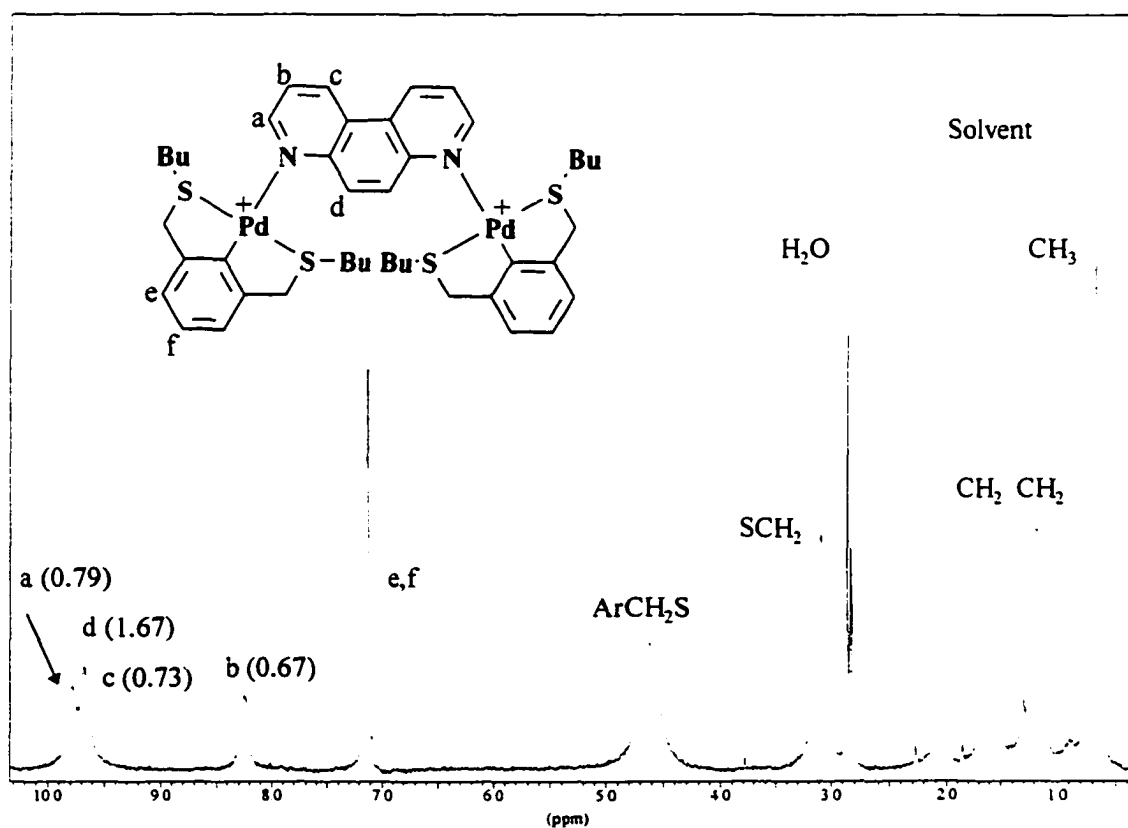
phenanthroline.



Figure 3.7 $^1H$ NMR spectrum in d6-acetone of Bu-Cleft. Numbers in brackets represent
downfield shifts of complexed 4,7-phenanthroline relative to free 4,7-phenanthroline

The $^1$H NMR spectrum of the Ph-Cleft is similar to the Bu-Cleft's, although the observed chemical shifts for the phenanthroline protons are not as great. This may be attributable to $\pi$-stacking interactions with the phenyl groups which cause upfield shifts.[78,79] The VT $^1$H NMR spectra are consistent with this since the phenanthroline region is temperature dependent. At room temperature, both the benzylic peak and the phenanthroline region are broad. As the temperature increases, the benzylic peak sharpens and there is a corresponding sharpening in the phenanthroline region. This sharpening of the phenanthroline region is not observed in the Bu-Cleft.

In both the Ph- and Bu-Cleft, the high temperature spectrum (344 K in $CD_2Cl_2$) exhibits a sharp singlet for the benzylic peak. This implies that there is free rotation about the Pd-N bond since the diastereotopic protons are observed in only one environment.

### 3.5.3 Mass Spectrometry

Molecular weights for both the Ph- and Bu-Cleft were determined by LSIMS and FAB mass spectrometry. Originally, samples were sent to University of Alberta Chemistry Department for FAB-MS. With this technique, fragmentation resulted in the peaks at 427 and 607 m/z for the Ph-Cleft and 387 and 568 m/z for the Bu-Cleft. The parent ion [M-BF$_4$]$^-$ could not be located for either the Bu-Cleft or Ph-Cleft.

m/z=427

m/z=607

m/z=387

m/z=568
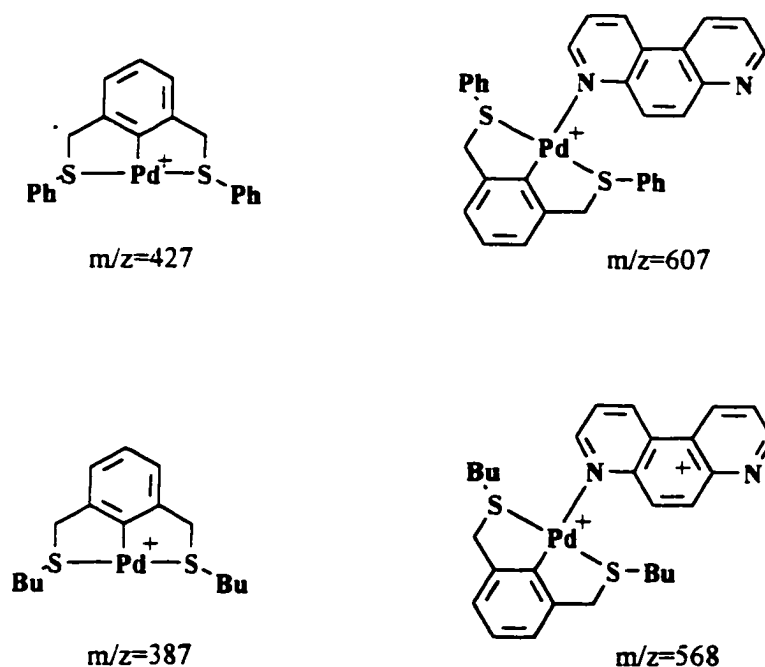
*Figure 3.8  Assigned fragments of the prominent peaks in the FAB and LSIMS of Ph-Cleft and Bu-Cleft.*

After several trials on LSIMS at the University of Windsor, the parent ion was found for both clefts. The peaks were very weak and poorly resolved. The Bu-Cleft parent ion was $[M-BF_4]^- = 1042.81$. The University of Birmingham satisfactorily resolved the parent ion $[M-BF_4]^* = 1122.75$ for the Ph-Cleft. Since there are six abundant isotopes of palladium (eighteen in all), the isotopic distribution provides an excellent fingerprint for the identification of the species. The observed isotopic distribution was in agreement with the calculated pattern.
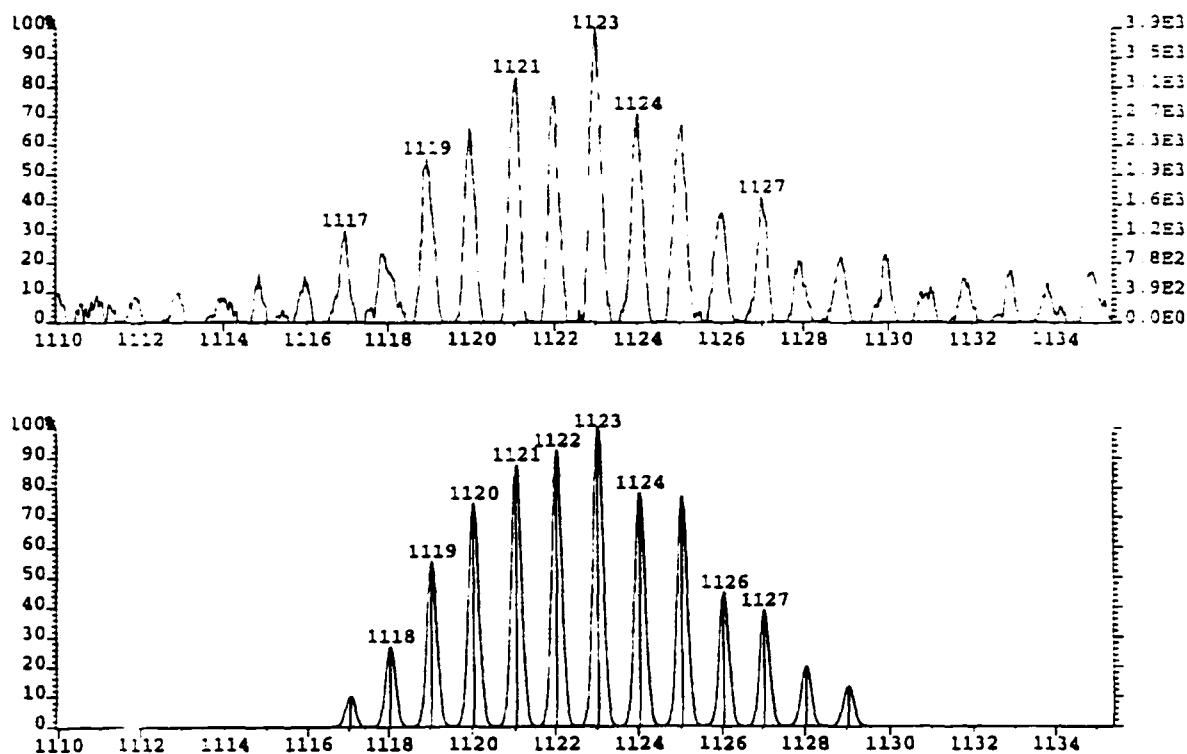
Figure 3.9 A comparison of the observed (top) and calculated (bottom) isotopic distribution of the parent ion for the Ph-Cleft

### 3.5.4 X-Ray Crystallography

The Bu-Cleft was characterized by X-ray crystallography. The complex crystallizes with four molecules per unit cell with no crystallographically imposed symmetry. As expected, the structure has two $Pd(BuS_2)$ groups coordinated to the corner piece, 4,7-phenanthroline. Consistent with the $Pd_2(PhS_4)(1,10\text{-phen})_2$ structure is the deviation from orthogonality between the coordination plane of the palladiums and the plane of the phenanthroline. In this case, the angles formed between the planes at Pd(1) and Pd(2) are 71.4° and 69.5° respectively. For steric reasons, the sulphurs at each metal adopt anti conformations. This results in one butyl group from each $Pd(PhS_2)$ group occupying the space directly above and below the cavity in the cleft and the other butyl

group oriented away from the cavity. A key factor in deciding whether the box structure could be formed was the angle between the two Pd-N bonds. To form the box, the angle should ideally be 60°. This angle in the crystal structure was a nearly ideal 60.57°. Occupying the cavity of the cleft is one of the $BF_4^-$ counter-ions. Pd(1)-F(4) and Pd(2)-F(2) distances are 3.93(2) and 3.99(3) Å respectively. A weak bifurcated hydrogen bond may exist between F(1) and C(38) and C(39) of phenanthroline. The distance from fluorine to both carbons is 3.34(2) Å. Each palladium exists in a slightly distorted square planar environment. Bond angles and distances are typical. Selected bond distances and angles can be found in appendix B.

Crystals of the Ph-Cleft were grown and X-ray diffraction data collected, but all attempts at solving it have failed. The crystals seem to be severely disordered. The unit cell and contents are consistent with the proposed formulation.
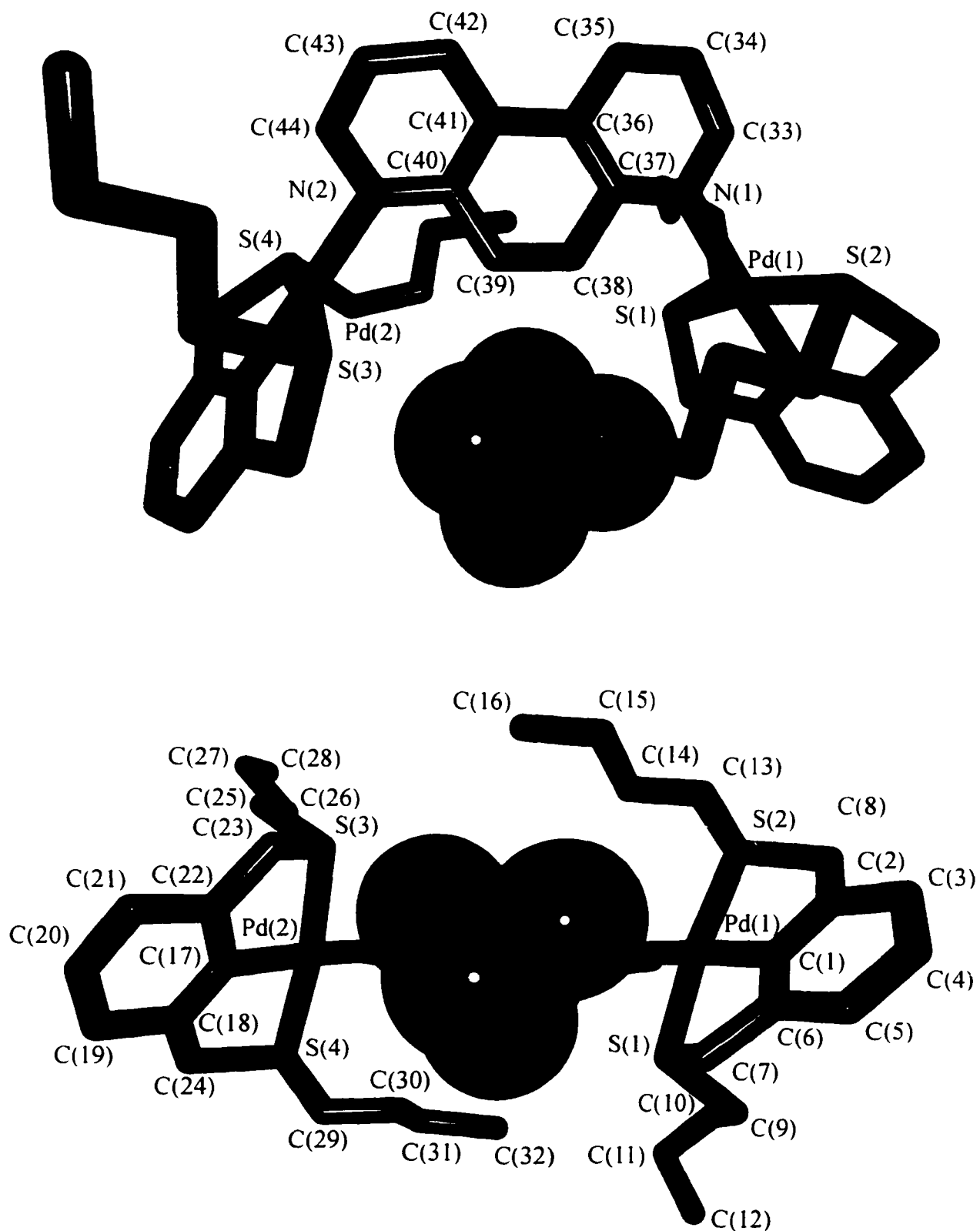
Figure 3.10 X-ray crystal structure of Bu-Cleft with two views. The BF₄ occupying the cavity of the cleft is shown with Van der Waals radii. The cleft is shown as a tube structure.

## 3.6  Results and Discussion of Molecular Boxes

### 3.6.1  Synthesis of Molecular Boxes

After successful characterization of the cleft structures, the synthesis of the molecular boxes was achieved using the compounds $Pd(BuS_4)$ and $Pd(PhS_4)$. The corner piece used was 4,7-phenanthroline. In contrast to the cleft, there are several possible products, the desired cyclic structure and various oligomeric materials. When mixed in a 1:1 ratio, $[Pd_2(RS_4)]$:4,7-phenanthroline, the sole product is the box structure. This is supported by $^1H$ NMR spectroscopic evidence,

### 3.6.2  $^1H$ NMR Spectroscopy

The $^1H$ NMR spectrum of the Bu-Box is shown below. Significant shifts occur to the phenanthroline protons as a consequence of their binding to the metal centre. These shifts are similar in magnitude to the Bu-Cleft. Integration of the phenanthroline peaks and the wall pieces indicates that the relative stoichiometry of the components is one to one. The determination of whether acyclic oligomeric material, the desired cyclic trimer or a combination of material was present in solution was not obvious from the $^1H$ NMR spectra. In the literature, there are several examples where a symmetric NMR spectrum has been taken as sufficient evidence that the cyclic product has been produced.[62,64,65] It was assumed that oligomeric material would produce extra or complicated signals in the $^1H$ NMR spectra, and there have been examples where this is the case.[72,73] If this were taken to be generally true then the $^1H$ NMR spectra indicates that the Bu- and Ph-Box have the desired cyclic structure.
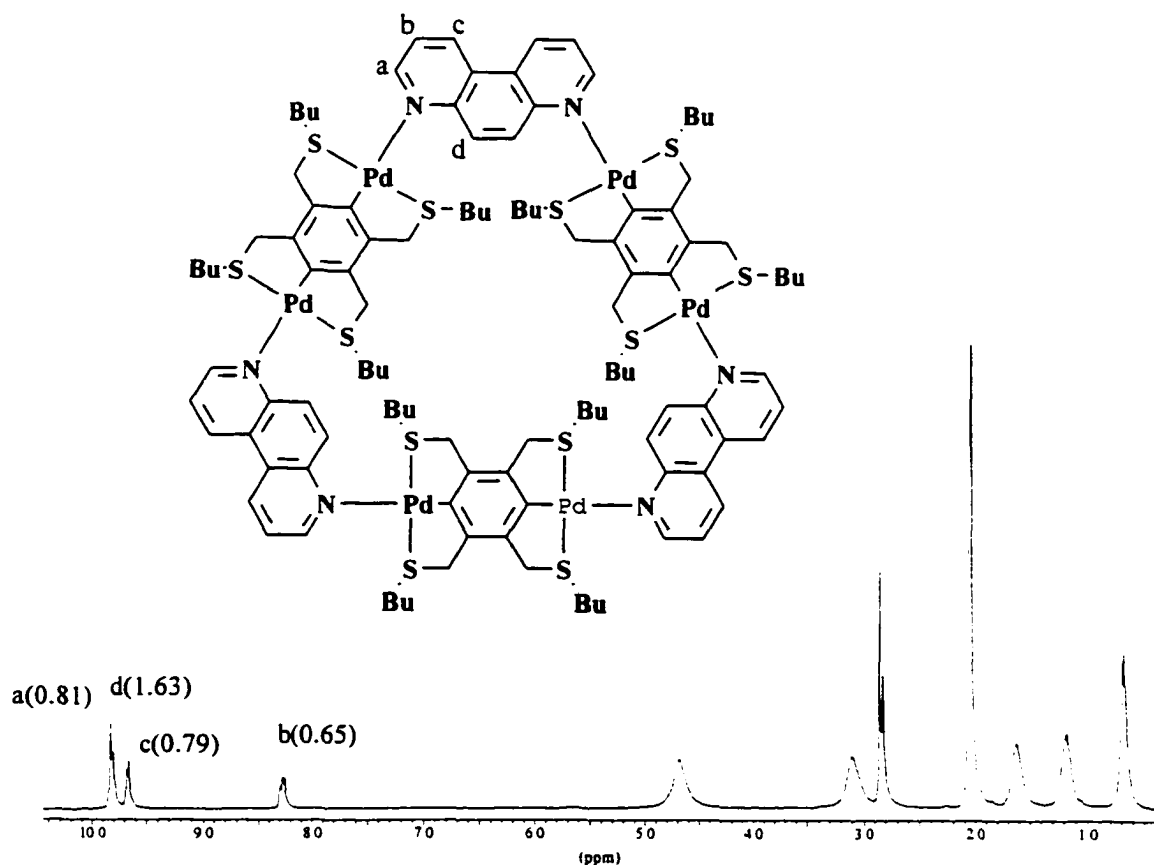
Figure 3.11 $^1H$ NMR spectrum of Bu-Box in d6-acetone. The numbers in brackets represent the downfield shift of complexed 4,7-phenanthroline relative to free 4,7-phenanthroline

The assembly of these pieces must occur in a stepwise process at some level, and the rate at which the system reaches a thermodynamic minimum will determine whether any intermediate pieces are observable. In this stepwise assembly, the order of addition of the compounds may be significant. Consider the reaction where one component has been added to an excess of the other. Statistically there will initially be one major compound with components assembled in a 2:1 ratio. This species must be in equilibrium with the precursor to the box which contains components in a 3:2 ratio. The final step is the formation of the box. Addition of the wall unit to the corner piece should most effectively

form the box since there are fewer structures leading to acyclic material. Experimentally

this is not observed. The excess components are always observed at their uncomplexed

positions in the ¹H NMR spectra and the ratio of complexed wall to corner piece is always

1:1. The consequence of this is that the molecular box must be the sole product of the

reaction and assembly must occur in a matter of seconds. Furthermore, the second and

final steps in the self-assembly process are kinetically faster than the first step.



2:1                              3:2                                1:1
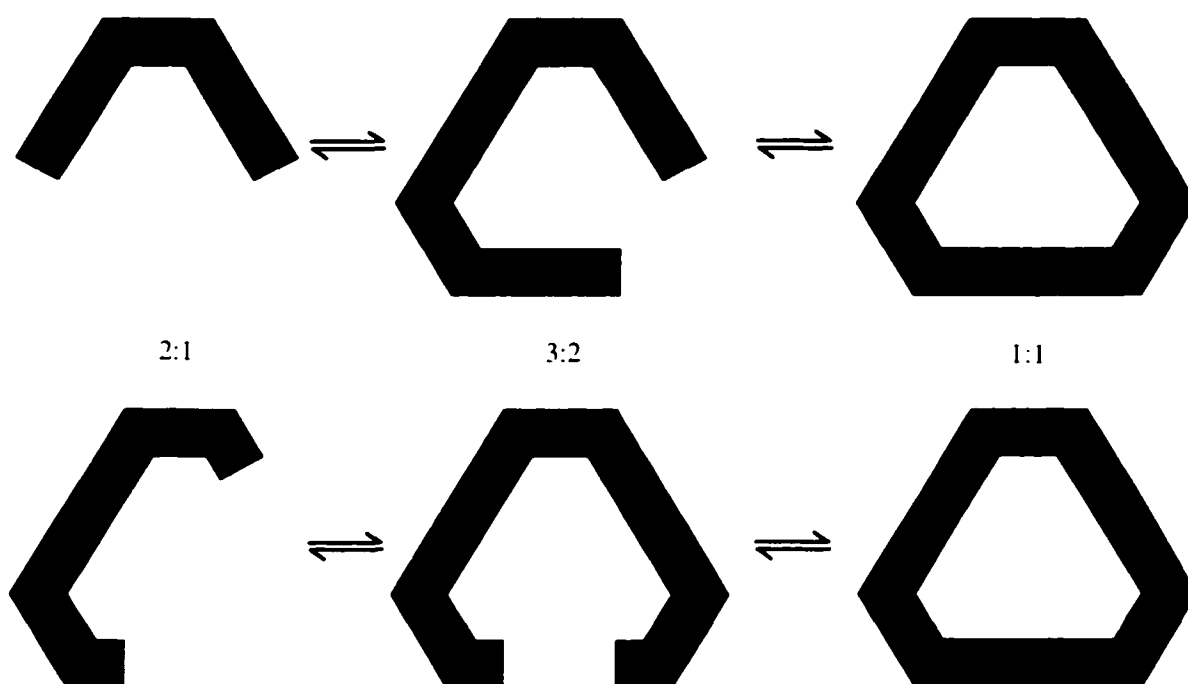


Figure 3.12 The schemes represent the stepwise assembly of a container when one
component is added to an excess of the other. Shown are the possible structures leading
to the assembly of the molecular box when the corner is added to an excess of wall (top
scheme) and the wall added to an excess of the corner units. (bottom scheme)

The high temperature ¹H NMR spectra for the Ph-Box displayed a doublet of

doublets for the benzylic protons. This is consistent with the cyclic structure proposed as

the benzylic protons are in different environments, inside and outside of the box. As well.

the phenanthroline region displays a temperature dependence similar to the Ph-Cleft This

is presumably due to π-stacking interactions of the pendant phenyl groups with the 4,7

phenanthroline as this behavior is not observed in the Bu-Cleft or the Bu-Box.
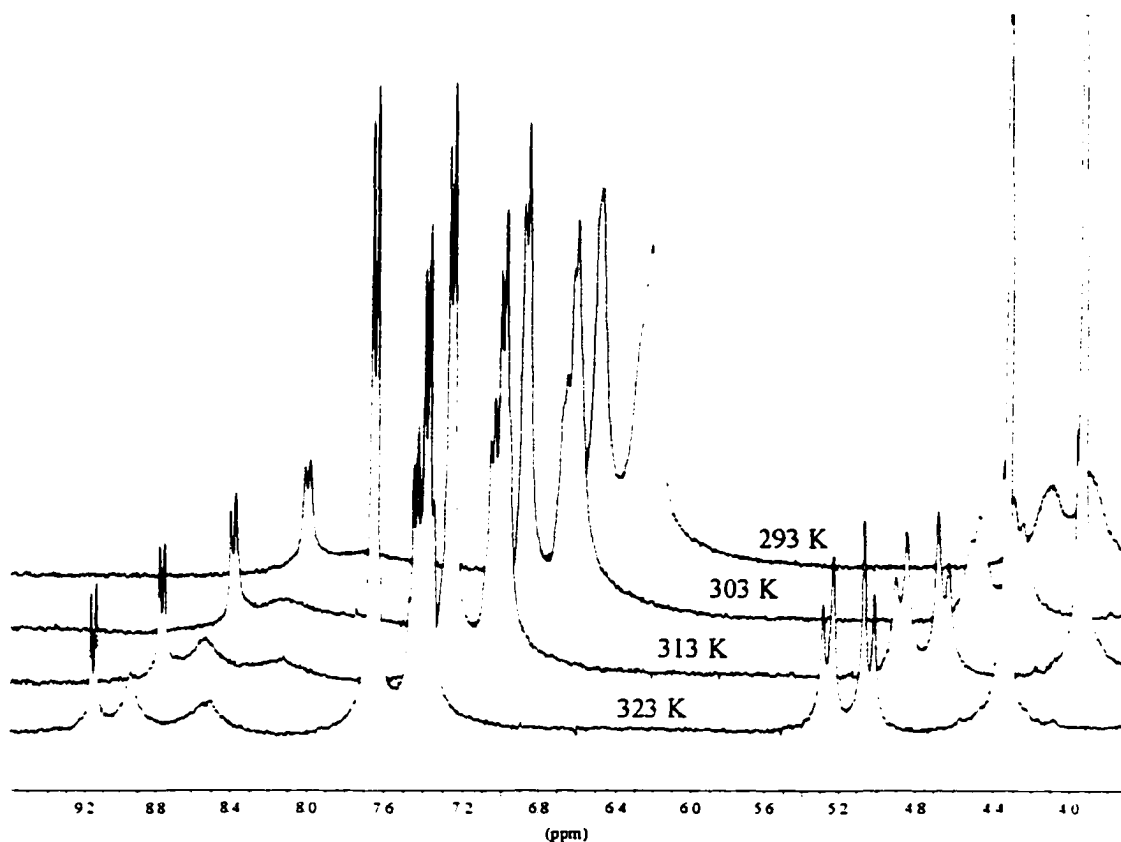


*Figure 3.13  VT 1H NMR spectra (CD₂Cl₂) of  Ph-Box showing high temperature(323K) doublet of doublets for the benzylic protons.  The phenanthroline region also demonstrates temperature dependence due to π-stacking interactions with the pendant phenyl groups.*

### 3.6.3  Mass Spectrometry

Given the difficulty encountered obtaining molecular weights of the clefts by mass

spectrometry, we were not optimistic that molecular weight information could be

obtained.  Samples were sent to the University of Alberta, and the University of

Birmingham for FAB-MS and to the University of Victoria for ESI-MS.  As well many

attempts were made here at the University of Windsor under LSIMS. There was

significant fragmentation with all the techniques and very few peaks were useful in

determining the degree of aggregation. In all the spectra of the Ph-Box only two peaks

were of interest. A weak peak at 1610.0 m/z found by FAB was assigned to $[M-2BF_4]^{2-}$

A peak at 1044 was found by LSI-MS and assigned to the species, $[M-3BF_4]^{3-}$ The Bu-

Box afforded only a single peak indicative of the degree of aggregation. A multiply

charged peak observed at 964 m/z corresponded to the species $[M-3BF_4]^{3-}$. The major

concern from the various mass spectrometry departments was that the boxes were

sufficiently soluble in non-competitive solvents to provide good spectra. The ability to

obtain a respectable NMR spectrum does not seem to be an adequate measure of the

solubility required for obtaining FAB-MS or ESI-MS results. In hind sight the use of $PF_6^-$

instead of $BF_4^-$ as a counter-ion may be more effective.

### 3.6.4 X-Ray Crystallography

From the initial syntheses of these molecular boxes, crystals could essentially be

grown overnight. The crystals were typically small and lost solvent within seconds.

Crystals of the Ph-Box could be grown only from methylene chloride and all attempts at

obtaining crystals using less volatile solvents failed. Crystals of the Bu-Box were grown

from acetone but could not be grown from other solvents. Attempts at obtaining a crystal

structure resulted in only a rough unit cell before the crystal decayed. The unit cell was

primitive and triclinic with Z=2 for the expected cell contents. These results coupled with

encouraging mass spec results and consistent $^1H$ NMR spectra was considered evidence

that these compounds had been successfully prepared in essentially quantitative yields. A

last effort was made at obtaining a crystal structure. A set of crystals of the Ph-Box was

sent to Siemens for the diffraction experiment on their new SMART CCD diffractometer

A very large set of data was collected, and subsequently solved to a degree that confirmed

the proposed structure. The structure is preliminary and is based on the triclinic space

group P1 with Z=4. Available crystallographic data is tabulated below.

*Table 3.1  Crystallographic Data for Ph-Box*

| | |
|---|---|
| Empirical Formula | $C_{144}H_{120}N_6S_{12}Pd_6B_6F_{24}$ |
| Fw | 3478.32 |
| a,Å | 21.8740(4) |
| b,Å | 24.5519(5) |
| c,Å | 27.1042(5) |
| $\alpha$ | 93.424(1) |
| $\beta$ | 99.810(1) |
| $\gamma$ | 103.406(1) |
| Crystal System | Triclinic |
| Space Group | *P1* |
| Vol. Å$^3$ | 13877.6(4) |
| Z | 4 |
| Diffractometer | Siemens SMART CCD |
| $\lambda$, Å (Mo K$\alpha$) | 0.71073 |
| T (°C) | -120 |

A paper recently published by Raymond has a crystal structure of a molecular box

which crystallized in the space group $I4_1$ and sits on a special position having $\bar{4}$

symmetry.[80] This paper contains the following excerpt "the success of this pre-designed,

symmetry-driven system supports the explanation of the formation of the highly

symmetrical clusters seen in nature.". How ironic that the Ph-Box, being rigid and having

such potential for high symmetry should crystallize in a space group with no symmetry,

*and* four molecules per asymmetric unit.

Figure 3.15 demonstrates the size of the cavity of the box. The diagram is a molecular model of the actual box with the phenyl groups projected away from the cavity For reference. $C_{60}$ fullerene has been placed in the centre of the cavity and Van der Waal radii of the molecules displayed as dotted spheres. $C_{60}$ is not in contact with the Van der Waal surface of the box. The atom to atom distances are taken from the actual crystal structure
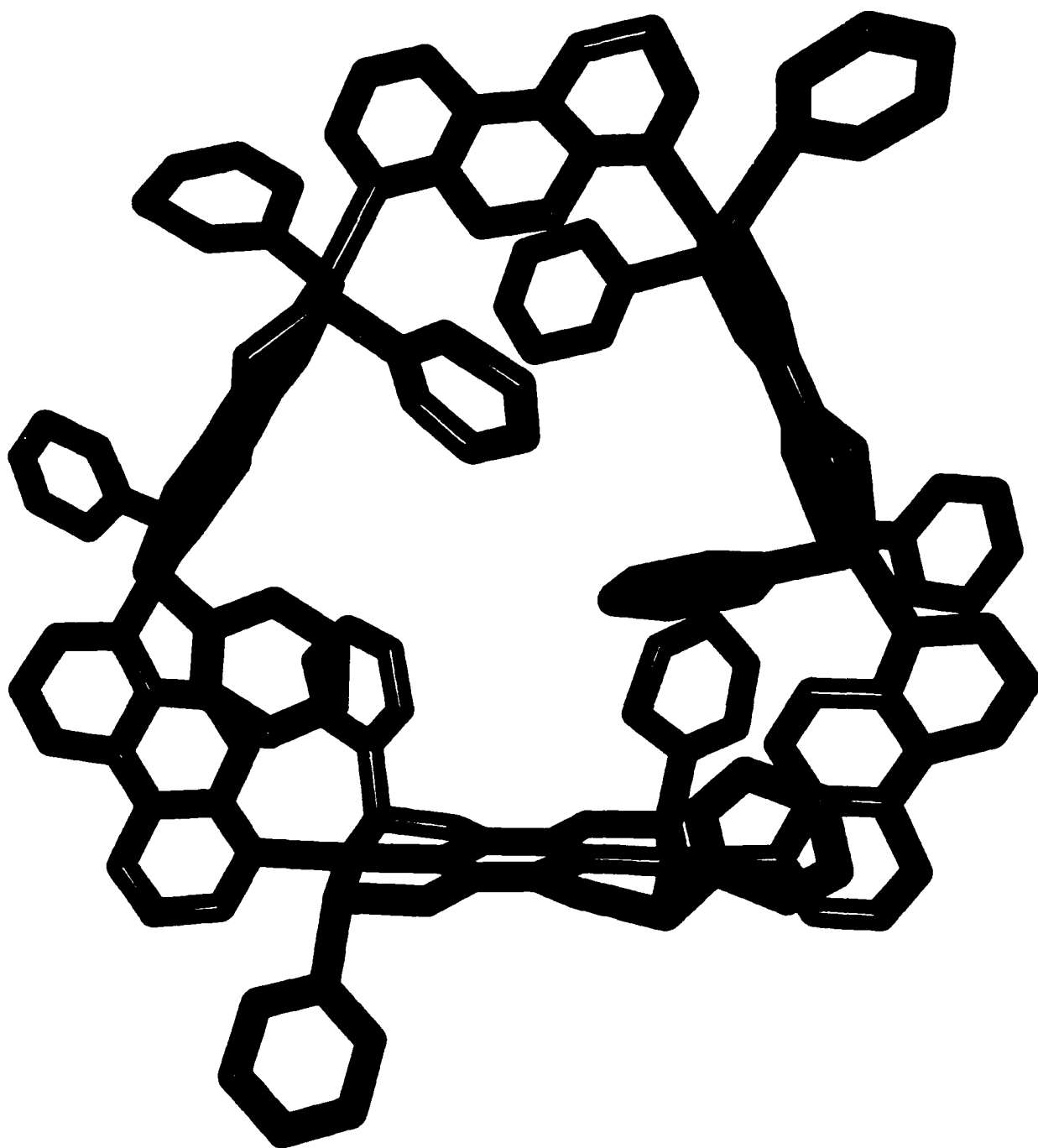
*Figure 3.14 Preliminary X-ray crystal structure of one of the molecules in the unit cell of the Ph-Box*
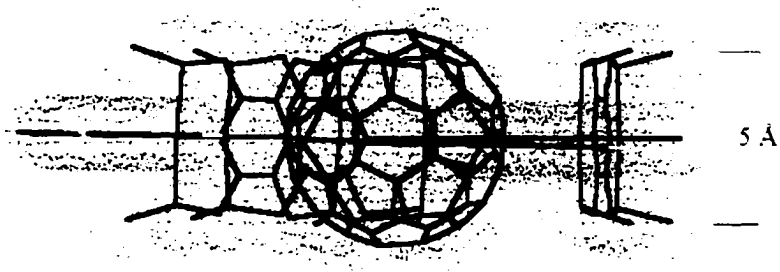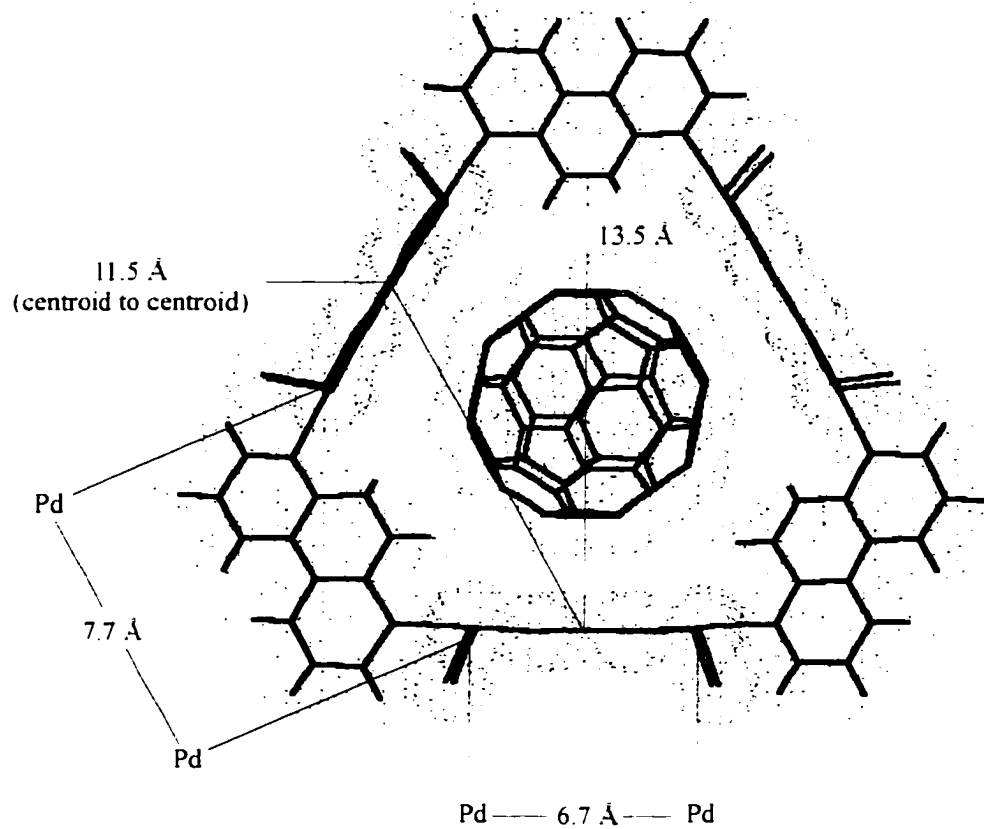
*Figure 3.15 Depiction of the cavity of the box. $C_{60}$ fullerene has been added for reference and shows no Van der Waal contact with the box*

## 3.7 Summary and Conclusions

The components selected from a molecular toolbox were used to construct molecular clefts and box structures via self-assembly. Components were mixed at room temperature and the products recovered in essentially quantitative yields. Characterization of these compounds was accomplished by $^1$H NMR spectroscopy, mass spectrometry and X-ray crystallography. The latter technique produced structures for the Bu-Cleft and the Ph-Box. Nature appears to build intricate shapes with ease. Chemists are just beginning to utilize some of the tools necessary for the construction of complex structures. Eventually applications ranging from catalysis, to nanoscale machines will result from the increasingly complex supramolecular architectures produced via self-assembly.

# APPENDIX A

## A.1 Diagrams of Synthesized Compounds
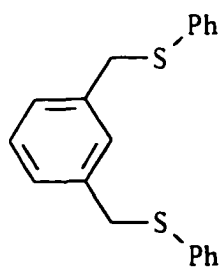
(1) $PhS_2$
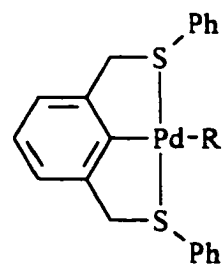
(2) $R=CH_3CN$
(3) $R=Cl$
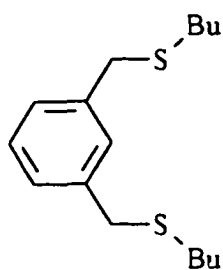
(4) $BuS_2$
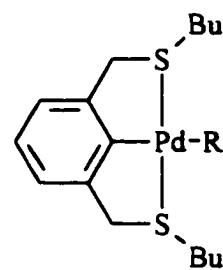
(5) $R=CH_3CN$
(6) $R=Cl$
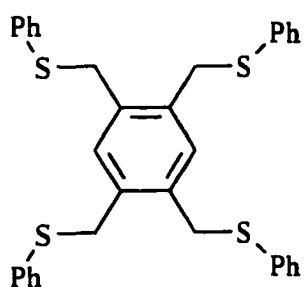
(7) $PhS_4$
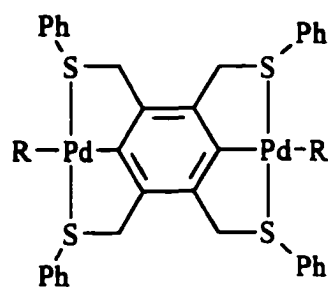
(8) $R=CH_3CN$
(9) $R=Cl$
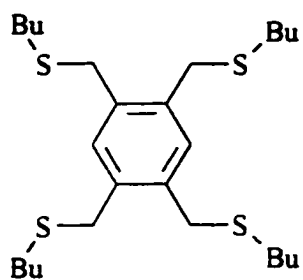
(10) BuS$_4$
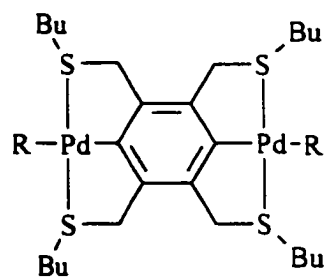
(11) R=CH$_3$CN
(12) R=I
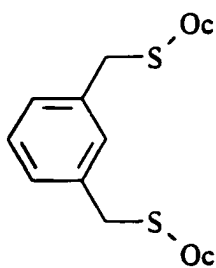
(13) OctS$_2$
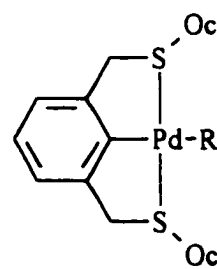
(14) R=CH$_3$CN
(15) R=Cl
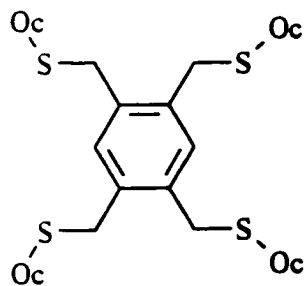
(16) OctS$_4$
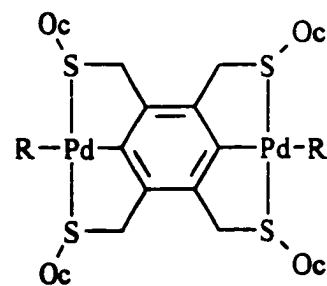
(17) R=CH$_3$CN
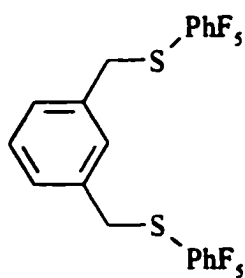
(18) F$_5$PhS$_4$
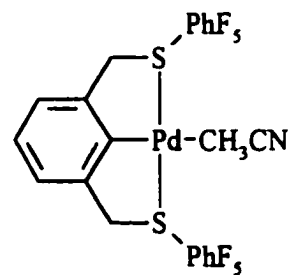
(19) R=CH$_3$CN
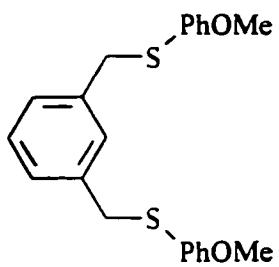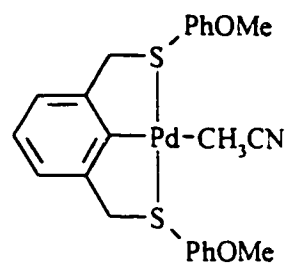
(21) X = BF$_4$

(22) X = CF$_3$SO$_3$

(20) MeOPhS$_4$
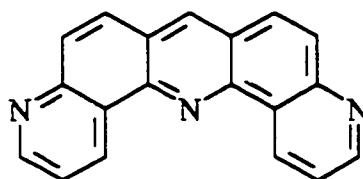
(23) Quino[5,6-b]1,7-phenanthroline
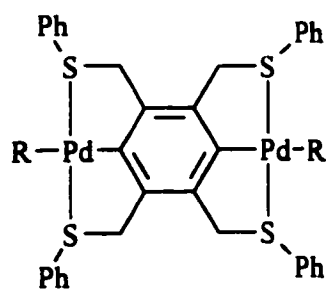
(24) R = 1,10-phenanthroline
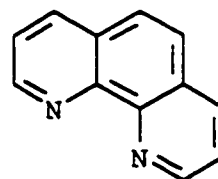
(25) R = Quinoline
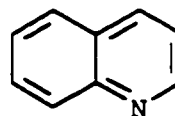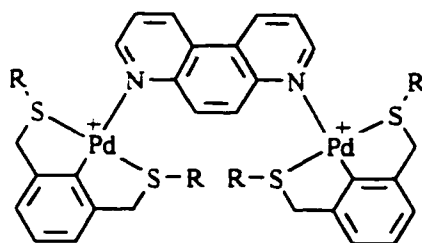
(26) R = Ph, Ph-Cleft
(27) R = Bu, Bu-Cleft
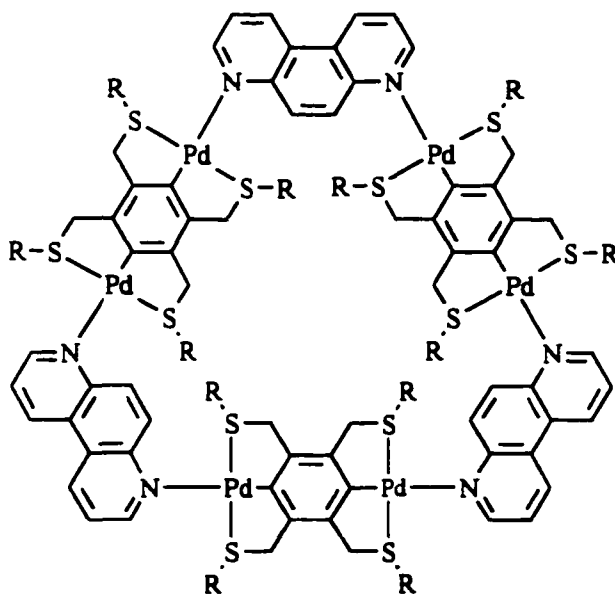


(28) R = Ph, Ph-Box
(29) R = Bu, Bu-Box

# APPENDIX B

## B.1  Supplementary Data for X-ray Structure Determinations

*Table B. 1 Details of Crystallographic Data Collection, Solution and Refinement for [Pd(PhS₂)(CH₃CN)][BF₄]*

| | |
|---|---|
| Empirical Formula | $C_{20}H_{17}S_2PdCl$ |
| Fw | 555.73 |
| a,Å | 15.631(13) |
| b,Å | 8.089(3) |
| c,Å | 18.191(10) |
| α | |
| β | 94.792(54) |
| γ | |
| Crystal System | Monoclinic |
| Space Group | $P2_1/n$ |
| Vol. $Å^3$ | 2291.969(2.05) |
| Z | 4 |
| $\mu$ $(cm^{-1})$ | 10.34 |
| $\rho_{calc}$, $g/cm^3$ | 1.61 |
| Diffractometer | Rigaku AFC6S |
| λ, Å (Mo Kα) | 0.7107 |
| T (°C) | 23 |
| scan type | ω-2θ |
| speed, deg $min^{-1}$ | 8 |
| No. Observations Unique | 3265 |
| No. Observations (I>3.00σ(I)) | 1512 |
| No. Variables | 256 |
| Reflection/Parameter Ratio | 5.9:1 |
| R,% | 4.9 |
| $R_w$ % | 4.0 |
| GOF | 2.02 |
| (Δ/σ)max | 2.11 |
| $\Delta\rho_{min}$, $e^-/Å^3$ | -0.571 |
| $\Delta\rho_{max}$, $e^-/Å^3$ | 0.8 |

Table B.2 Selected Positional Parameters and $B_{eq}$ for $[Pd(PhS_2)(CH_3CN)][BF_4]$

| atom | x | y | z | $B_{eq}$ |
|------|-----|-----|-----|-----|
| Pd(1) | 0.03308(6) | -0.0282(1) | -0.18288(6) | 4.26(5) |
| S(1) | 0.1687(2) | 0.0300(4) | -0.1302(2) | 4.9(2) |
| S(2) | -0.1136(2) | -0.0775(4) | -0.2002(2) | 5.0(2) |
| N(1) | 0.0391(7) | 0.092(1) | -0.2845(6) | 5.2(6) |
| C(1) | 0.249(1) | -0.041(2) | -0.2580(9) | 6.1(8) |
| C(2) | 0.320(1) | -0.034(2) | -0.2991(8) | 6.5(8) |
| C(3) | 0.392(1) | 0.039(2) | -0.273(1) | 7(1) |
| C(4) | 0.399(1) | 0.102(2) | -0.203(1) | 7(1) |
| C(5) | 0.3305(8) | 0.098(2) | -0.1593(8) | 5.4(8) |
| C(6) | 0.2563(7) | 0.025(2) | -0.1873(7) | 4.3(6) |
| C(7) | 0.1863(7) | -0.161(2) | -0.0763(7) | 5.0(7) |
| C(8) | 0.1006(8) | -0.198(1) | -0.0471(7) | 4.0(7) |
| C(9) | 0.0973(8) | -0.281(2) | 0.0191(8) | 4.6(8) |
| C(10) | 0.016(1) | -0.314(2) | 0.0423(8) | 5.3(8) |
| C(11) | -0.0574(8) | -0.266(2) | 0.0034(9) | 4.5(8) |
| C(12) | -0.0542(8) | -0.180(1) | -0.0621(8) | 3.9(7) |
| C(13) | 0.0275(8) | -0.149(1) | -0.0883(7) | 4.2(7) |
| C(14) | -0.1335(8) | -0.118(1) | -0.1054(8) | 5.0(7) |
| C(15) | -0.1285(7) | -0.271(2) | -0.2439(9) | 4.3(7) |
| C(16) | -0.1316(8) | -0.419(2) | -0.2063(7) | 5.2(8) |
| C(17) | -0.1430(9) | -0.566(2) | -0.244(1) | 7(1) |
| C(18) | -0.149(1) | -0.569(2) | -0.319(1) | 7(1) |
| C(19) | -0.145(1) | -0.424(3) | -0.357(1) | 9(1) |
| C(20) | -0.1353(9) | -0.273(2) | -0.319(1) | 6(1) |
| C(21) | 0.0427(9) | 0.150(2) | -0.3391(9) | 4.9(8) |
| C(22) | 0.0478(9) | 0.230(2) | -0.411(1) | 7(1) |

*Table B.3 Selected Bond Distances and Angles for [Pd(PhS₂)(CH₃CN)]/[BF₄]*

## Distances(Å)

| | | | |
|---|---|---|---|
| Pd(1)-S(1) | 2.301(3) | C(8)-C(9) | 1.38(2) |
| Pd(1)-S(2) | 2.323(4) | C(8)-C(13) | 1.37(2) |
| Pd(1)-N(1) | 2.10(1) | C(9)-C(10) | 1.39(2) |
| Pd(1)-C(13) | 1.99(1) | C(10)-C(11) | 1.36(2) |
| S(1)-C(6) | 1.79(1) | C(11)-C(12) | 1.38(2) |
| S(1)-C(7) | 1.84(1) | C(12)-C(13) | 1.42(2) |
| S(2)-C(14) | 1.81(1) | C(12)-C(14) | 1.50(2) |
| S(2)-C(15) | 1.76(1) | C(15)-C(16) | 1.38(2) |
| N(1)-C(21) | 1.10(2) | C(15)-C(20) | 1.37(2) |
| C(1)-C(2) | 1.39(2) | C(16)-C(17) | 1.37(2) |
| C(1)-C(6) | 1.39(2) | C(17)-C(18) | 1.36(3) |
| C(2)-C(3) | 1.33(2) | C(18)-C(19) | 1.37(3) |
| C(3)-C(4) | 1.36(3) | C(19)-C(20) | 1.40(3) |
| C(4)-C(5) | 1.39(2) | C(21)-C(22) | 1.47(2) |
| C(5)-C(6) | 1.36(2) | | |
| C(7)-C(8) | 1.51(2) | | |

## Angles (°)

| | | | |
|---|---|---|---|
| C(13)-Pd(1)-N(1) | 178.2(5) | C(13)-C(8)-C(7) | 118(1) |
| C(13)-Pd(1)-S(1) | 81.1(4) | C(9)-C(8)-C(7) | 120(1) |
| C(13)-Pd(1)-S(2) | 85.4(4) | C(8)-C(9)-C(10) | 117(1) |
| N(1)-Pd(1)-S(1) | 99.5(3) | C(11)-C(10)-C(9) | 123(1) |
| N(1)-Pd(1)-S(2) | 94.4(3) | C(10)-C(11)-C(12) | 120(1) |
| S(1)-Pd(1)-S(2) | 163.0(1) | C(11)-C(12)-C(13) | 118(1) |
| C(6)-S(1)-C(7) | 101.8(6) | C(11)-C(12)-C(14) | 122(1) |
| C(6)-S(1)-Pd(1) | 118.6(4) | C(13)-C(12)-C(14) | 119(1) |
| C(7)-S(1)-Pd(1) | 98.2(4) | C(8)-C(13)-C(12) | 120(1) |
| C(15)-S(2)-C(14) | 104.0(7) | C(8)-C(13)-Pd(1) | 121(1) |
| C(15)-S(2)-Pd(1) | 107.8(4) | C(12)-C(13)-Pd(1) | 118.9(9) |
| C(14)-S(2)-Pd(1) | 98.5(4) | C(12)-C(14)-S(2) | 111.2(9) |
| C(21)-N(1)-Pd(1) | 178(1) | C(20)-C(15)-C(16) | 119(1) |
| C(6)-C(1)-C(2) | 118(1) | C(20)-C(15)-S(2) | 117(1) |
| C(3)-C(2)-C(1) | 121(1) | C(16)-C(15)-S(2) | 124(1) |
| C(2)-C(3)-C(4) | 120(2) | C(17)-C(16)-C(15) | 121(1) |
| C(3)-C(4)-C(5) | 122(1) | C(18)-C(17)-C(16) | 121(2) |
| C(6)-C(5)-C(4) | 118(1) | C(17)-C(18)-C(19) | 119(2) |
| C(5)-C(6)-C(1) | 121(1) | C(18)-C(19)-C(20) | 120(2) |
| C(5)-C(6)-S(1) | 116(1) | C(15)-C(20)-C(19) | 120(2) |
| C(1)-C(6)-S(1) | 122.4(9) | N(1)-C(21)-C(22) | 179(2) |
| C(8)-C(7)-S(1) | 104.9(8) | | |
| C(13)-C(8)-C(9) | 122(1) | | |

Table B.4 Details of Crystallographic Data Collection, Solution and Refinement of [Pd(PhS2)Cl]

| Empirical Formula | $C_{20}H_{17}S_2PdCl$ |
|---|---|
| Fw | 463.33 |
| a, Å | 14.660(5) |
| b, Å | 17.806(2) |
| c, Å | 14.146(1) |
| $\alpha$ | 93.356(7) |
| $\beta$ | 91.132(17) |
| $\gamma$ | 88.506(17) |
| Crystal System | Triclinic |
| Space Group | P$\bar{1}$ (No. 2) |
| Vol. Å$^3$ | 3684(1) |
| Z | 8 |
| $\mu$ (cm$^{-1}$) | 13.57 |
| $\rho_{calc}$, g/cm$^3$ | 1.67 |
| Diffractometer | Rigaku AFC6S |
| $\lambda$, Å (Mo K$\alpha$) | 0.7107 |
| T (°C) | 23 |
| scan type | $\omega$-2$\theta$ |
| speed, deg min$^{-1}$ | 32 |
| No. Observations Unique | 12979 |
| No. Observations (I>3.00$\sigma$(I)) | 4886 |
| No. Variables | 466 |
| Reflection/Parameter Ratio | 10.5:1 |
| R, % | 5.2 |
| R$_w$ % | 5.1 |
| GOF | 1.65 |
| ($\Delta/\sigma$)max | 0.005 |
| $\Delta\rho_{min}$, e$^-$/Å$^3$ | -0.510 |
| $\Delta\rho_{max}$, e$^-$/Å$^3$ | 0.7 |

*Table B.5 Selected Positional Parameters and $B_{eq}$ for [Pd(PhS$_2$)Cl] Molecule I*

| atom | x | y | z | $B_{eq}$ |
|---|---|---|---|---|
| Pd(1) | 0.22631(7) | 0.21967(6) | 0.04864(8) | 3.46(6) |
| Cl(1) | 0.0660(2) | -0.1569(2) | 0.3229(3) | 4.5(2) |
| S(1) | 0.2144(3) | -0.0827(2) | 0.4959(3) | 4.0(2) |
| S(2) | 0.2618(3) | -0.2270(2) | 0.2195(3) | 4.1(2) |
| C(1) | 0.3613(8) | -0.1548(7) | 0.3796(9) | 3.2(3) |
| C(2) | 0.398(1) | -0.1133(7) | 0.460(1) | 3.7(3) |
| C(3) | 0.334(1) | -0.0780(7) | 0.531(1) | 4.0(3) |
| C(4) | 0.2403(9) | 0.1571(7) | -0.070(1) | 3.4(3) |
| C(5) | 0.327(1) | 0.1426(8) | -0.109(1) | 3.8(3) |
| C(6) | 0.336(1) | 0.0942(8) | -0.190(1) | 4.8(4) |
| C(7) | 0.189(1) | 0.0114(8) | 0.463(1) | 3.9(3) |
| C(8) | 0.2639(9) | -0.1641(7) | 0.128(1) | 3.5(3) |
| C(9) | 0.421(1) | -0.1945(7) | 0.319(1) | 3.7(3) |
| C(10) | 0.491(1) | -0.1079(8) | 0.474(1) | 4.9(4) |
| C(11) | 0.0746(9) | 0.6308(8) | -0.399(1) | 3.8(3) |
| C(12) | 0.105(1) | 0.6527(8) | -0.592(1) | 4.9(4) |
| C(13) | 0.445(1) | 0.6464(9) | -0.532(1) | 5.8(4) |
| C(14) | 0.125(1) | 0.2852(8) | -0.261(1) | 4.3(3) |
| C(15) | 0.0840(8) | 0.3260(7) | -0.1751(9) | 2.9(3) |
| C(16) | -0.0103(9) | 0.3244(7) | -0.159(1) | 3.4(3) |
| C(17) | -0.046(1) | 0.3621(8) | -0.080(1) | 4.1(3) |
| C(18) | 0.0098(8) | 0.3981(7) | -0.0153(9) | 3.2(3) |
| C(19) | 0.1019(8) | 0.3983(7) | -0.0276(9) | 2.8(3) |
| C(20) | 0.2784(8) | 0.5376(7) | -0.0287(9) | 3.0(3) |

*Table B.6 Selected Positional Parameters and $B_{eq}$ for [Pd(PhS$_2$)Cl] Molecule 2*

| atom | x | y | z | $B_{eq}$ |
|------|------|------|------|------|
| Pd(2) | 0.27584(7) | 0.36693(6) | -0.12536(7) | 2.91(5) |
| Cl(2) | 0.2347(3) | 0.7891(2) | -0.3044(3) | 5.3(2) |
| S(3) | 0.4144(3) | 0.7128(2) | -0.4380(3) | 4.9(2) |
| S(4) | 0.1033(3) | 0.7019(2) | -0.4753(3) | 4.3(2) |
| C(21) | 0.341(1) | 0.5866(8) | 0.012(1) | 4.6(3) |
| C(22) | 0.407(1) | 0.1807(8) | -0.065(1) | 5.1(4) |
| C(23) | 0.163(1) | 0.1235(8) | -0.118(1) | 3.8(3) |
| C(24) | 0.071(1) | 0.1402(8) | -0.079(1) | 5.0(4) |
| C(25) | 0.381(1) | -0.2458(8) | 0.241(1) | 4.8(3) |
| C(26) | 0.331(1) | -0.116(1) | 0.116(1) | 6.0(4) |
| C(27) | 0.364(1) | 0.6184(8) | -0.590(1) | 4.0(3) |
| C(28) | 0.368(1) | 0.5693(8) | -0.671(1) | 4.5(3) |
| C(29) | 0.449(1) | 0.6613(8) | -0.337(1) | 4.1(3) |
| C(30) | 0.3950(9) | 0.6125(8) | -0.297(1) | 3.8(3) |
| C(31) | 0.010(1) | 0.6480(8) | -0.332(1) | 4.8(3) |
| C(32) | 0.342(1) | 0.6599(9) | -0.018(1) | 5.4(4) |
| C(33) | 0.281(1) | 0.6843(8) | -0.082(1) | 5.0(4) |
| C(34) | 0.220(1) | 0.6361(8) | -0.125(1) | 4.6(3) |
| C(35) | 0.2178(9) | 0.5606(8) | -0.096(1) | 4.1(3) |
| C(36) | 0.260(1) | 0.0631(9) | -0.233(1) | 5.7(4) |
| C(37) | 0.175(1) | 0.0786(9) | -0.202(1) | 5.8(4) |
| C(38) | -0.009(1) | 0.1517(8) | 0.187(1) | 4.3(3) |
| C(39) | 0.0538(9) | 0.1347(8) | 0.119(1) | 3.6(3) |
| C(40) | 0.101(1) | 0.0659(8) | 0.119(1) | 4.6(3) |

*Table B.7 Selected Positional Parameters and $B_{eq}$ for [Pd(PhS$_2$)Cl] Molecule 3*

| atom | x | y | z | $B_{eq}$ |
|------|---|---|---|------|
| Pd(3) | 0 25791(8) | 0.71332(7) | -0.44751(8) | 3.66(6) |
| Cl(3) | 0.2092(3) | 0.2837(2) | 0.2024(3) | 4.7(2) |
| S(5) | 0.0730(3) | 0.1989(2) | 0.0314(3) | 4.2(2) |
| S(6) | 0 3820(3) | 0.2288(2) | 0.0474(3) | 4.5(2) |
| C(41) | 0 087(1) | 0.0150(8) | 0.188(1) | 5.0(4) |
| C(42) | 0 024(1) | 0.0372(9) | 0.258(1) | 5.0(4) |
| C(43) | 0.118(1) | 0.0487(8) | 0.507(1) | 4.6(3) |
| C(44) | 0.099(1) | 0.121(1) | 0.480(1) | 5.5(4) |
| C(45) | 0.190(1) | -0.1649(9) | 0.063(1) | 5.2(4) |
| C(46) | 0.189(1) | -0.118(1) | -0.011(1) | 6.4(4) |
| C(47) | 0.258(1) | -0.075(1) | -0.026(1) | 6.0(4) |
| C(48) | 0.513(1) | -0.1901(8) | 0.336(1) | 5.0(4) |
| C(49) | 0.547(1) | -0.1465(9) | 0.409(1) | 5.4(4) |
| C(50) | -0.025(1) | 0.1027(9) | 0.257(1) | 5.2(4) |
| C(51) | 0.377(1) | 0.107(1) | 0.159(1) | 5.6(4) |
| C(52) | 0.427(1) | 0.1620(8) | 0.128(1) | 3.7(3) |
| C(53) | -0.014(1) | 0.593(1) | -0.271(1) | 6.7(4) |
| C(54) | 0.090(1) | 0.507(1) | -0.341(1) | 7.0(5) |
| C(55) | 0.116(1) | 0.560(1) | -0.407(1) | 5.8(4) |
| C(56) | 0.512(1) | 0.5798(8) | -0.188(1) | 4.7(3) |
| C(57) | 0.565(1) | 0.6301(8) | -0.227(1) | 4.9(4) |
| C(58) | 0.536(1) | 0.6719(8) | -0.302(1) | 4.5(3) |
| C(59) | 0.312(1) | 0.4049(8) | -0.361(1) | 4.1(3) |
| C(60) | 0.2702(9) | 0.3384(8) | -0.362(1) | 3.5(3) |

*Table B.8 Selected Positional Paramters and $B_{eq}$ for [Pd(PhS₂)Cl] Molecule 4*

| atom | x | y | z | $B_{eq}$ |
|------|---|---|---|------|
| Pd(4) | 0.22716(7) | -0.15561(6) | 0.35607(8) | 3.30(6) |
| Cl(4) | 0.4383(2) | 0.3705(2) | -0.1458(3) | 4.7(2) |
| S(7) | 0.2791(2) | 0.4447(2) | 0.0106(2) | 3.3(2) |
| S(8) | 0.2497(2) | 0.2892(2) | -0.2573(2) | 3.4(2) |
| C(61) | 0.1421(8) | 0.3657(7) | -0.1059(9) | 2.8(3) |
| C(62) | 0.1631(9) | 0.4351(7) | 0.049(1) | 3.7(3) |
| C(63) | 0.331(1) | -0.070(1) | 0.035(1) | 8.0(5) |
| C(64) | 0.239(1) | 0.045(1) | 0.400(1) | 5.9(4) |
| C(65) | 0.215(1) | 0.119(1) | 0.375(1) | 7.0(5) |
| C(66) | 0.143(1) | 0.1552(9) | 0.419(1) | 5.6(4) |
| C(67) | 0.519(1) | 0.170(1) | 0.156(1) | 5.8(4) |
| C(68) | 0.555(1) | 0.119(1) | 0.217(1) | 7.2(5) |
| C(69) | 0.507(1) | 0.067(1) | 0.248(1) | 6.1(4) |
| C(70) | 0.417(1) | 0.054(1) | 0.222(1) | 7.8(5) |
| C(71) | 0.323(1) | 0.4419(9) | -0.445(1) | 5.4(4) |
| C(72) | 0.295(1) | 0.407(1) | -0.528(1) | 5.8(4) |
| C(73) | 0.260(1) | 0.336(1) | -0.532(1) | 7.6(5) |
| C(74) | 0.248(1) | 0.302(1) | -0.445(1) | 7.1(5) |
| C(75) | 0.026(1) | 0.524(1) | -0.276(1) | 6.1(4) |
| C(76) | 0.426(1) | 0.5698(8) | -0.223(1) | 4.7(3) |
| C(77) | 0.275(1) | 0.6456(7) | -0.563(1) | 3.6(3) |
| C(78) | 0.198(1) | 0.6227(8) | -0.619(1) | 4.0(3) |
| C(79) | 0.211(1) | 0.5719(9) | -0.695(1) | 5.5(4) |
| C(80) | 0.295(1) | 0.548(1) | -0.720(1) | 6.2(4) |

*Table B.9 Selected Bond Distances and Angles for [Pd(PhS₂)Cl]*

Angles(°)

| | | | |
|---|---|---|---|
| C(4)-Pd(1)-S(6) | 85.7(4) | C(40)-C(39)-S(5) | 121(1) |
| C(4)-Pd(1)-S(5) | 86.2(4) | C(78)-C(77)-Pd(3) | 119(1) |
| C(4)-Pd(1)-Cl(3) | 173.9(4) | C(27)-C(77)-Pd(3) | 121(1) |
| S(6)-Pd(1)-S(5) | 171.8(2) | C(3)-S(1)-Pd(4) | 99.6(5) |
| S(6)-Pd(1)-Cl(3) | 95.0(1) | C(8)-S(2)-C(25) | 102.3(6) |
| S(5)-Pd(1)-Cl(3) | 93.0(1) | C(8)-S(2)-Pd(4) | 106.6(5) |
| C(61)-Pd(2)-S(8) | 86.4(4) | C(25)-S(2)-Pd(4) | 99.8(5) |
| C(61)-Pd(2)-S(7) | 85.1(4) | C(13)-S(3)-C(29) | 100.8(7) |
| C(61)-Pd(2)-Cl(4) | 178.7(4) | C(13)-S(3)-Pd(3) | 102.1(5) |
| S(8)-Pd(2)-S(7) | 171.5(1) | C(29)-S(3)-Pd(3) | 107.5(5) |
| S(8)-Pd(2)-Cl(4) | 95.0(1) | C(11)-S(4)-C(12) | 103.4(7) |
| S(7)-Pd(2)-Cl(4) | 93.5(1) | C(11)-S(4)-Pd(3) | 102.6(5) |
| C(77)-Pd(3)-S(3) | 85.1(4) | C(12)-S(4)-Pd(3) | 99.7(5) |
| C(77)-Pd(3)-S(4) | 86.7(4) | C(39)-S(5)-C(24) | 103.6(7) |
| C(77)-Pd(3)-Cl(2) | 177.0(4) | C(39)-S(5)-Pd(1) | 102.7(5) |
| S(3)-Pd(3)-S(4) | 171.8(2) | C(24)-S(5)-Pd(1) | 100.6(5) |
| S(3)-Pd(3)-Cl(2) | 95.7(2) | C(52)-S(6)-C(22) | 101.1(7) |
| S(4)-Pd(3)-Cl(2) | 92.5(1) | C(52)-S(6)-Pd(1) | 106.4(5) |
| C(1)-Pd(4)-S(2) | 85.4(4) | C(22)-S(6)-Pd(1) | 100.8(5) |
| C(1)-Pd(4)-S(1) | 86.6(4) | C(20)-S(7)-C(62) | 102.8(6) |
| C(1)-Pd(4)-Cl(1) | 178.4(4) | C(20)-S(7)-Pd(2) | 105.4(4) |
| S(2)-Pd(4)-S(1) | 171.9(1) | C(62)-S(7)-Pd(2) | 99.6(4) |
| S(2)-Pd(4)-Cl(1) | 93.2(1) | C(60)-S(8)-C(14) | 101.2(6) |
| S(1)-Pd(4)-Cl(1) | 94.8(1) | C(60)-S(8)-Pd(2) | 109.7(5) |
| C(7)-S(1)-C(3) | 102.1(6) | C(14)-S(8)-Pd(2) | 102.1(5) |
| C(7)-S(1)-Pd(4) | 106.1(5) | C(9)-C(1)-Pd(4) | 121(1) |
| C(2)-C(3)-S(1) | 115(1) | C(2)-C(1)-Pd(4) | 120(1) |
| C(5)-C(4)-Pd(1) | 121(1) | C(35)-C(20)-S(7) | 122(1) |
| C(23)-C(4)-Pd(1) | 121(1) | C(21)-C(20)-S(7) | 118(1) |
| C(64)-C(7)-S(1) | 122(1) | C(5)-C(22)-S(6) | 113(1) |
| C(43)-C(7)-S(1) | 117(1) | C(23)-C(24)-S(5) | 113(1) |
| C(26)-C(8)-S(2) | 124(1) | C(9)-C(25)-S(2) | 113(1) |
| C(45)-C(8)-S(2) | 117(1) | C(30)-C(29)-S(3) | 123(1) |
| C(31)-C(11)-S(4) | 118(1) | C(51)-C(52)-S(6) | 122(1) |
| C(55)-C(11)-S(4) | 121(1) | C(67)-C(52)-S(6) | 116(1) |
| C(78)-C(12)-S(4) | 113(1) | C(59)-C(60)-S(8) | 124(1) |
| C(27)-C(13)-S(3) | 113(1) | C(74)-C(60)-S(8) | 116(1) |
| C(15)-C(14)-S(8) | 111(1) | C(19)-C(61)-Pd(2) | 123(1) |
| C(58)-C(29)-S(3) | 117(1) | C(15)-C(61)-Pd(2) | 119.8(9) |
| C(38)-C(39)-S(5) | 120(1) | C(19)-C(62)-S(7) | 113.0(9) |

*Table B.10 Details of Crystallographic Data Collection, Solution and Refinement for [Pd₂(PhS₄)(CH₃CN)₂][BF₄]₂*

| | |
|---|---|
| Empirical Formula | $C_{38}H_{34}S_4Pd_2B_2F_8N_2$ |
| Fw | 1033.35 |
| a,Å | 12.66(1) |
| b,Å | 12.702(5) |
| c,Å | 12.93(1) |
| α | |
| β | 98.39(10) |
| γ | |
| Crystal System | Monoclinic |
| Space Group | P2₁/n (No. 14) |
| Vol. Å³ | 2058(3) |
| Z | 2 |
| μ (cm⁻¹) | 11.23 |
| ρ_calc, g/cm³ | 1.67 |
| Diffractometer | Rigaku AFC6S |
| λ, Å (Mo Kα) | 0.7107 |
| T (°C) | 23 |
| scan type | ω-2θ |
| speed, deg min⁻¹ | 8 |
| No. Observations Unique | 3811 |
| No. Observations (I>3.00σ(I)) | 1059 |
| No. Variables | 127 |
| Reflection/Parameter Ratio | 8.3:1 |
| R,% | 7.4 |
| R_w % | 6.5 |
| GOF | 2.41 |
| (Δ/σ)max | 1.94 |
| Δρ_min, e⁻/Å³ | -0.651 |
| Δρ_max, e⁻/Å³ | 0.7 |

*Table B.11 Selected Positional Parameters and $B_{eq}$ for $[Pd_2(PhS_4)(CH_3CN)_2][BF_4]_2$*

| atom | x | y | z | $B_{eq}$ |
|------|------|------|------|------|
| Pd(1) | 0.1642(2) | 0.4139(2) | 0.8329(2) | 4.0(1) |
| S(1) | 0.0155(5) | 0.4028(6) | 0.7106(5) | 4.6(4) |
| S(2) | 0.2904(5) | 0.4023(6) | 0.9778(6) | 4.6(4) |
| N(1) | 0.261(2) | 0.355(2) | 0.728(2) | 6.3(6) |
| C(1) | 0.064(2) | 0.469(2) | 0.930(2) | 3.6(5) |
| C(2) | -0.041(2) | 0.481(2) | 0.893(2) | 3.8(5) |
| C(3) | 0.110(2) | 0.485(2) | 1.037(2) | 3.5(5) |
| C(4) | -0.087(2) | 0.459(2) | 0.775(2) | 4.6(6) |
| C(5) | 0.225(2) | 0.468(2) | 1.074(2) | 4.8(6) |
| C(6) | 0.004(2) | 0.267(2) | 0.724(2) | 4.4(6) |
| C(7) | -0.043(2) | 0.220(2) | 0.805(2) | 6.4(7) |
| C(8) | -0.058(3) | 0.113(3) | 0.810(3) | 10(1) |
| C(9) | -0.013(3) | 0.059(3) | 0.736(3) | 12(1) |
| C(10) | 0.027(3) | 0.093(3) | 0.655(3) | 10(1) |
| C(11) | 0.040(3) | 0.204(3) | 0.649(3) | 8.6(9) |
| C(12) | 0.275(2) | 0.267(2) | 1.000(2) | 5.5(7) |
| C(13) | 0.207(2) | 0.228(2) | 1.058(2) | 5.4(6) |
| C(14) | 0.197(3) | 0.119(3) | 1.066(3) | 8.4(9) |
| C(15) | 0.262(3) | 0.050(3) | 1.022(3) | 9(1) |
| C(16) | 0.329(3) | 0.091(3) | 0.970(3) | 8.9(8) |
| C(17) | 0.344(2) | 0.200(2) | 0.952(2) | 6.2(7) |
| C(18) | 0.320(3) | 0.312(2) | 0.688(3) | 8(1) |
| C(19) | 0.382(3) | 0.255(3) | 0.611(3) | 10(1) |

*Table B.12 Selected Bond Distances and Angles for [Pd₂(PhS₄)(CH₃CN)₂][BF₄]₂*

## Distances(Å)

| | | | |
|---|---|---|---|
| Pd(1)-S(1) | 2.279(7) | C(6)-C(7) | 1.42(4) |
| Pd(1)-S(2) | 2.284(7) | C(6)-C(11) | 1.38(4) |
| Pd(1)-N(1) | 2.09(3) | C(7)-C(8) | 1.38(5) |
| Pd(1)-C(1) | 2.03(3) | C(8)-C(9) | 1.36(6) |
| S(1)-C(4) | 1.79(3) | C(9)-C(10) | 1.30(6) |
| S(1)-C(6) | 1.74(2) | C(10)-C(11) | 1.41(5) |
| S(2)-C(5) | 1.80(3) | C(12)-C(13) | 1.32(4) |
| S(2)-C(12) | 1.76(3) | C(12)-C(17) | 1.42(4) |
| N(1)-C(18) | 1.11(4) | C(13)-C(14) | 1.39(4) |
| C(1)-C(2) | 1.35(3) | C(14)-C(15) | 1.38(5) |
| C(1)-C(3) | 1.44(3) | C(15)-C(16) | 1.27(5) |
| C(2)-C(3) | 1.41(4) | C(16)-C(17) | 1.42(5) |
| C(2)-C(4) | 1.58(3) | C(18)-C(19) | 1.54(5) |
| C(3)-C(5) | 1.49(3) | | |

## Angles(°)

| | | | |
|---|---|---|---|
| C(1)-Pd(1)-N(1) | 178(1) | C(2)-C(4)-S(1) | 109(2) |
| C(1)-Pd(1)-S(1) | 85.7(8) | C(3)-C(5)-S(2) | 112(2) |
| C(1)-Pd(1)-S(2) | 86.5(8) | C(7)-C(6)-C(11) | 120(3) |
| N(1)-Pd(1)-S(1) | 91.9(8) | C(11)-C(6)-S(1) | 118(2) |
| N(1)-Pd(1)-S(2) | 95.7(8) | C(7)-C(6)-S(1) | 123(2) |
| S(1)-Pd(1)-S(2) | 166.9(2) | C(6)-C(7)-C(8) | 121(3) |
| C(4)-S(1)-C(6) | 106(1) | C(7)-C(8)-C(9) | 113(3) |
| C(4)-S(1)-Pd(1) | 104(1) | C(8)-C(9)-C(10) | 130(4) |
| C(6)-S(1)-Pd(1) | 94(1) | C(9)-C(10)-C(11) | 116(4) |
| C(5)-S(2)-C(12) | 106(1) | C(6)-C(11)-C(10) | 119(3) |
| C(12)-S(2)-Pd(1) | 96(1) | C(13)-C(12)-C(17) | 121(3) |
| C(21)-S(2)-Pd(1) | 102(1) | C(13)-C(12)-S(2) | 124(2) |
| C(18)-N(1)-Pd(1) | 167(3) | C(17)-C(12)-S(2) | 115(2) |
| C(2)-C(1)-Pd(1) | 119(2) | C(14)-C(13)-C(12) | 119(3) |
| C(3)-C(1)-Pd(1) | 117(2) | C(13)-C(14)-C(15) | 122(3) |
| C(2)-C(1)-C(3) | 124(2) | C(14)-C(15)-C(16) | 117(3) |
| C(1)-C(2)-C(3) | 119(2) | C(17)-C(16)-C(15) | 127(3) |
| C(1)-C(2)-C(4) | 122(2) | C(12)-C(17)-C(16) | 114(3) |
| C(3)-C(2)-C(4) | 119(2) | N(1)-C(18)-C(19) | 167(5) |
| C(1)-C(3)-C(5) | 122(2) | | |

*Table B.13 Details for Crystallographic Data Collection, Solution and Refinement for [Pd₂(PhS₄)Cl₂]*

| | |
|---|---|
| Empirical Formula | $C_{34}H_{28}S_4Pd_2Cl_2$ |
| Fw | 848.54 |
| a,Å | 10.170(2) |
| b,Å | 10.073(2) |
| c,Å | 15.344(2) |
| α | |
| β | 94.406(10) |
| γ | |
| Crystal System | Monoclinic |
| Space Group | $P2_1/c$ (No. 14) |
| Vol. Å³ | 1567.297(4) |
| Z | 2 |
| μ (cm⁻¹) | 16.10 |
| $\rho_{calc}$, g/cm³ | 1.80 |
| Diffractometer | Rigaku AFC6S |
| λ, Å (Mo Kα) | 0.7107 |
| T (°C) | 23 |
| scan type | ω-2θ |
| speed, deg min⁻¹ | 8 |
| No. Observations Unique | 3100 |
| No. Observations (I>3.00σ(I)) | 1789 |
| No. Variables | 190 |
| Reflection/Parameter Ratio | 8.8:1 |
| R,% | 3.3 |
| $R_w$ % | 2.6 |
| GOF | 1.33 |
| (Δ/σ)max | 0.001 |
| $\Delta\rho_{min}$, e⁻/Å³ | -0.390 |
| $\Delta\rho_{max}$, e⁻/Å³ | 0.55 |

Table B.14 Selected Positional Parameters and $B_{eq}$ for $[Pd_2(PhS_4)Cl_2]$

| atom | x | y | z | $B_{eq}$ |
|---|---|---|---|---|
| Pd(1) | 0.59749(5) | 0.21961(5) | 0.90018(3) | 2.42(2) |
| Cl(1) | 0.6663(2) | 0.0234(2) | 0.8267(1) | 3.65(9) |
| S(1) | 0.7885(2) | 0.3356(2) | 0.8824(1) | 2.89(8) |
| S(2) | 0.4047(2) | 0.1274(2) | 0.9411(1) | 2.74(8) |
| C(1) | 0.8800(6) | 0.3021(7) | 0.9842(4) | 3.1(3) |
| C(2) | 0.9661(6) | 0.1951(7) | 0.9838(5) | 3.3(4) |
| C(3) | 1.0415(7) | 0.1613(7) | 1.0592(5) | 4.0(4) |
| C(4) | 1.0338(7) | 0.2368(9) | 1.1341(5) | 4.4(4) |
| C(5) | 0.9482(8) | 0.341(1) | 1.1348(5) | 4.8(4) |
| C(6) | 0.8701(7) | 0.3757(8) | 1.0599(5) | 4.3(4) |
| C(7) | 0.2740(6) | 0.1516(7) | 0.8591(4) | 2.5(3) |
| C(8) | 0.2032(7) | 0.0420(7) | 0.8302(5) | 3.7(4) |
| C(9) | 0.0950(8) | 0.0552(9) | 0.7705(5) | 5.1(5) |
| C(10) | 0.0564(8) | 0.179(1) | 0.7424(5) | 4.8(4) |
| C(11) | 0.1235(7) | 0.2894(9) | 0.7707(5) | 4.8(4) |
| C(12) | 0.2354(7) | 0.2763(8) | 0.8291(4) | 3.9(4) |
| C(13) | 0.5410(6) | 0.3831(6) | 0.9587(4) | 2.2(3) |
| C(14) | 0.3637(6) | 0.2495(6) | 1.0221(4) | 3.0(3) |
| C(15) | 0.7281(6) | 0.5029(7) | 0.8968(4) | 2.8(3) |
| C(16) | 0.6094(5) | 0.5030(7) | 0.9503(4) | 2.1(3) |
| C(17) | 0.4320(6) | 0.3811(6) | 1.0104(4) | 2.0(3) |

*Table B.15 Selected Bond Distances and Angles for [Pd₂(PhS₄)Cl₂]*

## Distances (Å)

| | | | |
|---|---|---|---|
| Pd(1)-Cl(1) | 2.406(2) | C(7)-C(8) | 1.373(9) |
| Pd(1)-S(1) | 2.301(2) | C(7)-C(12) | 1.384(9) |
| Pd(1)-S(2) | 2.300(2) | C(8)-C(9) | 1.383(9) |
| Pd(1)-C(13) | 1.982(6) | C(9)-C(10) | 1.37(1) |
| S(1)-C(1) | 1.788(6) | C(10)-C(11) | 1.36(1) |
| S(1)-C(15) | 1.813(7) | C(11)-C(12) | 1.399(8) |
| S(2)-C(7) | 1.776(6) | C(13)-C(16) | 1.405(8) |
| S(2)-C(14) | 1.819(6) | C(13)-C(17) | 1.412(7) |
| C(1)-C(2) | 1.389(9) | C(14)-C(17) | 1.514(8) |
| C(1)-C(6) | 1.387(9) | C(15)-C(16) | 1.510(8) |
| C(2)-C(3) | 1.381(9) | C(16)-C(17) | 1.394(8) |
| C(3)-C(4) | 1.39(1) | | |
| C(4)-C(5) | 1.37(1) | | |
| C(5)-C(6) | 1.391(9) | | |

## Angles (°)

| | | | |
|---|---|---|---|
| C(13)-Pd(1)-S(2) | 85.9(2) | C(8)-C(7)-S(2) | 117.6(5) |
| C(13)-Pd(1)-S(1) | 84.7(2) | C(12)-C(7)-S(2) | 122.6(5) |
| C(13)-Pd(1)-Cl(1) | 179.0(2) | C(7)-C(8)-C(9) | 120.5(7) |
| S(2)-Pd(1)-S(1) | 169.27(7) | C(10)-C(9)-C(8) | 119.4(7) |
| S(2)-Pd(1)-Cl(1) | 94.66(6) | C(11)-C(10)-C(9) | 121.4(7) |
| S(1)-Pd(1)-Cl(1) | 94.75(6) | C(10)-C(11)-C(12) | 119.5(8) |
| C(1)-S(1)-C(15) | 103.1(3) | C(7)-C(12)-C(11) | 119.6(7) |
| C(1)-S(1)-Pd(1) | 100.8(2) | C(16)-C(13)-C(17) | 118.7(6) |
| C(15)-S(1)-Pd(1) | 99.2(2) | C(16)-C(13)-Pd(1) | 120.7(4) |
| C(7)-S(2)-C(14) | 101.1(3) | C(17)-C(13)-Pd(1) | 120.7(5) |
| C(7)-S(2)-Pd(1) | 111.0(2) | C(17)-C(14)-S(2) | 112.3(4) |
| C(14)-S(2)-Pd(1) | 99.1(2) | C(16)-C(15)-S(1) | 111.1(5) |
| C(6)-C(1)-C(2) | 120.3(7) | C(17)-C(16)-C(13) | 120.8(5) |
| C(6)-C(1)-S(1) | 124.4(6) | C(17)-C(16)-C(15) | 121.1(6) |
| C(2)-C(1)-S(1) | 115.3(5) | C(13)-C(16)-C(15) | 118.1(6) |
| C(3)-C(2)-C(1) | 119.8(7) | C(16)-C(17)-C(13) | 120.5(6) |
| C(2)-C(3)-C(4) | 119.8(7) | C(16)-C(17)-C(14) | 121.7(5) |
| C(5)-C(4)-C(3) | 120.4(7) | C(13)-C(17)-C(14) | 117.8(6) |
| C(4)-C(5)-C(6) | 120.6(8) | | |
| C(1)-C(6)-C(5) | 119.1(7) | | |
| C(8)-C(7)-C(12) | 119.6(6) | | |

*Table B.16 Details of Crystallographic Data Collection, Solution and Refinement for [Pd₂(PhS₄)(1,10-phen)₂][BF₄]₂ ·2CH₂Cl₂*

| Empirical Formula | $C_{57}H_{46}S_4N_4Pd_2B_2F_8Cl_2$ |
|---|---|
| Fw | 1372.57 |
| a,Å | 11.856(7) |
| b,Å | 21.171(13) |
| c,Å | 11.896(7) |
| α | |
| β | 94.394 |
| γ | |
| Crystal System | Monoclinic |
| Space Group | $P2_1/a$ (No. 14) |
| Vol. Å³ | 2977.120(5.9) |
| Z | 2 |
| μ (cm⁻¹) | 9.00 (Diff Abs) |
| $\rho_{calc}$, g/cm³ | 1.53 |
| Diffractometer | Rigaku AFC6S |
| λ, Å (Mo Kα) | 0.7107 |
| T (°C) | 23 |
| scan type | ω-2θ |
| speed, deg min⁻¹ | 16 |
| No. Observations Unique | 5520 |
| No. Observations (I>3.00σ(I)) | 1714 |
| No. Variables | 235 |
| Reflection/Parameter Ratio | 6.9:1 |
| R,% | 6.9 |
| $R_w$ % | 6.5 |
| GOF | 2.03 |
| (Δ/σ)max | 0.003 |
| $\Delta\rho_{min}$, e⁻/Å³ | -6.22 |
| $\Delta\rho_{max}$, e⁻/Å³ | 0.6 |

Table B.17 Selected Positional Parameters and $B_{eq}$ for $[Pd_2(PhS_4)(1,10-Phen)_2][BF_4]_2$

| atom | x | y | z | $B_{eq}$ |
|------|------|------|------|------|
| Pd(1) | 0.1113(1) | 0.12126(8) | 0.1557(1) | 3.33(7) |
| Cl(1) | 0.688(1) | 0.0666(6) | 0.1345(9) | 18(1) |
| Cl(2) | 0.821(1) | 0.1779(5) | 0.0905(8) | 13.6(8) |
| S(1) | 0.1284(5) | 0.1698(3) | -0.0133(4) | 3.8(3) |
| S(2) | 0.0228(4) | 0.0680(3) | 0.2963(4) | 3.4(3) |
| N(1) | 0.183(1) | 0.1977(7) | 0.258(1) | 3.1(8) |
| N(2) | 0.305(1) | 0.0880(7) | 0.254(1) | 3.7(8) |
| C(1) | 0.328(2) | 0.105(1) | -0.033(2) | 6.7(6) |
| C(2) | 0.431(3) | 0.095(2) | -0.071(2) | 11(1) |
| C(3) | 0.471(2) | 0.145(1) | -0.140(2) | 8.3(7) |
| C(4) | 0.412(2) | 0.195(1) | -0.170(2) | 6.8(6) |
| C(5) | 0.308(2) | 0.205(1) | -0.129(2) | 5.2(5) |
| C(6) | 0.266(2) | 0.159(1) | -0.059(1) | 4.0(5) |
| C(7) | 0.044(1) | 0.117(1) | -0.105(1) | 3.8(4) |
| C(8) | 0.027(1) | 0.0539(9) | -0.052(1) | 2.6(4) |
| C(9) | 0.041(1) | 0.0505(9) | 0.066(1) | 2.7(4) |
| C(10) | 0.021(1) | -0.0066(8) | 0.116(1) | 2.5(4) |
| C(11) | 0.046(1) | -0.0093(8) | 0.240(1) | 2.7(4) |
| C(12) | 0.098(2) | 0.070(1) | 0.429(1) | 3.3(4) |
| C(13) | 0.156(2) | 0.0185(9) | 0.478(1) | 3.4(4) |
| C(14) | 0.218(2) | 0.026(1) | 0.584(2) | 4.4(5) |
| C(15) | 0.215(2) | 0.086(1) | 0.633(2) | 4.5(5) |
| C(16) | 0.159(2) | 0.132(1) | 0.589(2) | 5.4(5) |
| C(17) | 0.098(2) | 0.128(1) | 0.485(1) | 4.1(4) |
| C(18) | 0.126(2) | 0.254(1) | 0.248(2) | 5.8(5) |
| C(19) | 0.163(2) | 0.304(1) | 0.327(2) | 7.5(7) |
| C(20) | 0.250(2) | 0.294(1) | 0.394(2) | 6.2(6) |
| C(21) | 0.314(2) | 0.241(1) | 0.409(2) | 4.7(5) |
| C(22) | 0.400(2) | 0.227(1) | 0.485(2) | 4.9(5) |
| C(23) | 0.453(2) | 0.175(1) | 0.494(2) | 5.1(5) |
| C(24) | 0.426(1) | 0.123(1) | 0.416(1) | 3.7(4) |
| C(25) | 0.487(2) | 0.068(1) | 0.413(2) | 4.4(5) |
| C(26) | 0.459(2) | 0.024(1) | 0.333(2) | 6.1(6) |
| C(27) | 0.367(2) | 0.037(1) | 0.257(2) | 3.9(4) |
| C(28) | 0.336(2) | 0.134(1) | 0.333(1) | 3.8(4) |
| C(29) | 0.275(2) | 0.192(1) | 0.331(2) | 3.9(4) |
| C(30) | 0.748(3) | 0.110(3) | 0.047(3) | 24(5) |

*Table B.18 Selected Bond Distances and Angles for [Pd$_2$(PhS$_j$)(1,10-phen)$_2$][BF$_4$]$_2$*

## Distances (Å)

| | | | |
|---|---|---|---|
| Pd(1)-S(1) | 2.281(5) | C(8)-C(10) | 1.36(2) |
| Pd(1)-S(2) | 2.333(5) | C(9)-C(10) | 1.38(2) |
| Pd(i)-N(1) | 2.16(1) | C(10)-C(11) | 1.48(2) |
| Pd(1)-C(9) | 1.98(2) | C(12)-C(13) | 1.39(2) |
| Cl(1)-C(30) | 1.60(4) | C(12)-C(17) | 1.40(2) |
| Cl(2)-C(30) | 1.73(6) | C(13)-C(14) | 1.42(2) |
| S(1)-C(6) | 1.77(2) | C(14)-C(15) | 1.40(3) |
| S(1)-C(7) | 1.81(2) | C(15)-C(16) | 1.27(3) |
| S(2)-C(11) | 1.80(2) | C(16)-C(17) | 1.39(2) |
| S(2)-C(12) | 1.75(2) | C(18)-C(19) | 1.46(3) |
| N(1)-C(18) | 1.37(3) | C(19)-C(20) | 1.28(3) |
| N(1)-C(29) | 1.34(2) | C(20)-C(21) | 1.36(3) |
| N(2)-C(27) | 1.31(2) | C(21)-C(22) | 1.35(2) |
| N(2)-C(28) | 1.39(2) | C(21)-C(29) | 1.45(2) |
| C(1)-C(2) | 1.34(3) | C(22)-C(23) | 1.27(3) |
| C(1)-C(6) | 1.38(3) | C(23)-C(24) | 1.46(3) |
| C(2)-C(3) | 1.44(3) | C(24)-C(25) | 1.37(3) |
| C(3)-C(4) | 1.31(3) | C(24)-C(28) | 1.41(2) |
| C(4)-C(5) | 1.39(3) | C(25)-C(26) | 1.35(3) |
| C(5)-C(6) | 1.39(2) | C(26)-C(27) | 1.38(3) |
| C(7)-C(8) | 1.49(2) | C(28)-C(29) | 1.42(2) |
| C(8)-C(9) | 1.40(2) | | |

## Angles(°)

| | | | |
|---|---|---|---|
| C(9)-Pd(1)-N(1) | 177.8(6) | C(1)-C(2)-C(3) | 115(3) |
| C(9)-Pd(1)-S(1) | 85.9(5) | C(4)-C(3)-C(2) | 124(3) |
| C(9)-Pd(1)-S(2) | 80.0(5) | C(3)-C(4)-C(5) | 120(3) |
| N(1)-Pd(1)-S(1) | 95.9(4) | C(4)-C(5)-C(6) | 118(2) |
| N(1)-Pd(1)-S(2) | 97.8(4) | C(1)-C(6)-C(5) | 120(2) |
| S(1)-Pd(1)-S(2) | 157.7(2) | C(1)-C(6)-S(1) | 122(2) |
| C(6)-S(1)-C(7) | 102.5(9) | C(5)-C(6)-S(1) | 118(2) |
| C(6)-S(1)-Pd(1) | 111.2(7) | C(8)-C(7)-S(1) | 113(1) |
| C(7)-S(1)-Pd(1) | 99.5(6) | C(10)-C(8)-C(9) | 123(2) |
| C(12)-S(2)-C(11) | 105.8(9) | C(25)-C(24)-C(23) | 124(2) |
| C(12)-S(2)-Pd(1) | 114.0(6) | C(28)-C(24)-C(23) | 116(2) |
| C(11)-S(2)-Pd(1) | 94.8(6) | C(26)-C(25)-C(24) | 120(2) |
| C(29)-N(1)-C(18) | 120(2) | C(25)-C(26)-C(27) | 117(2) |
| C(29)-N(1)-Pd(1) | 124(1) | N(2)-C(27)-C(26) | 127(2) |
| C(18)-N(1)-Pd(1) | 116(1) | N(2)-C(28)-C(24) | 120(2) |
| C(27)-N(2)-C(28) | 116(2) | N(2)-C(28)-C(29) | 119(2) |
| C(2)-C(1)-C(6) | 123(3) | C(24)-C(28)-C(29) | 121(2) |

| | | | |
|---|---|---|---|
| N(1)-C(29)-C(28) | 119(2) | C(12)-C(13)-C(14) | 120(2) |
| N(1)-C(29)-C(21) | 124(2) | C(15)-C(14)-C(13) | 116(2) |
| C(28)-C(29)-C(21) | 118(2) | C(16)-C(15)-C(14) | 124(2) |
| Cl(1)-C(30)-Cl(2) | 121(2) | C(15)-C(16)-C(17) | 122(2) |
| C(10)-C(8)-C(7) | 119(2) | C(16)-C(17)-C(12) | 118(2) |
| C(9)-C(8)-C(7) | 117(2) | N(1)-C(18)-C(19) | 117(2) |
| C(10)-C(9)-C(8) | 118(2) | C(20)-C(19)-C(18) | 118(3) |
| C(10)-C(9)-Pd(1) | 121(1) | C(19)-C(20)-C(21) | 129(3) |
| C(8)-C(9)-Pd(1) | 121(1) | C(22)-C(21)-C(20) | 131(2) |
| C(8)-C(10)-C(9) | 119(1) | C(22)-C(21)-C(29) | 118(2) |
| C(8)-C(10)-C(11) | 125(2) | C(20)-C(21)-C(29) | 112(2) |
| C(9)-C(10)-C(11) | 116(2) | C(23)-C(22)-C(21) | 126(2) |
| C(10)-C(11)-S(2) | 108(1) | C(22)-C(23)-C(24) | 121(2) |
| C(13)-C(12)-C(17) | 120(2) | C(25)-C(24)-C(28) | 120(2) |
| C(13)-C(12)-S(2) | 125(2) | | |
| C(17)-C(12)-S(2) | 115(1) | | |

*Table B.19 Details of Crystallographic Data Collection, Solution and Refinement of Bu-Cleft*

| Empirical Formula | $C_{36}H_{58}N_2S_4Pd_2B_2F_8$ |
|---|---|
| Fw | 1033.51 |
| a,Å | 16.837(14) |
| b,Å | 17.058(8) |
| c,Å | 19.335(8) |
| $\alpha$ | |
| $\beta$ | 112.852(45) |
| $\gamma$ | |
| Crystal System | Monoclinic |
| Space Group | $P2_1/n$ (No. 14) |
| Vol. $Å^3$ | 5117.4(5.6) |
| Z | 4 |
| $\mu$ $(cm^{-1})$ | 27.83 |
| $\rho_{calc}$, $g/cm^3$ | 1.34 |
| Diffractometer | Rigaku AFC5S |
| $\lambda$, Å (Mo K$\alpha$) | 0.7107 |
| T (°C) | 23 |
| scan type | $\omega$-2$\theta$ |
| speed, deg $min^{-1}$ | 8 |
| No. Observations Unique | 9686 |
| No. Observations (I>3.00$\sigma$(I)) | 2303 |
| No. Variables | 272 |
| Reflection/Parameter Ratio | 8.5:1 |
| R,% | 8.4 |
| $R_w$ % | 7.2 |
| GOF | 2.65 |
| ($\Delta/\sigma$)max | 2.65 |
| $\Delta\rho_{min}$, $e^-/Å^3$ | -0.627 |
| $\Delta\rho_{max}$, $e^-/Å^3$ | 1.1 |

*Table B.20 Selected Positional Parameters and $B_{eq}$ for Bu-Cleft*

| atom | x | y | z | $B_{eq}$ |
|------|------|------|------|------|
| Pd(1) | 0.6751(1) | 0.2371(1) | 0.0835(1) | 5.2(1) |
| Pd(2) | 0.4106(1) | 0.1792(1) | 0.3354(1) | 5.3(1) |
| S(1) | 0.6750(5) | 0.1050(5) | 0.1075(4) | 6.7(5) |
| S(2) | 0.6626(6) | 0.3618(5) | 0.0338(5) | 8.7(5) |
| S(3) | 0.3339(5) | 0.2794(5) | 0.2584(4) | 7.7(5) |
| S(4) | 0.4649(5) | 0.0671(5) | 0.4050(4) | 6.9(5) |
| N(1) | 0.725(1) | 0.274(1) | 0.199(1) | 7(1) |
| N(2) | 0.533(1) | 0.237(1) | 0.3734(9) | 5(1) |
| C(1) | 0.638(1) | 0.203(1) | -0.022(1) | 4.1(6) |
| C(2) | 0.637(2) | 0.257(2) | -0.074(1) | 6.1(7) |
| C(3) | 0.605(2) | 0.235(2) | -0.152(1) | 6.2(7) |
| C(4) | 0.573(2) | 0.159(2) | -0.171(1) | 5.3(6) |
| C(5) | 0.570(2) | 0.107(2) | -0.122(1) | 5.8(7) |
| C(6) | 0.604(2) | 0.130(2) | -0.042(1) | 5.0(6) |
| C(7) | 0.597(2) | 0.076(2) | 0.016(2) | 7.9(8) |
| C(8) | 0.677(2) | 0.335(2) | -0.053(2) | 9.2(9) |
| C(9) | 0.777(2) | 0.066(2) | 0.102(2) | 12(1) |
| C(10) | 0.853(4) | 0.082(4) | 0.177(4) | 26(2) |
| C(11) | 0.884(4) | 0.041(4) | 0.254(4) | 28(2) |
| C(12) | 0.899(8) | -0.031(7) | 0.225(7) | 61.0(7) |
| C(13) | 0.539(2) | 0.373(2) | -0.009(2) | 12(1) |
| C(14) | 0.508(3) | 0.383(2) | 0.051(2) | 14(1) |
| C(15) | 0.403(3) | 0.388(2) | 0.002(2) | 13(1) |
| C(16) | 0.371(3) | 0.403(3) | 0.062(2) | 16(1) |
| C(17) | 0.297(2) | 0.119(2) | 0.303(2) | 5.9(7) |
| C(18) | 0.292(2) | 0.057(2) | 0.342(2) | 6.5(7) |
| C(19) | 0.206(2) | 0.018(2) | 0.313(2) | 8.2(9) |
| C(20) | 0.145(2) | 0.051(2) | 0.255(2) | 9(1) |
| C(21) | 0.148(2) | 0.113(2) | 0.220(2) | 9(1) |
| C(22) | 0.231(2) | 0.152(2) | 0.243(2) | 7.0(8) |
| C(23) | 0.241(2) | 0.223(2) | 0.200(2) | 9(1) |
| C(24) | 0.360(2) | 0.030(2) | 0.405(2) | 7.7(8) |
| C(25) | 0.288(2) | 0.335(2) | 0.314(2) | 8.6(9) |
| C(26) | 0.357(2) | 0.377(2) | 0.374(2) | 8.8(9) |
| C(27) | 0.307(2) | 0.439(2) | 0.404(2) | 13(1) |
| C(28) | 0.373(3) | 0.485(2) | 0.464(2) | 15(1) |
| C(29) | 0.481(2) | -0.002(2) | 0.342(2) | 8.9(9) |
| C(30) | 0.546(2) | 0.017(2) | 0.310(2) | 11(1) |
| C(31) | 0.628(3) | 0.025(2) | 0.368(2) | 14(1) |
| C(32) | 0.699(3) | 0.033(3) | 0.326(2) | 17(1) |
| C(33) | 0.805(2) | 0.297(2) | 0.230(2) | 6.8(8) |

| | | | | |
|------|----------|----------|----------|--------|
| C(34) | 0.851(2) | 0.319(2) | 0.306(2) | 10(1) |
| C(35) | 0.806(2) | 0.311(2) | 0.351(2) | 7.7(8) |
| C(36) | 0.717(2) | 0.285(2) | 0.321(1) | 5.1(6) |
| C(37) | 0.682(2) | 0.267(2) | 0.245(1) | 5.0(6) |
| C(38) | 0.593(1) | 0.240(1) | 0.214(1) | 4.7(6) |
| C(39) | 0.547(1) | 0.232(1) | 0.256(1) | 4.5(6) |
| C(40) | 0.581(2) | 0.250(1) | 0.335(1) | 4.4(5) |
| C(41) | 0.668(2) | 0.276(2) | 0.368(2) | 6.5(7) |
| C(42) | 0.699(2) | 0.295(2) | 0.444(2) | 9.0(9) |
| C(43) | 0.645(2) | 0.282(2) | 0.481(2) | 9(1) |
| C(44) | 0.563(2) | 0.256(2) | 0.445(2) | 7.1(7) |

*Table B.21 Selected Bond Distances and Angles for Bu-Cleft*

### Distances (Å)

| | | | |
|---|---|---|---|
| Pd(1)-S(1) | 2.300(9) | C(11)-C(12) | 1.4(1) |
| Pd(1)-S(2) | 2.310(9) | C(13)-C(14) | 1.45(7) |
| Pd(1)-N(1) | 2.15(2) | C(14)-C(15) | 1.64(5) |
| Pd(1)-C(1) | 1.98(2) | C(15)-C(16) | 1.49(7) |
| Pd(2)-S(3) | 2.306(9) | C(17)-C(18) | 1.32(4) |
| Pd(2)-S(4) | 2.312(8) | C(17)-C(22) | 1.38(4) |
| Pd(2)-N(2) | 2.15(2) | C(18)-C(19) | 1.49(5) |
| Pd(2)-C(17) | 2.04(3) | C(18)-C(24) | 1.39(4) |
| S(1)-C(7) | 1.82(3) | C(19)-C(20) | 1.32(4) |
| S(1)-C(9) | 1.88(4) | C(20)-C(21) | 1.27(5) |
| S(2)-C(8) | 1.84(4) | C(21)-C(22) | 1.45(5) |
| S(2)-C(13) | 1.93(4) | C(22)-C(23) | 1.51(5) |
| S(3)-C(23) | 1.82(3) | C(25)-C(26) | 1.47(4) |
| S(3)-C(25) | 1.82(4) | C(26)-C(27) | 1.60(6) |
| S(4)-C(24) | 1.88(4) | C(27)-C(28) | 1.48(5) |
| S(4)-C(29) | 1.79(4) | C(29)-C(30) | 1.48(6) |
| N(1)-C(33) | 1.30(4) | C(30)-C(31) | 1.40(5) |
| N(1)-C(37) | 1.36(4) | C(31)-C(32) | 1.69(8) |
| N(2)-C(40) | 1.31(4) | C(33)-C(34) | 1.42(4) |
| N(2)-C(44) | 1.32(3) | C(34)-C(35) | 1.37(5) |
| C(1)-C(2) | 1.36(4) | C(35)-C(36) | 1.46(4) |
| C(1)-C(6) | 1.36(4) | C(36)-C(37) | 1.38(3) |
| C(2)-C(3) | 1.43(4) | C(36)-C(41) | 1.46(5) |
| C(2)-C(8) | 1.48(4) | C(37)-C(38) | 1.45(3) |
| C(3)-C(4) | 1.40(4) | C(38)-C(39) | 1.34(4) |
| C(4)-C(5) | 1.31(4) | C(39)-C(40) | 1.44(3) |
| C(5)-C(6) | 1.48(4) | C(40)-C(41) | 1.42(4) |
| C(6)-C(7) | 1.49(4) | C(41)-C(42) | 1.39(4) |
| C(9)-C(10) | 1.55(7) | C(42)-C(43) | 1.39(6) |
| C(10)-C(11) | 1.5(1) | C(43)-C(44) | 1.35(4) |

### Angles(°)

| | | | |
|---|---|---|---|
| S(1)-Pd(1)-S(2) | 168.2(3) | S(4)-Pd(2)-N(2) | 94.2(6) |
| S(1)-Pd(1)-N(1) | 96.2(7) | S(4)-Pd(2)-C(17) | 82.9(9) |
| S(1)-Pd(1)-C(1) | 84.0(8) | N(2)-Pd(2)-C(17) | 177(1) |
| S(2)-Pd(1)-N(1) | 95.6(7) | Pd(1)-S(1)-C(7) | 97(1) |
| S(2)-Pd(1)-C(1) | 84.3(8) | Pd(1)-S(1)-C(45) | 105(1) |
| N(1)-Pd(1)-C(1) | 176.0(8) | Pd(1)-S(2)-C(8) | 97(1) |
| S(3)-Pd(2)-S(4) | 170.1(3) | Pd(1)-S(2)-C(13) | 100(1) |
| S(3)-Pd(2)-N(2) | 95.7(6) | Pd(2)-S(3)-C(23) | 98(1) |
| S(3)-Pd(2)-C(17) | 87.2(9) | Pd(2)-S(3)-C(25) | 106(1) |

| | | | |
|---|---|---|---|
| Pd(2)-S(4)-C(24) | 97(1) | N(2)-C(40)-C(39) | 119(2) |
| Pd(2)-S(4)-C(29) | 106(1) | N(2)-C(40)-C(41) | 123(2) |
| Pd(1)-N(1)-C(33) | 119(2) | N(2)-C(44)-C(43) | 121(3) |
| Pd(1)-C(1)-C(2) | 118(2) | Pd(1)-N(1)-C(37) | 124(2) |
| Pd(1)-C(1)-C(6) | 119(2) | C(33)-N(1)-C(37) | 117(2) |
| C(2)-C(1)-C(6) | 122(2) | Pd(2)-N(2)-C(44) | 113(2) |
| S(1)-C(7)-C(6) | 109(2) | Pd(2)-C(17)-C(18) | 119(2) |
| S(2)-C(8)-C(2) | 106(2) | Pd(2)-C(17)-C(22) | 114(2) |
| N(1)-C(33)-C(34) | 127(3) | S(3)-C(23)-C(22) | 110(2) |
| N(1)-C(37)-C(36) | 124(2) | S(4)-C(24)-C(18) | 110(2) |

# REFERENCES

[1] J.M. Lehn, *Pure Appl. Chem*, **1978**, 50, 871.

[2] J.-M. Lehn, *Acc. Chem. Res.*, **1978**, 11, 49.

[3] C. J. Pedersen, *J. Am. Chem. Soc.*, **1967**, 89, 7017.

[4] J. M. Lehn, *Angew. Chem., Intl. Ed. Engl.*, **1988**, 27, 89.

[5] D.J. Cram, T. Kaneda, R.C. Helgeson, S.B. Brown, C.B. Knobler, E.F. Maverick, K.N. Trueblood, *J. Am. Chem. Soc.*, **1985**, 107, 3645.

[6] D.J. Cram, J. Weiss, R.C. Helgeson, C.B. Knoberl, A.E. Dorigo, K.N. Houk, *J. Chem. Soc., Chem. Commun.*, **1988**, 407.

[7] D. J. Cram, *Angew. Chem., Intl. Ed. Engl.*, **1988**, 27, 1009.

[8] L.G. Mackey, H.L. Anderson, J.K.M. Sanders, *J. Chem. Soc., Chem. Commun.*, **1992**, 43-44.

[9] M. C. Thompson, D. H. Busch, *J. Am. Chem. Soc.*, **1962**, 84, 1762.

[10] J.-P. Sauvage, C.O. Dietrich-Buchecker, J. Guilhem, C. Pascard, *Angew. Chem. Int. Ed. Engl.*, **1990**, 29, 1154-56

[11] C.L. Brown, D. Philp, L.R. Stoddart, *Synlett.*, **1991**, 462-464.

[12] P.R. Ashton, C.G.Claessens, W.Hayes, S. Menzer, J.F. Stoddart, A.J.P. White, D.J. Williams, *Angew. Chem., Intl. Ed. Engl.*, **1995**, 34, 1862.

[13] G. Wald, *Sci. Am.*, **1954**, 191, 44-53.

[14] R. D. Hancock, *Acc. Chem. Res.*, **1990**, 23, 253-57.

[15] B. P. Hay, *Coord. Chem. Rev.*, **1993**, 126, 177-236.

[16] H.L. Anderson, *Inorg. Chem*, **1994**, 33, 972-81.

[17] M. Fujita, Y. J. Kwon, O. Sasaki, K. Yamaguchi, K. Ogura, *J. Am. Chem. Soc.*, **1995**, 117, 7287-7288.

[18] H. Sleiman,P.Baxter,J.M. Lehn, K.Rissanen, *J. Chem. Soc., Chem. Commun.*, **1995**, 715.

[19] M.T. Youinou, N. Rahmouni, J. Fischer, J.A. Osborn, *Angew. Chem., Intl. Ed. Engl.*, **1992**, 31, 733.

[20] P.Baxter, J.M. Lehn, J. Fischer, M.T. Youinou, *Angew. Chem., Intl. Ed. Engl.*, **1994**, 33, 2284.

[21] A. F. Williams, C. Piguet, G. Bernardinelli, *Angew. Chem., Intl. Ed. Engl.*, **1991**, 30, 1490.

[22] E. Constable, S.M. Elder, J. Healy, M.D. Ward, *J. Am. Chem. Soc.*, **1990**, 112, 4590.

[23] M.T. Youinou, R. Ziessel, J.M. Lehn, *Inorg. Chem*, **1991**, 30, 2144.

[24] T.M. Garrett, U. Koert, J.-M. Lehn, A. Rigault, D. Meyer, J. Fischer, *J. Chem. Soc., Chem. Commun.*, **1990**, 557.

[25] C. Piguet, G.Bernardinelli, J.G.Bunzli,S. Petoud and G. Hopfgartner, *J. Chem. Soc., Chem. Commun.*, **1995**, 2575.

[26] W. Huck, F. van Veggel, B.L. Kropman, D. Blank, E.G. Keim, M. Smithers, D.N. Reinhoudt, *J. Am. Chem. Soc.*, **1995**, 117, 8293.

27 S. Serroni, G. Denti, S. Campagna, A. Juris, M. Ciano, V. Balzani, *Angew. Chem., Intl. Ed. Engl.*, **1992**, 31, 1493.

28 C. Dietrich-Buchecker, J.P. Sauvage, *New. J. Chem.*, **1992**, 16, 277.

29 M.Fujita, F.Ibukuro, K. Yamaguchi, K. Ogura, *J. Am. Chem. Soc.*, **1995**, 117, 4175-76.

30 F. Diederich, C. Dietrich-Buchecker, J-F. Nierengarten, J.-P. Sauvage, *J. Chem. Soc., Chem. Commun.*, **1995**, 781.

31 M. Saunders, J. B. Hyne, *J. Chem. Phys.*, **1958**, 29, 1319-1323.

32 S.J. Loeb, G.K.H. Shimizu, *J. Chem. Soc., Chem. Commun.*, **1993**, 1395-97.

33 D.M. Grove, G. van Koten, J.N. Louwen, J.G. Noltes, A.L. Spek, J.J.C. Ubbels, *J. Am. Chem. Soc.*, **1982**, 104, 6609.

34 J. Errington, W.S. McDonald, B.L. Shaw, *J. Chem. Soc. Dalton Trans.*, **1980**, 2312.

35 J. Dupont, N. Beydoun, M. Pfeffer, *J. Chem. Soc. Dalton Trans.*, **1989**, 1715.

36 W. Offermann, F. Vogtle, *Angew. Chem., Intl. Ed. Engl.*, **1980**, 19, 464-465.

37 J. Rohrich, K. Mullen, *J. Org. Chem.*, **1992**, 57, 2374-2379.

38 Y. Dai, K.H. Meier, *Chem. Ber.*, **1994**, 127, 1533-1535.

39 K. Campbell, I. Schaffner, *J. Am. Chem. Soc.*, **1945**, 67, 86-89.

40 E. W. Abel, R. P. Bush, F.J. Hopton, *J. Chem. Soc., Chem. Commun.*, **1966**, 58.

41 E. W. Abel, S. K. Bhargave, K. G. Orrell, *Prog. Inorg. Chem.*, **1984**, 32, 1.

42 D.S. Stephenson, G. Binsch, Program 365, Quantum Chemistry Program Exchange, Indiana University, Bloomington, IN. 47405.

43 P.A. Bates, M.N. Meah, A.J. Deeming, M.B. Hursthouse, *J. Chem. Soc. Dalton Trans.*, **1988**, 2193-2199.

44 C.V. Senoff, *Inorg. Chem*, **1978**, 8, 2320-2322.

45 S. Yamazaki, *Inorg. Chem*, **1982**, 21, 1638.

46 Z. Taira, S. Yamazaki, *J. Am. Chem. Soc.*, **1986**, 59, 649.

47 N.C. Stephenson, *J. Inorg. Nucl. Chem.*, **1962**, 24, 797.

48 M. Yamashita, H. Ito, K. Torumi, T. Ito, *Inorg. Chem*, **1983**, 22, 1566.

49 S. Yamazaki, *Inorg. Chem*, **1982**, 21, 1638.

50 Z. Taira, S. Yamazaki, *Bull. Chem. Soc. Jpn.*, **1986**, 59, 649.

51 B.A Frenz, J.A. Ibers, *Inorg. Chem*, **1972**, 11, 1109.

52 K. Wieghardt, E. Schoffmann, B. Nuber, H. Weiss, *Inorg. Chem*, **1986**, 25, 2877.

53 B.A. Frenz, J.A. Ibers, *Inorg. Chem*, **1972**, 11, 1109.

54 C.W. Reimann, S. Block, A. Perloff, *Inorg. Chem*, **1966**, 5, 1185.

55 A.J. Graham, R.H. Fenn, *J. Organomet. Chem.*, **1970**, 25, 173.

56 G. W. Bushnell, K.R. Dixon, M.A. Khan, *Can. J. Chem.*, **1974**, 52, 1367.

57 S. Yamazaki, *Polyhedron*, **1985**, 4, 1915.

58 S. McCasland, *J. Org. Chem.*, **1946**, 11, 277.

59 A.W. Maverick, S.C. Buckingham, Q. Yao, J.R. Bradbury, G.G. Stanley, *J. Am. Chem. Soc.*, **1986**, 108, 7430.

[60] M. Fujita, J. Yazaki, K. Ogura, *J. Am. Chem. Soc.*, **1990**, 112, 5645.

[61] M. Fujita, J. Yazaki, K. Ogura, *Tetrahedron Lett.*, **1991**, 32, 5589

[62] P.J. Stang, D.H. Cao, *J. Am. Chem. Soc.*, **1994**, 116, 4981.

[63] P.J. Stang, D.H. Cao, S. Saito, A.M. Arif, *J. Am. Chem. Soc.*, **1995**, 117, 6273.

[64] P.J. Stang, B. Olenyuk, J. Fan, A.M. Arif, *Organometallics*, **1996**, 15, 904.

[65] P.J. Stang, P.J. Whiteford, *Organometallics*, **1994**, 13, 3776.

[66] C.A. Hunter, L.D. Sarson, *Angew. Chem., Intl. Ed. Engl.*, **1994**, 33, 2313.

[67] X. Chi, A.J. Guerin, R.A. Haycock, C.A. Hunter, L.D. Sarson, *J. Chem. Soc., Chem. Commun.*, **1995**, 2563.

[68] X. Chi, A.J. Guerin, R.A. Haycock, C.A. Hunter, L.D. Sarson, *J. Chem. Soc., Chem. Commun.*, **1995**, 2567.

[69] P.M. Stricklen, E.J. Volcko, J.G. Verkade, *J. Am. Chem. Soc.*, **1983**, 105, 2494.

[70] R. Ziessel, M.-T. Youinou, *Angew. Chem., Intl. Ed. Engl.*, **1993**, 32, 877.

[71] F. Bitscch, C. O. Dietrichh-Buchecker, A. Khemiss, J. P. Sauvage, A. Van Dorsselaer, *J. Chem. Soc., Chem. Commun.*, **1991**, 115, 4023-4024.

[72] M. Fujita, S. Nagao, K. Ogura, *J. Am. Chem. Soc.*, **1995**, 117, 1649.

[73] M. Fujita, F. Ibukruo, H. Hagihara, K. Ogura, *Nature.*, **1994**, 367, 720.

[74] J.-F. Nierengarte, C.O. Dietrich-Buckecker, J.-P. Sauvage, *J. Am. Chem. Soc.*, **1994**, 116, 375.

[75] K. C. Russell, E. Leize, A. Van Dorsselaer, J. M. Lehn, *Angew. Chem., Intl. Ed. Engl.*, **1995**, 34, 209-213.

[76] P. R. Ashton, C. L. Brown, J. R. Chapman, R. T. Gallagher, J. F. Stoddart, *Tetrahedron Lett.*, **1992**, 33, 7771-7774.

[77] E.Leize, A. Van Dorsselaer, R. Kramer, J.-M. Lehn, *J. Chem. Soc., Chem. Commun.*, **1993**, 990.

[78] S.C. Zimmerman, W. Wu, Z. Zeng, *J. Am. Chem. Soc.*, **1991**, 113, 196.

[79] S. Goswami, A.D. Hamilton, *J. Am. Chem. Soc.*, **1989**, 111, 3425.

[80] T. Beissel, R. Powers, K.N. Raymond, *Angew. Chem., Intl. Ed. Engl.*, **1996**, 35, 1084.

# Curriculum Vitae:  Jeffrey Ronald Hall

| | |
|---|---|
| **Address:** | Department of Chemistry and Biochemistry<br>University of Windsor<br>Windsor, Ontario, Canada N9B 3P4 |
| **Birthplace:** | Windsor, Ontario, Canada |
| **Birthdate:** | March 28, 1968 |
| **Citizenship:** | Canadian |

**Education:**

| | |
|---|---|
| B. Sc., 1993 | Honours Chemistry<br>University of Windsor<br>Windsor, Ontario, Canada |
| M. Sc., 1996 | Inorganic/Organometallic Chemistry<br>University of Windsor<br>Windsor, Ontario, Canada |

**Scholarships and Awards**

Undergraduate Student Presentation Award
*XXV*$^{th}$ *Inorganic Discussion Weekend*, London, Ontario, **1993**

**Experience**

Graduate Student
University of Windsor, Windsor, Ont. Canada (1993-1996)

Teaching Assistant
University of Windsor, Windsor, Ont. Canada (1993-1996)

Undergraduate 4$^{th}$ Year Project
University of Windsor, Windsor, Ont. Canada (1992)

**Publications**

S. Wang, J.C. Zheng, J.R. Hall, "Crystal Structure and Magnetic Properties of a Cubane-Type Copper Compound [Cu$^{II}$(2,2,6,6-Tetramethyl-3,5-heptanedionato)(ethoxo)]$_4$ ", *Polyhedron*, **1994**, 13, 1039-1044

**Presentations**

C. N. Deslippe, J. R. Hall, S. J. Loeb. "The Self-Assembly of Metal-Based Molecular Hexagons" *212th Meeting of the American Chemical Society*, Orlando, USA., **1996**

C.N. Deslippe, J. R. Hall, S. J. Loeb, "The Self-Assembly of Metal-Based Molecular Hexagons" *31st International Conference on Coordination Chemistry*, Vancouver, British Columbia, **1996**

J. R. Hall, S. J. Loeb, "Metal-Based Molecular Polygons and Clefts" *78th Canadian Chemical Conference and Exhibition*, Guelph, Ontario, **1995**

J. R. Hall, S. J. Loeb, "Metal-Based Molecular Polygons and Clefts" *XXVIIth Inorganic Discussion Weekend*, Hamilton, Ontario, **1995**

J. R. Hall, J. E. Kickham, S. J. Loeb, S. L. Murphy, "Molecular Recognition Via Simultaneous First- and Second-sphere Coordination" *XIXth International Symposium on Macrocyclic Chemistry*, Lawrence, Kansas, USA, **1994**

J. R. Hall, S.W. Wang, "A Non-Linear Regression Program for Magnetic Susceptibility" *XXVth Inorganic Discussion Weekend*, London, Ontario, **1993**

# IMAGE EVALUATION
# TEST TARGET (QA-3)

150mm

6"
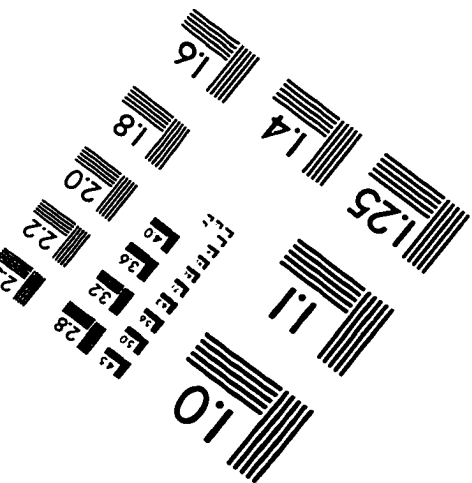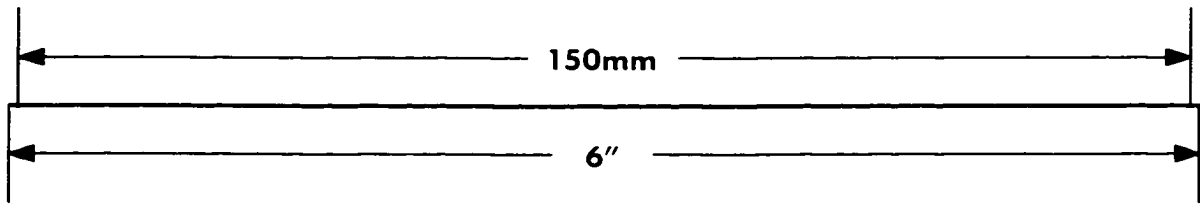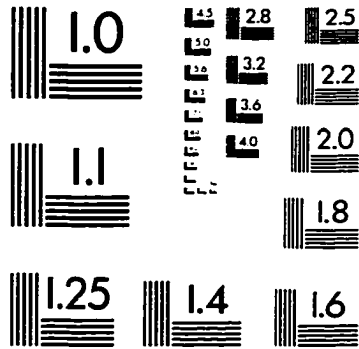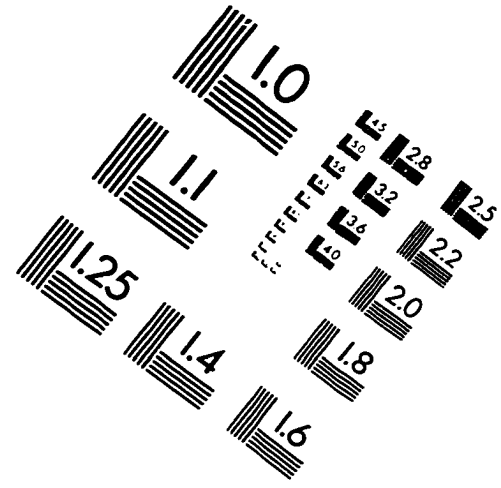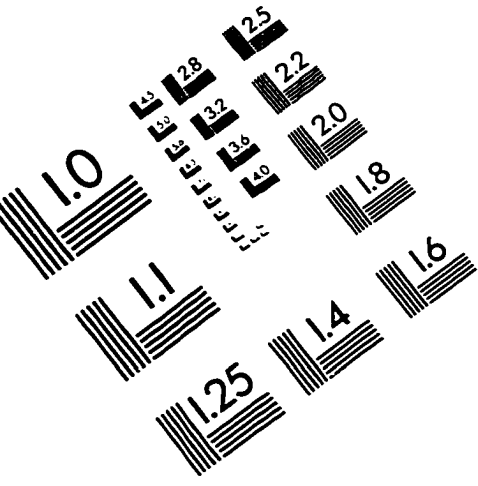
APPLIED IMAGE, Inc
1653 East Main Street
Rochester, NY 14609 USA
Phone: 716/482-0300
Fax: 716/288-5989

© 1993, Applied Image, Inc., All Rights Reserved